

Copyright
by
Katherine Taylor
2012

**The Dissertation Committee for Katherine Taylor Certifies that this is the approved
version of the following dissertation:**

**THE HOST RESPONSE TO VENEZUELAN EQUINE
ENCEPHALITIS VIRUS**

Committee:

Dr. Slobodan Paessler, Supervisor

Dr. Mark Estes, Co-Supervisor

Dr. Judy Aronson

Dr. David Beasley

Dr. Gerald Campbell

Dr. Dirk Werling

Dean, Graduate School

**THE HOST RESPONSE TO VENEZUELAN EQUINE
ENCEPHALITIS VIRUS**

by

Katherine Gwen Taylor, B.S.

Dissertation

Presented to the Faculty of the Graduate School of

The University of Texas Medical Branch

in Partial Fulfillment

of the Requirements

for the Degree of

Doctor of Philosophy

The University of Texas Medical Branch

May 2012

Dedication

This work is dedicated to my parents and grandparents who taught me the importance of wisdom and knowledge, and blessed me with the gift of education.

Acknowledgements

Kevin who was always there for me; Jessie whose empathy made life brighter; my friends and fellow graduate students; and Drs. Slobodan Paessler and Mark Estes who mentored me throughout this project.

The Host Response to Venezuelan Equine Encephalitis Virus

Publication No. _____

Katherine Gwen Taylor, Ph.D.

The University of Texas Medical Branch, 2012

Supervisor: Slobodan Paessler

Viruses are currently the most common cause of encephalitis. Arboviruses in the *Alphavirus* genus in the family *Togaviridae* contain multiple viruses capable of causing human encephalitis. Of these, VEEV represents the most significant human pathogen. However, no licensed vaccines or therapeutics are available. A comprehensive understanding of the host response to a pathogen is integral in the development of both. By using intranasal infection with TC83, the vaccine attenuated strain of VEEV, we are able to mimic VEEV encephalitis as well as evaluate the vaccine candidate. Intranasal infection with TC83 in different mouse strains led to development of three models of infection: (1) non-lethal infection with complete viral clearance from the brain in C57BL/6 mice (2) lethal infection in C3H/HeN mice and (3) persistent viral infection of the brain in α/β T-cell receptor deficient (TCR KO) mice. All three strains display a similar viral kinetic and brain pathology. Further comparison of the host response among these models derived key immune mediated factors in protection and pathogenesis. Proinflammatory cytokine kinetics and levels in the brain differentiate lethal

(BL6) and non-lethal infection (C3H). Furthermore, significant differences in gene transcription in the brain appeared between strains. These factors indicated a role for natural killer cells in pathogenesis. Subsequent loss and gain of function studies in the natural killer cell compartment in C3H mice demonstrated a pathogenic role for this cell type. In TCR KO mice, $\alpha\beta$ T-cells appear to be required for clearance of virus, but are not needed to prevent lethal infection as virus persists in the brain for 90 days post-infection. Histological signs of inflammation remain to 30 days post-infection. In addition, MCP-1, RANTES, and IL-12p40 levels remain elevated above controls to 90 days post-infection. These cytokines may be useful in the identification of viral infection without requiring isolation of the virus. Loss and gain of function studies in BL6 mice indicate that IL-12p40 appears to aid in recovery early in infection of BL6 mice, but may enhance pathogenesis later in infection. In addition, in a model of virulent VEEV encephalitis, IL-12p40 appears to be pathogenic as vaccinated mice recover more rapidly in the absence of IL-12p40. However, this effect is dependent on the presence of adoptively transferred antigen-specific T-cells. In summary, C3H mice survive in the absence of functional NK cells indicating the importance of this cell population. T-cells in BL6 are not required for survival, and absence of T-cells establishes chronic infection with a detectable chronic host response. This establishes a novel model to study T-cells in viral clearance as well as the chronic responses to infection in the brain.

Table of Contents

List of Tables	xii
List of Figures	xiv
Chapter 1: Overview of Encephalitic Alphaviruses	1
Medical Importance	2
History	4
Transmission cycles and geographic range.....	5
Molecular biology of the Alphavirus genus.....	8
Virus spread	10
Pathogenic sequence of alphaviral infection in humans	10
Conclusion	12
Chapter 2: Host Response to Alphaviral Infection	14
TC83	15
Efficacy studies of TC83 vaccination in animal models.....	16
TC83 virulence and pathogenesis in mouse models.....	18
Intranasal TC83 infection of C3H mice is representative of VEEV encephalitis	19
C3H susceptibility is not linked to MHC, but may result from changes to the immune response.....	20
CNS Entry	23
Immune Response	25
Innate Immune Response.....	29
Type I Interferon.....	29
Natural killer cells.....	35
Type II IFN.....	39
Adaptive Immune Response	40
B-cells	41
T-cells.....	42
Conclusions	44

Chapter 3: Study Purpose and Design.....	46
Study Purpose.....	46
Hypothesis.....	48
Chapter 4: Methods.....	50
Animal Use:.....	50
Statistical analysis:.....	50
Rationale.....	51
Virus52	
Rationale.....	52
Viral replication in the tissues.....	52
Organ preparation.....	52
Plaque Assay.....	53
Statistical Analysis.....	53
Rationale.....	53
Histopathology.....	54
Statistical Analysis.....	54
Microarray analysis.....	55
Total RNA preparation and GeneChip processing.....	55
Statistical analysis.....	55
Bioplex analyses of cytokine and chemokine expression.....	56
Statistical analysis.....	56
Additional Methods:.....	56
Chapter 5: A Comparative Model of Lethal and Non-Lethal TC83-Encephalitis	57
Characterization of a comparative model of lethal and non-lethal TC83-encephalitis.....	59
High-levels of mortality in C3H mice, but complete survival in BL6 mice characterize intranasal TC83 infection.....	59
Both C3H and BL6 mice display high-titer viral load in the brain and low-titer viral load in peripheral organs.....	60
Similar pathology and histology scores in lethally infected C3H and resistant BL6 mice.....	62
Characterization of lethal and non-lethal host response to TC83-encephalitis.	62

High-level production of neutralizing antibody at 6 dpi characterizes TC83 infected BL6 and C3H mice.....	63
Transcriptome analysis identified immune and inflammatory genes in lethal and non-lethal host responses.....	64
Cytokine levels indicate T-cell and NK cell involvement in TC83 infection.....	71
Depletion of NK cells reverses the infection outcome in C3H mice..	74
NK cells may increase viral burden in the host.....	76
NK cell depleted and TC83 infected mice develop lethal encephalitis following adoptive transfer of naïve NK cells.....	77
NK cells do not affect level of inflammation in the brain, but may alter phenotype of infiltrating inflammatory cells.....	80
Additional methods.....	82
Adoptive transfer.....	82
NK-cell depletion.....	83
Flow cytometric analysis.....	83
NK cell depletion alters cytokine profiles.....	84
Discussion.....	87
Chapter 6: A model of viral persistence following acute TC83-encephalitis in mice.....	91
Characterization of a comparative model of viral persistence and clearance following acute TC83-encephalitis in mice.....	92
TCR KO mice develop acute encephalitis followed by low level, unresolved viral infection of the brain.....	92
TCR KO, but not BL6 or IL-12p40 KO mice develop asymptomatic, non-lethal chronic TC83 infection of the brain.	94
Characterization of chronic viral isolates.....	97
TCR KO mice display a chronic inflammatory response in the brain.....	99
An on-going pro-inflammatory cytokine response characterizes chronically infected TCR KO mice.....	99
Cytokine profiles identify chronically infected TCR KO mice.....	102
Whole transcriptome analysis of the brain indicates significant alterations of the host response.....	104

T-cell absence mediates a chronic infection and inflammatory response of the brain.....	106
A proposed role for IL-12p40 in TC83 infection of BL6 and C3H mice...106	
IL-12p40 treatment of C3H mice extends mean time to death, lessens disease, and reduces viral load in the brain.....	107
IL-12p40 treatment of IL-12p40 KO mice reduces symptomatic disease and viral load in the brain.	109
Clinical hematology and biochemistry parameters vary little between infection in early IL-12p40 treated mice, untreated mice, and uninfected, untreated mice at eight dpi.....	110
The effect of IL-12p40 on TC83 infection of C3H and BL6 mice....	111
A potential role for IL-12p40 in wild-type VEEV infection.....	111
Discussion	113
Chapter 7: Conclusions.....	116
Bibliography	122
Vita Error! Bookmark not defined.	

List of Tables

Table 1: Characteristics of the New World encephalitic alphaviruses.....	3
Table 2: Efficacy of TC83 vaccination in inbred mouse strains.....	17
Table 3: Survival following TC83 infection in inbred mouse strains.	18
Table 4: Response of C3H and BL6 mouse strains following intranasal TC83 infection.	47
Table 5: Description of genetically modified strains utilized in studies.	50
Table 6: Histological scores of brain tissue from C3H and BL6 mice following intranasal TC83 infection at 6 dpi. Overall scores represent mean determined from means for individual brain sections.	62
Table 7: Serum neutralizing antibody response between C3H and BL6 mice at six dpi.	63
Table 8: Histological scores of brain tissue from NK cell depleted and NK cell competent C3H mice following intranasal TC83 infection at 6 dpi. Overall score represents the mean of all individual brain sections.....	81
Table 9: Serum neutralizing antibody at 12 dpi in TC83 infected TCR KO and BL6 mice.	97
Table 11: Cytokine protein levels at one, six, 30, and 90 dpi that are significantly elevated ($p<0.05$) in : (1) chronically infected TCR KO mice compared to sham (2) BL6 infected compared to sham (3) TCR KO infected animals compared to BL6 infected.....	103

Table 10: Fold change in IL-12p40 and related cytokine gene expression in infected BL6 and TCR KO mice compared to sham controls.....105

List of Figures

- Figure 1: Transmission cycles of the New World encephalitic alphaviruses. Humans and equines represent secondary hosts that are not typically involved in enzootic viral transmission cycles. However, infection of humans and equines results in epidemic or epizootic outbreaks of disease respectively. Ability of secondary hosts to transmit the virus is pathogen dependent..... 6
- Figure 2: Geographic distribution of alphaviruses capable of causing encephalitis.8
- Figure 3: Biphasic nature of alphavirus infection in viral spread, immune response, and disease. 11
- Figure 4: Pathogenesis of intranasal TC83 infection in C3H and BL6 mice. (A) Survival was significantly lower in infected C3H (n=9) mice compared to infected BL6 mice (n=3) or saline controls (n=3). (B) Infected C3H mice displayed significantly greater weight loss than infected BL6 mice or saline controls at nine dpi. BL6 mice lost significantly more weight and maintained significantly lower weights than saline controls starting at five dpi. (* denotes $p < 0.05$ compared to saline controls, ^ denotes $p < 0.05$ between infected groups). 58
- Figure 5: Similar viral kinetic in the brain between C3H and BL6 mice following intranasal TC83 infection. At one and six dpi, C3H mice and BL6 mice have no significant difference in viral load as determined by plaque assay. ($p < 0.01$). At 34 dpi, BL6 mice have no infectious virus present in the brain. The one surviving C3H animal had no virus present in the brain at 90 dpi. (n=3/group/time point)..... 59

Figure 6: Infectious virus in peripheral organs of TC83 infected C3H (n=3) and BL6 mice (n=3) at six dpi determined by plaque assay. No virus was observed in any of the tested replicates at either one dpi or 34 dpi. No significant difference in viral load between for any group comparison was demonstrated ($p < 0.01$).60

Figure 7: Meningitis and perivascular cuffing in TC83 infected C3H and BL6 mice at 6 dpi. Sham infected mice had normal brain architecture. 61

Figure 8: Comparison of genes with 2-fold or more differential expression between TC83 infected C3H and BL6 mice and saline controls. Numbers in green represent 2-fold or greater decrease in expression compared to saline. Numbers in red represent 2-fold or greater increase. C3H and BL6 shared expression of 516 up-regulated and 19 down regulated genes. C3H expressed 34 up-regulated and 5 down-regulated genes not expressed by BL6. BL6 mice uniquely expressed 363 up-regulated and 64 down-regulated genes..... 64

Figure 9: Analysis of top functional categories. Differentially expressed genes involved several overlapping categories related to immune and inflammatory function (antigen presentation, cell and humoral immunity, and inflammatory response) in the brain homogenates of infected mice compared to sham infected mice. 66

Figure 10: Alterations in immune/inflammatory functional response following TC83 infection of C3H and BL6 mice. Heat map plot of differentially expressed immune/inflammatory transcripts (from functional categories representing antigen presentation, cell-mediated immune response, humoral immune response, and inflammatory response) for C3H and BL6 infected mice. The green bar on the right indicates genes differentially expressed between BL6 and saline control. The red bar represents genes differentially expressed between C3H and saline control. The blue bar represents genes differentially expressed in interaction analysis of C3H and BL6 infected mice. Genes differentially expressed between C3H infected mice and BL6 infected mice are highlighted in yellow. Rows are arranged by hierarchical clustering following Z-score transformation of the normalized data. Columns represent mock-infected and TC83-infected animals at six dpi. Columns represent mock-infected C3H (M25 and M20), BL6 (M1, M5) TC83-infected C3H (M3, M13, and M5), BL6 (M60, M61, M63) transcripts from brain homogenates at 6 days post challenge. . 67

Figure 11: Inverse patterns of IL-2 expression over time in the brain in non-lethal and lethal infections. Lethally infected C3H mice (n=3) demonstrate significantly lower levels of IL-2 at one dpi, but at six dpi have significantly higher levels of IL-2 compared to saline treated C3H mice (n=2). Non-lethal infection of BL6 mice (n=3) results in early, significant increase of IL-2 at one day post-infection compared to saline treated BL6 mice (n=2), but by six dpi is not significantly different from control BL6 mice (*,p<0.05;** , p<0.005 compared to sham-infected controls) (n=3/group). 71

Figure 12: Significant differences in production of KC, MCP-1 and IL-12p40 at six dpi in the brain between lethal and non-lethal infections. (A) KC levels are significantly higher in lethally infected C3H mice compared to non-lethally infected BL6 mice. KC levels in C3H infected mice are significantly higher compared control C3H mice, but not in infected BL6 mice compared to control BL6 mice. (B) MCP-1 levels in infected mice are significantly elevated above control BL6 and C3H mice respectively. MCP-1 levels are significantly higher in lethally infected C3H mice compared to non-lethally infected BL6 mice. (C) IL-12p40 levels are significantly elevated in infected mice, C3H and BL6, compared to C3H and BL6 saline controls respectively (*p<0.05;** p≤0.005) (n=3/TC83 group, n=2/saline group)..... 72

Figure 13: Unique cytokines expression profiles in the brains of C3H and BL6. All comparisons represent infected mice compared to sham control mice. C3H mice display significantly higher levels of MIP-1β, IL-1β, IL-1α, IL-5, IL-10, G-CSF, IL-6, IL-12p70, IL-3, and IL-17 compared to saline treated control C3H mice. In contrast, infected BL6 mice have significant differences only in MIP1β and IL-5 expression compared to saline treated control BL6 mice. No significant differences in IFN-γ expression were observed between groups though infected mice, C3H and BL6, show a trend to increased IFN-γ expression. Note the changing scale. (*p<0.05, **p<0.005)) 73

Figure 14: NK cell depletion reverses the outcome of the infection in C3H mice. (A) Depletion of NK-cells from C3H mice (n=3) resulted in 100% survival compared to 100% mortality in NK competent C3H mice who had a mean day to death of eight days (n=5) (p=0.0082). (B) Weight loss was significantly greater in infected NK competent C3H compared to NK cell depleted mice at six and eight dpi. For both infected NK-cell depleted and wt C3H weight loss was significantly greater compared to saline controls at both six and eight dpi. (C) NK-cell depleted mice had 80% survival rate, significantly higher than NK-cell competent mice. (n=10). There was no significant difference in survival between NK-cell depleted, infected mice (n=10) and saline controls (n=4). Survival in NK-cell competent infected mice (n=10) was significantly lower than saline controls (n=4). (D) Weight loss was significantly more in infected NK-cell competent C3H compared to NK-cell depleted mice at six and nine dpi. Significantly greater weight loss in NK-cell depleted mice compared to sham infected, depleted controls was maintained from six through 17 dpi. NK-cell competent C3H infected mice lost significantly more weight compared to saline controls. (*, p<0.05 compared to sham-infected control; ^ p<0.05 compared to TC83-infected group). 75

Figure 15: Viral load in the brain at eight and six dpi. (A) Viral load in the brain did not differ between NK-cell depleted and competent mice at eight dpi. Virus was not present in the brains of saline controls. (B) Viral load in the brain was significantly decreased in NK-cell depleted mice compared to NK-cell competent mice at six dpi (p=0.0422). Virus was not present in the brains of saline controls..... 76

Figure 16: Viral load in liver, lung and spleen at one dpi from TC83 infected NK-cell competent (n=3) and depleted C3H mice (n=3) determined by plaque assay. No significant difference viral load was observed between any group comparison (p<0.05)..... 77

Figure 17: Survival rates are similar when anti-asialo GM1 treatment is halted at one day prior to infection and counteracted with mouse anti-rabbit polyclonal IgG (maR-IgG). C3H mice receiving polyclonal rabbit IgG had 50% mortality (n=2). Mice in the asialo-GM1 treated group that were NK-cell depleted as previously (n=2) responded with 100% survival. Mice in the experimental group depleted of NK cells and receiving maR-IgG (n=2) responded with 100% survival..... 78

Figure 18: Pathogenesis resulting from reconstitution of naive NK-cell cells in previously resistant NK-cell depleted C3H mice. Treatment with anti-asialo GM1 antibody was halted one day prior to infection and counteracted with treatment with mouse anti-rabbit IgG. Mice received either 10^7 naive NK cells (n=5) or an equivalent amount of saline (n=3) i.p. 24 hours prior to infection. (A) Reconstitution of depleted mice with purified naive NK-cells, reverted disease phenotype to uniform mortality. This was significantly different than NK-cell depleted mice that did not receive NK-cells that had a 40% survival rate (p=0.0495). (B) Weight loss was not significantly different between groups at any time point post infection. Surviving NK-cell depleted mice showed weight gain indicative of survival between eight and 20 dpi..... 79

Figure 19: Meningitis and perivascular and vascular cuffing are similar between NK cell competent and NK cell depleted mice at six dpi. Sham infected controls depleted of NK cells demonstrate normal brain architecture..... 80

Figure 20: Alterations in the cellular immune response in the brain and spleen following NK-cell depletion and TC83 infection at six dpi. Analysis was performed by flow cytometry and represents cells pooled from 3 mice/group. Splenic B220+ cell populations were decreased in infected mice compared to saline controls, but depletion in saline controls increased these populations compared to saline competent controls. CD4+ cells were increased in infected mice compared to saline, NK-competent controls, but not saline NK-depleted controls. NK-cells are ablated in the spleens of TC83 and sham infected NK-cell depleted mice. In the brain, a trend toward increased infiltration of CD4+ and B220+ cells was observed. NK-cell populations and sham infected controls are not shown in the brain as too few events were recorded for analysis.... 82

Figure 21: Alterations in cytokine profiles in the brain NK cell competent and depleted C3H at one and six dpi. (A, B) In infected NK-cell competent C3H (n=3), IL-12p40, G-CSF and RANTES levels are elevated above saline controls (n=3). (A) IL-12p40 levels are higher in infected NK-cell competent C3H than depleted mice (n=3). (C) IL-3, IL-4, and IL-5 cytokines are higher in infected wt C3H, but not NK-depleted, than controls. (D) IL-10, GM-CSF, and IFN- γ levels are elevated in infected mice. (E) IL-9 and IL-13 are elevated in infected mice compared to controls. TNF- α levels are only elevated in NK-cell competent C3H. (*, $p < 0.05$, compared to saline control) (^, $p = 0.05$ compared to infected BL6)..... 86

Figure 22: Significantly higher IFN- β production occurs in infected and sham NK-cell depleted mice compared to NK-competent mice at one and six dpi. (A) At one dpi, infected and sham mice depleted of NK-cells show significant elevation of IFN- β compared to infected and sham animals given a control antibody. (B) At six days post-infection, NK-competent, infected mice have significantly higher levels of IFN- β than sham controls. NK-cell depleted mice maintain significantly higher IFN- β levels compared to NK-cell competent mice (* $p < 0.05$, ** $p < 0.005$) (n=3/group)..... 87

Figure 23: Weight loss and viral load in the brain of TCR KO mice intranasally infected with 10^7 or 10^8 pfu or TC83. Control mice received PBS or 10^7 pfu of SIN/ZPC (n=3/group). (A) TC83 infected TCR KO mice lost significantly more weight than SIN/ZPC or PBS controls and maintained weight loss to 34 dpi. (B) At six dpi, a significantly higher viral load is present in the brains of TC83 infected mice compared to saline controls. SIN/ZPC infected mice display low virus levels. At 13 dpi, TCR KO mice infected with 10^7 pfu TC83 had significantly higher virus levels in the brain than PBS or SIN/ZPC controls. TC83 infected TCR KO mice maintained infectious virus in the brain to 33 dpi. (* denotes group compared to saline; ^, compared to SIN/ZPC) (p<0.05). 93

Figure 24: Weight loss and viral load in the brains of TCR KO, IL-12p40 KO, and BL6. (A) TCR KO and BL6 mice maintained significantly greater weight loss than sham controls to 61 dpi. IL-12p40 KO maintained significantly greater weight loss to 13 dpi, and no significant difference was observed by 22 dpi. Dashed line indicates separate experiment. (B) Viral load peaked at six dpi for TCR KO and BL6, but virus was maintained in the brain to 90 dpi in TCR KO mice. IL-12p40 KO mice had an expected viral load at eight dpi. Points represent individual mice (n=3/group) (p<0.05 - * denotes group compared to sham-infected; ^, compared to infected BL6). 95

Figure 25: Viral load in the peripheral organs of BL6 (n=3) and TCR KO (n=3) mice infected intranasally with TC83 at six dpi. Virus levels were determined by plaque assay. No virus was found in the liver. No significant difference in viral load was observed in lung or spleen (p<0.05). 96

Figure 26: No significant changes in plaque size from original inoculum in chronically infected mice at 30 (n=1), 60 (n=1), and 90 (n=3) dpi. Plaque morphology does differ with some plaques displaying well defined edges and others appearing more unfocused at the periphery. 98

Figure 27: Neutrophil infiltrates, activated microglia, meningitis, and perivascular cuffing in the brains of TCR KO mice infected intranasally with TC83 at 30 dpi. Microglia also show signs of activation with elongated processes. 99

Figure 28: Expression of IL-12p40 and related cytokines over time. IL-12p40 levels are significantly higher than controls in BL6 and TCR KO mice at 6 dpi, but only in TCR KO mice at 30 dpi. IL-17 and IL-12p70 levels are significantly higher in TCR KO mice, but not BL6 at six dpi compared to controls. IL-12p70 levels are significantly higher in infected TCR KO mice compared to BL6. No differences between sham infected and TCR KO mice were observed. (* denotes $p < 0.05$ compared to sham-infected; ^, denotes $p < 0.05$ compared to infected BL6)100

Figure 29: Chronic elevation of RANTES, IL-12p40, and MCP1 in the brains of infected TCR KO mice. IL-12p40 is significantly different from controls at six and 30 dpi in TCR KO mice. RANTES is significantly different at six and 60 dpi TCR KO mice compared to controls. In addition, RANTES is significantly higher compared to infected BL6 mice.101

Figure 30: IFN- β levels in the brains of infected and sham infected TCR KO mice at 13 and 33 dpi (n=3/group). IFN- β levels display a trend toward elevation at 13 and 33 dpi compared to sham-infected controls. No significant difference between groups was observed. ($p < 0.05$).....102

Figure 31: IL-12p40 treatment of C3H mice delays time to death and reduces symptomatic disease following intranasal TC83 infection. Two treatments were given to TC83 infected mice; the early treatment group received 300 ng of IL-12p40 daily from zero to four dpi and the late treatment group from five to eight dpi. (A) TC83 infected C3H mice treated early (n=3) had a MTD of 14 dpi. The late treatment (n=4) and untreated (n=2) infected mice had MTD of 10 and 9 dpi respectively. Untreated (n=3) and treated (n=2) sham infected mice survived completely. There was no significant difference in survival curves in TC83 infected mice ($p < 0.05$). (B) Infected mice treated early lost less weight than untreated or late treatment groups. (* represents comparison to PBS control, * $p < 0.05$, ** $p < 0.005$, *** $p < 0.001$, **** $p < 0.0001$).....108

Figure 32: IL-12p40 treatment of C3H mice reduces viral load in the brain following TC83 infection at eight dpi. Both early (n=3) and late (n=1) treatment groups displayed a trend toward lower viral load in the brain at 8 dpi compared to untreated, infected mice (n=2). No significant differences were observed for any group comparison ($p < 0.05$).....109

Figure 33: IL-12p40 KO mice treated early with IL-12p40 monomer display less symptomatic disease and lower viral load in the brain. Early treatment (n=3) results in more rapid recovery as measured by weight loss, but later treatment (n=3) has no effect on recovery of weight compared to untreated, infected mice (n=2). Sham infected mice treated early (n=2) maintain lower weights than untreated, sham infected mice (n=2). Viral load in the brain is reduced in mice treated early with IL-12p40 compared to mice receiving treatment later or untreated mice. This difference was not significant. ($p < 0.05$) (* represents comparison to PBS control, * $p < 0.05$, ** $p < 0.005$, *** $p < 0.001$, **** $p < 0.0001$)110

Figure 34: T-cell mediated recovery in TCR KO and IL-12p40 KO mice. IL12p40 KO mice (n=5) had a 67% survival rate following VEEV challenge. IL-12p40 KO receiving T-cells (n=10) had a 33% survival rate, but this was not significantly different. TCR KO mice had 0% survival in the absence of T-cells (n=5), but in recipient groups had a 29% survival rate, a significant difference (n=10). IL-12p40 KO mice receiving T-cells weighed more than recipient TCR KO mice and IL-12p40 KO mice that did not receive T-cells between nine and 18 dpi. (*denotes $p < 0.05$ in comparison the recipient of the same strain; ^denotes $p < 0.05$ to recipient of the different strain; `denotes $p < 0.05$ compared to the control and recipient of the different strain).....112

Chapter 1: Overview of Encephalitic Alphaviruses

While nearly 100 different agents are associated with encephalitis, the arthropod borne viruses (arboviruses) are one of the most important life-threatening causes of infection (83). With more than 20 viruses known to cause human encephalitis, arboviruses represent a significant number of emerging infectious diseases both in the United States and world-wide (83). The *Alphavirus* genus in the family *Togaviridae* contains three viruses capable of causing human encephalitis: Venezuelan equine encephalitis virus (VEEV), eastern equine encephalitis virus (EEEV), and western equine encephalitis virus (WEEV). WEEV and EEEV are endemic to the United States and South America. VEEV circulates in Central and South America; however, spread of epidemic outbreaks has resulted in disease in southern Texas in North America. No specific therapy or vaccine is currently available against these viruses. Fatality rates from arboviral encephalitis range from 1-50% depending on the strain of virus, age of the host, and immune status of the host (83; 31; 30; 32).

The presence of viable mosquito vectors in non-endemic areas of the globe makes the encephalitic alphaviruses of significant concern to public health efforts. In addition to representing a group of emerging infectious diseases, these viruses are possible agents of bioterrorism (25; 65; 174; 185). Additionally, many of the encephalitic alphaviruses are highly stable as an aerosol, cause significant mortality or incapacitating disease, and grow rapidly in easily utilized, readily available cell culture systems. This combination of factors makes this group of viruses of significant interest for biodefense in the United States (65; 173).

MEDICAL IMPORTANCE

The *Alphavirus* genus within the *Togaviridae* family was first described as the group A complex, one of the original serological groups of arboviruses characterized by serum neutralization, complement-fixation, and hemagglutination inhibition. This group of viruses now represents enveloped, plus stranded RNA viruses (137; 138). Pathogenic alphaviruses of man can be roughly grouped further by a combination of phylogenetics, geographical circulation, and disease manifestation into two groups. Viruses circulating in the Old World (Europe, Asia, and Africa) typically cause arthralgia, malaise and/or rash. Of the Old World alphaviruses, only Semliki Forest Virus (SF) is associated with naturally occurring encephalitis in man (58; 185). New World (South and North America) alphaviral infections result in a flu-like syndrome that may progress to neurological involvement. New World encephalitic alphaviruses include EEE, WEE, and VEE complex viruses. Of these the primary causes of neurological involvement and lethal encephalitis are WEE, EEE, and VEE viruses (Table 1) (185).

The Centers for Disease Control and Prevention (CDC) suggest that 10,000-20,000 cases of encephalitis are reported annually in the United States with the majority being mild (177). Other reported incidences of viral encephalitis range from less than 1 to as high as 8.8 per 100,000 person-years varying substantially with viral etiology, geographic, social, demographic factors, and reporting system (128; 32). The availability of vaccines and the involvement of a vector, as is the case of the arboviral encephalitides, influence probability and severity of encephalitis (177). Of the cases of encephalitis reported to the CDC, the incidence of arboviral encephalitis (SLE, WEE, VEE, EEE, La Crosse, and other California serogroup viruses) is typically between 150-3,000 cases/year though substantial variation results from occurrence and intensity of

Table 1: Characteristics of the New World encephalitic alphaviruses.

Characteristic	WEE		EEE		VEE	
Geographic Range	Western and Mid-western US, western Canada, South and Central America	(71, 85)	Eastern and Gulf Coast, Southern US, eastern Canada, Central America, Caribbean	(14, 15)	Southern US, South and Central America, Caribbean	(104; 103; 167; 183; 175)
Primary host	Birds	(11)	Birds	(57)	Mammals	(13; 12)
Amplification species	Finches, sparrows, equines	(11, 39, 103)	Wading birds, passerine songbirds, starlings	(21, 59, 70)	Equines	(160)
Mosquito Vector	<i>Aedes, Culex</i>	(56)	<i>Culiseta, Aedes, Mansonia</i>	(20, 45, 73, 90)	<i>Culex, Psorophora, Ochleratatus</i>	(47; 175)
Age group	Infants, children, and adults greater than 50	(11, 66)	Children, elderly	(11, 23, 26, 27, 82)	Infants, children, elderly(143)	(44; 25; 175)
Mortality %	3 to 15	(17, 18, 66)	30-70%	82)	<1%	(143)
Sequelae	Occasional	(24, 29, 58)	Frequent	(18)	In children	(111)

epidemic outbreaks. Overall mortality rates due to encephalitis are typically less than one percent, but vary widely with pathogen (128; 31; 30; 32).

Both mortality and incidence are increased in pediatric groups that are, as a result, considered high-risk for severe disease. Regardless of etiology, incidence rates of encephalitis increase dramatically in pediatric populations under the age of one to 18.4/100,000 child-years and overall incidence of 10.5/100,000 child-years in children less than 15 (102). While data specific to the arboviral encephalitides is not specifically

available, incidence rates are typically inversely correlated with age though both elderly and immune-compromised populations are also considered high-risk. Unsurprisingly, case fatality rates and severe disease are also much higher in pediatric populations (25; 121) (Table 1).

Despite the high incidence and mortality rates in pediatric populations and the unpredictable nature of arboviral epidemics, few licensed vaccines and therapies are available for specific treatment. For the New World encephalitic alphaviruses, no specific therapy is available. Disease treatment is achieved through conservative management of symptoms (11; 32). However, current treatment efforts are not always effective, and neurological sequelae of indeterminate duration are not uncommon following CNS involvement (32). In addition, prevention tools are limited and no licensed human vaccines are available for EEEV, VEEV, and WEEV.

HISTORY

Records of fatal encephalitis in horses in the northeastern United States date to the 19th centuries and reports of *peste loca* in South America exist back further though etiology of these infections is uncertain (108; 170; 60). Throughout the early 20th century, sporadic outbreaks of encephalitis in horses continued to occur along the Atlantic seaboard of the United States as well as in regions of South America. In 1930, WEEV became the first of the encephalitic alphaviruses isolated from the brain of an infected equine, and isolation of EEEV closely followed (125; 166; 165). In 1936, an outbreak of equine disease in Venezuela similar to EEE and WEE epidemics presented isolates not neutralized by either EEE or WEE antisera. VEEV was subsequently discovered as a causative pathogen of equine disease in South America (14; 105; 106). Isolation of virus from human cases of encephalitis associated with epizootic outbreaks closely followed for all three of the viruses (46; 69; 27). However, the mild, febrile nature

of the majority of cases resulted in delayed recognition of these viruses as a significant cause of disease in man until the 1950's (175; 173; 132).

The seasonally cyclic nature of outbreaks with largely summer occurrence of epidemic disease and subsequent disappearance in fall and winter months suggested the transmission by a mosquito vector, and Kelser first demonstrated transmission of WEE virus by mosquitoes (96). Recognition of the mosquito-borne nature of the other encephalitic alphaviruses closely followed (25).

TRANSMISSION CYCLES AND GEOGRAPHIC RANGE

Alphaviruses maintain circulation in enzootic and epizootic cycles via transmission between mosquito vector and vertebrate mice (Figure 1). The nature of the vertebrate host determines the maintenance of virus in epizootic or enzootic cycles. The natural vertebrate host acts as the primary source of mosquito infection in which the virus replicates, but no symptomatic disease presents. Secondary vertebrates develop symptomatic disease where the ability to transmit the virus back to mosquitoes varies based on virus strain and infected host species. For the encephalitic alphaviruses, the primary host is typically murine or avian (Table 1) (25). In epizootic or epidemic cycles, infected mosquitoes transmit the virus to a secondary host, usually man or equine. Large outbreaks of disease occur when infected secondary hosts act as amplifier of virus replication and transmission generating a high titer viremia permitting further infection of mosquito, and, subsequently, host populations. The ability of the secondary host to amplify the virus furthering epidemic spread varies based on virus and host (174; 173; 185). Epizootic outbreaks in equines frequently signal the beginning of epidemic spread of virus followed by subsequent disease in humans.

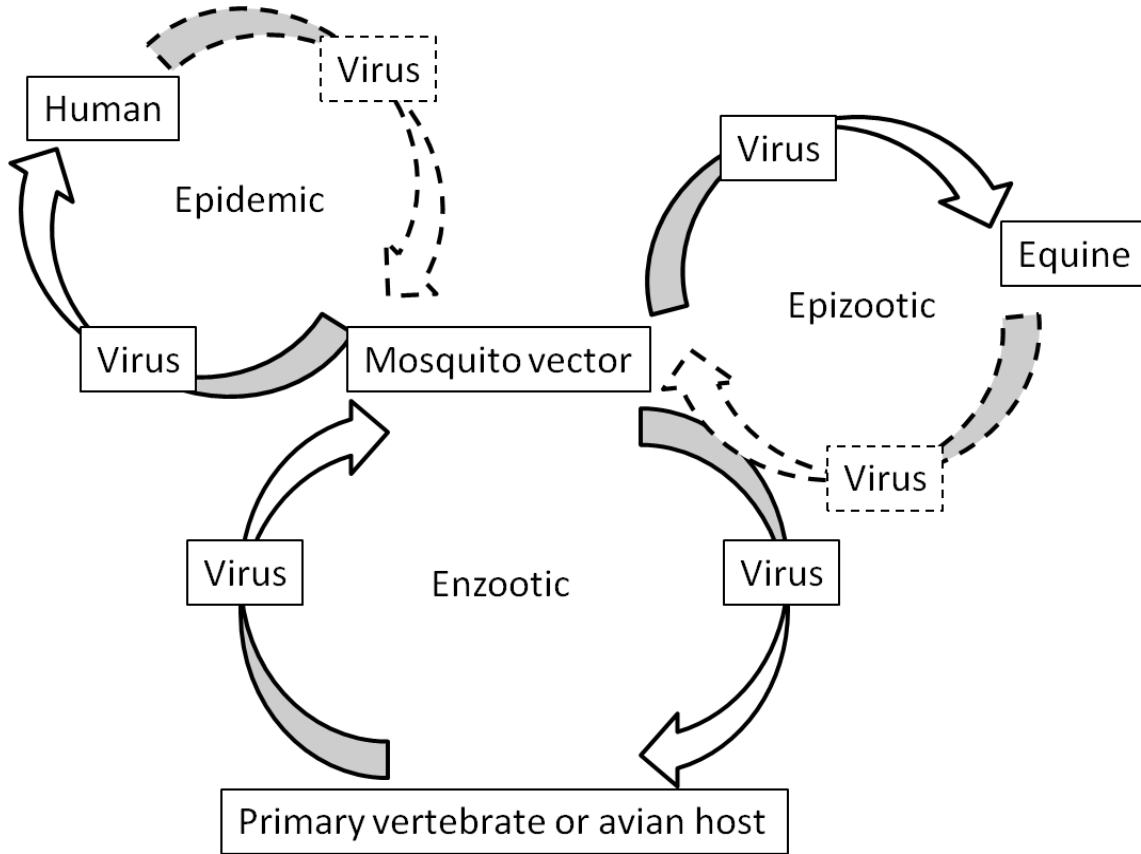


Figure 1: Transmission cycles of the New World encephalic alphaviruses. Humans and equines represent secondary hosts that are not typically involved in enzootic viral transmission cycles. However, infection of humans and equines results in epidemic or epizootic outbreaks of disease respectively. Ability of secondary hosts to transmit the virus is pathogen dependent.

EEE, WEE, and VEE viruses have been isolated from horses, humans, and other vertebrate species, namely birds. For the VEE complex viruses these include, pigeons and rodents (spiny rat, forest mouse, spiny mouse, pocket mouse, terrestrial rice rat, short tailed cane mouse) (151; 58). Additionally, VEE complex viruses have been isolated from mules and donkeys. Seropositive results by either serum neutralization or Hemagglutination inhibition identified a number of other domestic and wild species including dogs, goats, pigs, sheep, cattle, opossum, cotton mouse, cotton rat, deer mouse,

western harvest mouse, chill toothed kangaroo rat, white tailed antelope squirrel, blacktailed jackrabbit, nuttall and desert cottontail, and kit fox. Additionally, big and little brown, eastern pipistrell, and long eared bats are readily infected though the significance of these mice in transmission is uncertain (151).

Geographic limits are based on the arthropod vectors' specific ecological systems. All three of the primary New World encephalitic viruses, EEEV, WEEV, VEEV, are found in North, Central, and South America (Figure 2). However, as their name suggests, EEEV and WEEV are found along the Pacific and Atlantic seaboard respectively in the U.S (Figure 2). WEEV range extends west of the Mississippi River, and EEEV extends east. Both viruses have been found in eastern and western Canada respectively. WEEV has been isolated as far south as Argentina. Highlands J virus from the WEE complex has occasionally been associated with encephalitis in horses. EEEV isolates have also been identified from Arkansas, Minnesota, South Dakota, and Texas as well as the Caribbean islands where primarily North American variants are found. The South American variant of the EEEV occurs in parts of Central and South America particularly along the Gulf Coast. The southern isolates of WEEV and EEEV are primarily enzootic, and rarely cause human disease while the North American variants are more commonly associated with epizootic outbreaks (33) (Figure 2).

In contrast, epizootic VEEV strains (I-AB and I-C) are found in South and Central America with most epidemics occurring in northern and western South America. However, outbreaks of disease have spread into adjacent countries including the southern U.S. and Mexico as seen in the 1969 outbreak that began in Ecuador and spread northward reaching Texas in 1971 (175; 33). Enzootic strains of VEE are found in Mexico and parts of the U.S. as well as South and Central America. Three reports of Everglades virus (EVE) with encephalitis in man exists (26). EVE is a subtype II VEE

complex virus. The most closely related strains to EVE are enzootic, subtype I D strains. Subtype ID strains are progenitors of subtype IAB and IC strains responsible for major epidemics and epizootics (177). Old World alphaviruses Semliki Forest virus (SFV) and Ross River virus are rarely associated with encephalitis in man (178; 92; 116; 150; 132) (Figure 2). Thus, the nature of encephalitic virus' transmission cycles restricts geographic range resulting in distinct regions of circulating enzootic and epizootic strains.

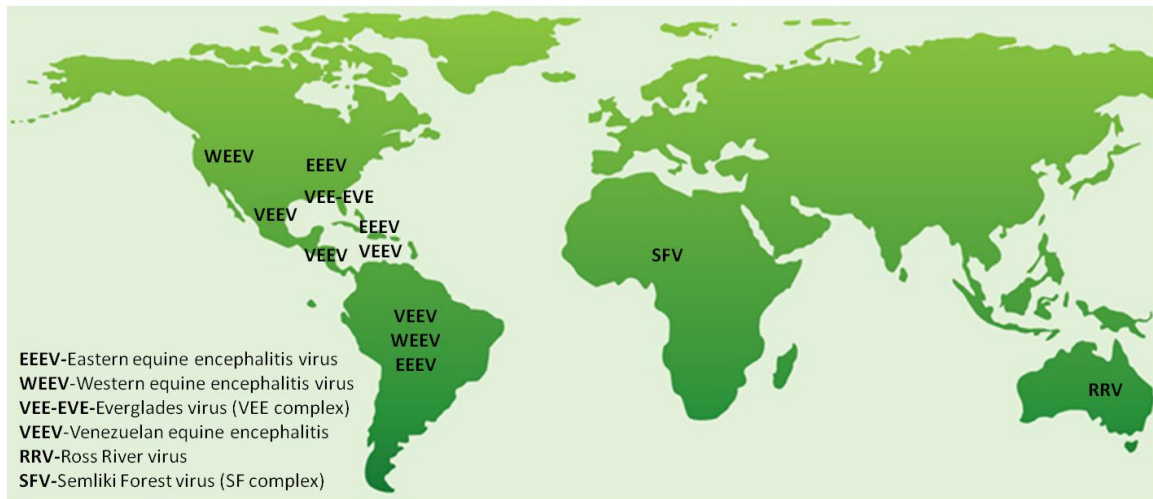


Figure 2: Geographic distribution of alphaviruses capable of causing encephalitis.

MOLECULAR BIOLOGY OF THE ALPHAVIRUS GENUS

The virions of the encephalitic alphaviruses contain an icosohedral nucleocapsid made of 240 copies of the capsid protein and a single-stranded, positive-sense RNA genome surrounded by a lipid envelope derived from the plasma membrane of infected cells. The genomic RNA is composed of 5' region encoding non structural proteins (NsP) and 3' region encoding structural proteins resulting in a length of approximately 12 kilobases. The first two-thirds of the genome encode non-structural proteins NsP1, NsP2, NsP3 and NsP4 that are involved primarily in viral genome replication and polyprotein

processing (48; 58). After viral entry into the cytoplasm of cells, a nonstructural polyprotein is translated and utilized in the production of full-length negative-sense RNA. The negative-sense RNA is then utilized as a template for the generation of genomic RNA as well as a subgenomic mRNA (26S) identical to the 3' one-third of the genome. The structural proteins are encoded in the 3' third of the genome and translated from the 26S subgenomic promoter resulting in production of the five protein products, the capsid (C), and envelope proteins 1-3 (E1-E3) and 6K (148; 58). E1/E2 glycoprotein heterodimers are embedded in the lipid envelope and are considered the primary targets for adaptive, antigen specific immunity, both humoral and cell-mediated (134; 148). The structural proteins are also capable of interfering with host defense mechanisms (1; 153). Specifically, greater virulence is associated with alterations in the genome conferring resistance to early anti-viral innate immune response,

Changes in the viral genome and subsequent virulence level are associated with phylogenetic and geographic divergence. Closely related strains of arboviruses can differ significantly in their ability to cause human disease. Geographically restricted strains of EEE endemic to North America cause fatal human and equine cases whereas EEE strains endemic in South America are not associated with diagnosed illness in either humans or equines (155; 117; 50). North American strains of WEE are also associated with epidemic disease whereas South American strains are solely epizootic (18). In contrast, VEE epidemic and epizootic strains are found in South America, though epidemic outbreaks have resulted in spread of disease to North America (175). Studies of virulence for all WEE and EEE strains demonstrated differential host responses corresponding to epidemiologic traits of individual strains; epizootic strains associate with neurovirulence and neuroinvasion and enzootic strains typically causing neither in

experimental models (18; 155; 117; 50). However, enzootic VEEV (ZPC738) displays no difference in neurovirulence in rodents or humans (131).

VIRUS SPREAD

Due to nature of infection and prevalence of asymptomatic infections, much of what is known about virus spread has been determined utilizing experimental animal models. As the mosquito feeds on the experimental host, virus is deposited extravascularly with infected saliva (168). For VEEV infection, virus is first observed in the draining lymph node (DLN), but replication at site of inoculation rapidly follows (8). VEEV targets dendritic cells (DC), particularly Langerhan's cells, and lymphocytes resulting in the rapid viral spread to the DLN through migration of these cell populations. Langerhan's cells are specialized DC of the skin. Infection of the DC and lymphocytes fuels a high titer serum viremia (49, 25). Blood and lymph borne virus then seeds tissues beyond the inoculation site. These include other lymphoid and reticuloendothelial tissues such as LN, spleen, thymus, Peyer's patches, and pancreas and skeletal muscle (49) (59; 113; 127; 84). As the viral replication and viremia continues, spread occurs to secondary sites of replication which include the brain and spinal cord neurons (58). Historically, the overall magnitude and duration of viremia was thought to influence the neuroinvasive ability of the virus. While tropism for other cells of the CNS apart from neurons is uncertain, alphaviruses may replicate in the meningeal cells, ependymal cells, and other glial cell populations such as astrocytes and microglia (Figure 3) (126; 149; 43).

PATHOGENIC SEQUENCE OF ALPHAVIRAL INFECTION IN HUMANS

Encephalitis refers to inflammation of the brain (83). In the context of the arboviral encephalitides, encephalitis is typically a complication of systemic infection and results in acute infection of the brain with focal or diffuse inflammation of the brain

parenchyma (11). Neurovirulence of the New World encephalitic alphaviruses associates with efficient and rapid spread of virus throughout the cells of the central nervous system (CNS), particularly neuronal cells, resulting in pathogenesis. Independently of viral spread and replication, disease development also depends on the host response (58; 145).

Disease symptoms in patients mimic the experimentally derived biphasic nature of both the immune response and viral replication. In patients, as the initial innate immune response and viral propagation exponentially grow, a fever develops associated with a mild, flu-like illness. The fever temporarily abates, but patients develop a secondary fever that signals the blood and lymph spread of virus to target tissues. During this phase clinical encephalitis may develop (25). This phase also signals initiation of the adaptive, antigen specific immune response (Figure 3).

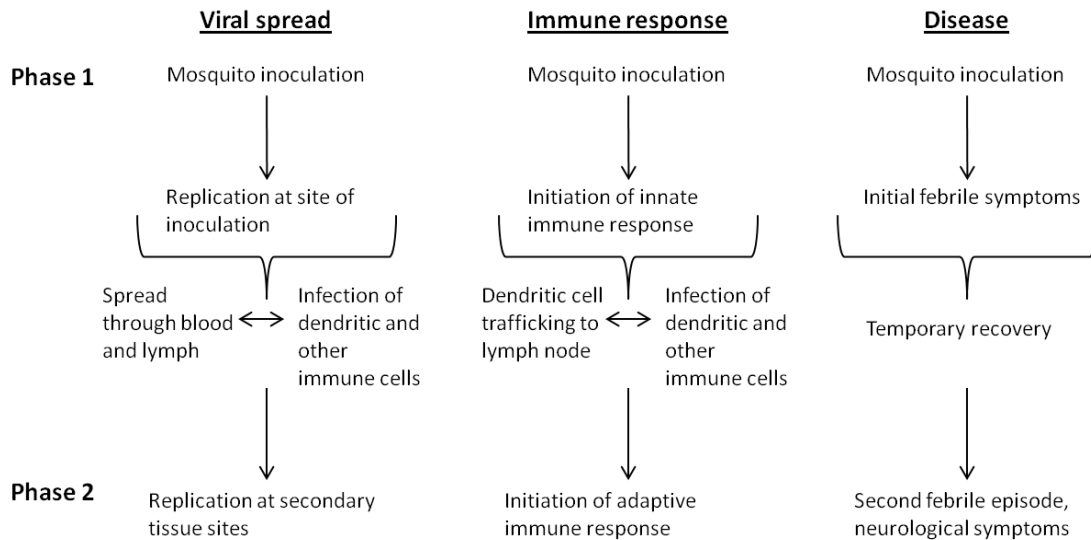


Figure 3: Biphasic nature of alphavirus infection in viral spread, immune response, and disease.

Following neurological complications, mortality typically results from cerebral edema or vasomotor instability (121). Typical lesions in fatal cases appear as severe inflammation of the gray matter with neuronal degeneration, infiltration of inflammatory

cells, gliosis, perivascular cuffing and hemorrhages (58). In the event of recovery following development of neuropathology, neurological morbidity often occurs ranging from personality changes, mental retardation, spasticity, to chronic ataxia. Focal deficits typically resolve over a period of months with initial recovery taking days to weeks. Severity of sequelae is loosely associated with incidence of coma and seizures (121). However, despite the close phylogenetic relationship the three New World encephalitic alphaviruses share, mortality, severity of sequelae, duration of acute and secondary disease, and location/pattern of brain lesions vary substantially between these pathogens (174; 118; 159).

CONCLUSION

The encephalitic alphaviruses represent a significant group of emerging infectious diseases causing incapacitating, flu-like illness with occasional mortality associated with neurological symptoms. This group of viruses is of significant interest to biodefense efforts in the U.S. However, no specific vaccines or therapeutics are available to prevent or treat disease in humans.

The three viruses are phylogenetically closely related and the E1 and E2 glycoproteins of each are the primary targets of the host adaptive immune response. Despite phylogenetic relationship, the viruses vary significantly in geographic range due to differences in mosquito vectors and primary host mice. In addition, mosquito vectors, vertebrate hosts, mortality rates, severity of sequelae, and duration of each phase of disease vary by pathogen. Secondary hosts that develop significant disease include humans and equines for all three viruses. Equines amplify WEEV and VEEV sufficiently to transmit back to mosquito populations intensifying epidemic outbreaks (Table 1). Viral spread in secondary hosts is similar between the three viruses: initial replication at site of inoculation, viral spread via blood and lymph, and seeding of secondary sites of

replication such as neurons. The biphasic febrile disease is congruent with the replication and spread of virus as well as initiation of the innate and subsequently adaptive host response (Figure 3).

In some experimental models, neuroinvasion and viral replication in the CNS occurs in the absence of significant clinical symptoms or mortality (133; 184). Neuroinvasion, neurotropism, age, and the acute (innate) and secondary (adaptive) individual host response all influence severity of disease and outcome following CNS invasion. As detailed in the next chapter, understanding differences in the host response and susceptibility to infection is key in determining effective therapeutic and prophylactic approaches to mitigate pathogenesis. However, little is currently known about the specific host response to alphavirus encephalitis and the influence of individual variability on outcome.

Chapter 2: Host Response to Alphaviral Infection

Neurovirulent viruses alter the highly sensitive microenvironment and critical functioning of the central nervous system (CNS). Initial viral replication, viremia, neuroinvasiveness and neurotropism combined lead to neurovirulence. For the encephalitic alphaviruses, virulence reflects severity of neurological disease. The molecular character of the virus as well as the host immune response influences each individual component of virulence (58).

Indicative of the importance of host control at the site of initial replication, intracerebral or intranasal inoculation of some alphaviruses causes fatal disease in experimental models while subcutaneous or intraperitoneal infection results in a clinical syndrome without lethality or severe neuropathology (58). Viremia duration and magnitude may partly determine invasion of the CNS, but successful neurotropic qualities determine the extent of viral damage to the CNS. The mechanisms the immune-competent host uses to prevent neuroinvasion are uncertain. Viral invasion without associated symptomatic illness has been reported in experimental models for alphavirus encephalitis (184). In the majority of infected individuals, the host response appears to be sufficient to prevent CNS damage, and most cases remain asymptomatic. In WEE epidemics, only 1/1000 infected individuals actually develop clinical encephalitis with only 3% of these cases resulting in fatality (Table 1) (141). Similar statistics are observed for VEEV and EEEV though mortality in EEEV infections is significantly higher (25). Case fatality rates for EEEV average 35% while VEEV rates average less than 1%, but can be as high as 15% in pediatric populations (25,153, 177). However, severity of disease manifestations and mortality with all of these viruses is much higher in pediatric populations, and the cause of age related susceptibility remains poorly defined. This is

reflected in experimental situations where variability in age or strain of mouse results in a range of disease (117). Thus, viruses that are apparently intrinsically of low virulence cause severe disease in some patients, and the specific host factors accounting for occasional neuropathology are unknown (23; 33; 185).

Neurovirulence is a combination of a faulty, ineffective or pathogenic host response, and the virus' ability to avoid host defense mechanisms and successfully replicate. Drug and vaccine development relies on modifying virus-host interactions. Thus, understanding this relationship produces effective therapies. (67). This chapter introduces current literature on neurovirulence of alphaviral infections with a focus on the innate and adaptive host response. An emphasis is placed on VEEV, particularly the vaccine strain TC83, as this is the focus of the remainder of this publication. In addition to studying the a vaccine strain of VEEV, utilizing TC83 extended time to death in mice, permitted work in the BSL2, and removed select agent restrictions.

TC83

The attenuated vaccine strain of VEEV, TC83, was developed by serial passage of VEEV IA/B Trinidad donkey (TrD) strain in guinea pig heart cells. The investigational new drug status (IND) of the vaccine strain permits vaccination of at risk laboratory and military personnel. However, vaccinees receiving TC83 display high rates of adverse events and poor rates of seroconversion (42; 28; 136; 132). TC83-derived viruses that kill hamsters and mice were isolated from the throats of human vaccinees and from hamsters after a single passage of the vaccine. (81; 82). Combined, these data indicate TC83 is poorly immunogenic and presents significant safety concerns.

The virus was originally derived by 83 serial passages in guinea pig heart cells (16). The strain contains 12 nucleotide mutations (98; 97). No alterations were found in the open reading frame coding the viral polyprotein or in the nonstructural proteins. Six

of nine dominant mutations found in the RNAs from plaque purified virus appeared in the E2 surface glycoprotein. E2 contains all five of the nucleotide changes producing non-conservative amino acid substitutions (82). In contrast, only two mutations in E1 were found; one silent and one that did not alter the protein character. An additional nucleotide difference was found in the non-coding region preceding the 5' end of the 26S mRNA (5'UTR) (82; 98; 97).

Unsurprisingly, the attenuated phenotype of TC83 results from the changes in E2 glycoprotein and the 5' UTR. E2-120 is a major structural determinant of attenuation, but genome nucleotide position 3 in the 5' UTR is also significant to the attenuated phenotype (97). E2 mutations increase glycoprotein binding to heparan sulfate *in vitro*. The other mutation occurs in the 5' UTR and increases viral sensitivity to type I interferon (IFN), an antiviral cytokine (97; 17; 176; 91). The attenuating mutation in the E2 protein increases viral replication *in vitro* (98, 99). In contrast, more rapid peripheral clearance occurs *in vivo* likely due to more efficient removal by the reticuloendothelial system and the increased type I IFN sensitivity conferred by the 5' UTR mutation (156; 79; 39).

In mice, TC83 virulence depends on age and strain of mouse utilized. The virus is highly lethal in new born mice following subcutaneous (s.c.) or intracerebral (i.c.) inoculation, but avirulent when given by s.c. routes of inoculation in adult mice of various genetic backgrounds (41; 131; 159).

Efficacy studies of TC83 vaccination in animal models.

Vaccination efficacy for TC83 varies between C57BL/6 (BL6), BALB/c, and C3H/HeN inbred mouse strains, and survival rates depend on vaccination and challenge route. Subcutaneous (s.c.), intraperitoneal (i.p.), and intradermal (i.d.) vaccination prior to s.c. challenge results in 100% survival in BL6 and BALB/c mice (85). C3H mice

respond in a similar manner with 100% survival following s.c vaccination and s.c. challenge (Table 2) (64; 63). However, survival rates of s.c. vaccinated C3H mice dropped to 20-33% with more rigorous aerosol challenge route (Table 2) (64). Vaccination with attenuated strain V3526 also failed to completely protect C3H mice and only 60% survived infection (63). V3526 is a live-attenuated virus derived by site-directed mutagenesis from a virulent clone of the VEEV-TrD strain. V3526 was intended for use as a vaccine candidate in humans (63). 100% of BALB/c mice survived in the same scenario with both

Table 2: Efficacy of TC83 vaccination in inbred mouse strains.

Strain	Vaccination	Challenge	Percent survival	Age/sex	Reference
BALB/c	ip, sc, id	sc	100%	NA/female	(85)
	sc	aerosol	100%		(63)
	aerosol	sc	100%	4-6 weeks/ female	(63)
	aerosol	aerosol	95%		(63)
C57BL/6	ip, sc, id	sc	100%	NA/female	(85)
C3H/HeN	sc	sc	100%	4-6 weeks/ female	(64; 63)
	sc	aerosol	20-33%	4-8 weeks/female	(38)
	aerosol	aerosol	50%*		(63)
	aerosol	sc	ND [^]	4-6 week s/ female	(63)
CBA/Ca	ip, sc, id	sc	100%	NA/female	(85)
C.C3	sc	aerosol	100%	4-8 weeks/female	(38)

*NA-not available

vaccines, but aerosol TC83 vaccination and aerosol challenge in BALB/c mice decreased survival to 95% (63). The low survival rates in C3H mice indicate an inability to develop

a protective immune response following vaccination, but reasons for lower survival is unknown.

TC83 virulence and pathogenesis in mouse models

Level of virulence in naïve mice also varies by genetic background of the host and route of infection. Again, C3H mice are more susceptible than BALB/c or C57BL/6 strains to infection with TC83 (Table 3). Survival rates in C3H mice range from 0-10% following intracerebral (i.c.), aerosol, or intranasal (i.n.) infections. In contrast, 100% of BALB/c mice survive (157; 117; 89). However, BALB/c mice display symptomatic disease to 14 dpi and display aggressive behavior after i.c. infection (117). 100% of BL6 mice survive i.n. infection (89). Thus, by a variety of routes of infection and under multiple vaccination conditions, C3H mice are more susceptible to TC83 infection than BALB/c or BL6 strains.

Table 3: Survival following TC83 infection in inbred mouse strains.

Mouse strain	Route	Percent survival	Age/Sex	Reference
BALB/c	aerosol	100%	6-8 weeks/female	(157)
	i.c.	100%*	6-8 weeks/NA	(117)
C57BL/6	i.n.	100%	NA/female	(89)
C3H/HeN	aerosol	0%	6-8 weeks/female	(157)
	i.c.	0%	6-8 weeks/NA	(117)
	i.n.	0-10%	NA/female	(89)

*NA-not available

Viral spread and inflammation in BALB/c and C3H mice is similar at early time points following TC83 aerosol infection. In one study, viral antigen levels and dissemination in the brain were similar between strains from two dpi to five dpi (159). After five dpi, an increase in TC83 antigen was noted in C3H mice compared to BALB/c.

All C3H mice maintained levels of viral antigen in the brain similar to five dpi to 10 dpi. In contrast, viral antigen was absent in all but one BALB/c animal at 10 dpi (157). Severity of brain lesions was not different early in infection, but at 10 dpi, C3H mice had more severe brain lesions compared to BALB/c. In addition, more brain lesions were present in caudal regions of C3H mice compared to BALB/c.

Aerosol infection with VEEV-TrD caused less discernible differences in disease phenotype between C3H and BALB/c than similar infection with TC83. However, Steele, et al. noted C3H mice displayed milder inflammatory infiltrates than BALB/c at five dpi but a trend toward more severe lesions. The authors' attributed the severity of lesions in C3H mice following both VEEV-TrD and TC83 infection to an impaired ability to mount an effective cellular immune response (157). Thus, studies of VEEV and TC83 virulence in C3H mice indicate an impaired host response.

TC83 presents a definitively more severe disease phenotype in C3H mice compared to BALB/c. The increased disease in C3H mice may be due to a defective immune response. However, the precise reasons for the enhanced virulence in C3H mice are unknown.

Intranasal TC83 infection of C3H mice is representative of VEEV encephalitis

TC83 encephalitis in C3H mice accurately mimics VEEV-encephalitis though less caudal spread of TC83 occurs in the brain in comparison to VEEV-TrD infection of C3H mice (157). TC83-infected C3H mice have been used as a model for anti-viral evaluation; however, key differences in the response of different inbred strains of mice may affect the utility of C3H mice for this purpose (87; 89). The similarities in TC83 and VEEV infection make intranasal infection with TC83 in C3H mice a useful model of VEEV-like encephalitis. While virulent forms of VEEV represent natural isolates, the rapid death of the murine host limits studies of the correlates of protective immunity to

primary infection. In addition, the virulent strains of VEEV must be used at the ABSL3/BSL3 level and require handling as a select agent. In contrast, TC83 infection results in a longer disease course in mice, and can be utilized at the ABLS2/BSL2 level enhancing the repertoire of research tools available. Furthermore, TC83 infection allows comparison to resistant mouse strains. This may aid in deriving the host factors contributing to susceptibility in naïve individuals.

C3H susceptibility is not linked to MHC, but may result from changes to the immune response.

Different genetic backgrounds in inbred mouse strains result in changes in mortality and immune response in other infectious disease models. Haplotypes vary by genetic background: C3H mice have H2^k; BL6 have H2^b; and BALB/c have H2^d. The dichotomy in the T-cell response between BALB/c and C57BL6 mice is one of the more commonly recognized haplotype-specific differences in the immune response (70; 66). This useful phenotype resulted in novel discoveries for *Mycobacterium tuberculosis* and some parasitic diseases to name a few (70; 135; 169; 66).

However, susceptibility in C3H mice to TC83 is not linked to the H2^k haplotype. BALB/c mice with an H2^k background (C.C3-H2^k) completely survive aerosol infection with VEEV following TC83 vaccination. In contrast, only 33% of wild-type C3H mice survive (64). Thus, susceptibility in C3H mice appears to be independent of MHC, but the basis for mortality may be linked to other alterations in immune functioning.

The decreased immunogenicity of both TC83 and V3526 strains in C3H mice may be linked to differences in processing and presentation of antigen by dendritic cells (DC). For example, more pronounced thymic hypocellularity results in BL6 mice compared to C3H following *cis*-urocoanic acid exposure. The authors' postulated alterations in DC processing and presentation as a cause (139). A like effect may explain

the differences in disease following VEEV infection of inbred strains. Additionally, changes in dendritic cell reactivity and expression of toll-like receptors (TLR) between C57BL/6 and BALB/c mice mark differential outcome to bacterial infection(114). Thus, decreased TC83 vaccine efficacy in C3H mice may be linked to changes in antigen processing and presentation.

Differences in mucosal IgA might also explain the differences in mortality seen in C3H mice. The Mouse Phenome Database indicated that 9-12 week female C3H mice have significantly lower levels of IgA than BL6 mice. C3H mice displayed lower levels of IgA in vaginal and bronchial washes following TC83 vaccination, but both BALB/c and C3H mice developed similar high titer virus neutralizing antibody in the serum. Thus, the significance of IgA level is uncertain especially since virus invades the brains of both mouse strains and distribution of viral antigen in the brain remains similar to five dpi (64; 157).

In *Mycobacterium tuberculosis* (*M. tb*) infection, the MHC locus partly determines the host's susceptibility by affecting the antigen specific CD4⁺ T-cell response. BL6 mice are more resistant to *M. tb* infection, and their CD4⁺ T-cells demonstrate more robust IFN- γ production after *in vitro* stimulation compared to C3H mice. However, C3H mice with an H2^b background (C3.Sw-H2b/SnJ) and wild-type C3H were equally susceptible (90). Thus, T-cell recognition of *M. tb* antigen is haplotype specific, but susceptibility depends on MHC-independent factors unique to each strain.

In the case of group A streptococcus (GAS) infections, vaccination overcomes the innate genetic susceptibility of C3H mice and results in a resistant phenotype similar to BALB/c mice. Protection in C3H depended on T-cell dependent antibody production and may relate to antigen specificity required for protection. In contrast, following TC83

infection, C3H and BALB/c display similar serum antibody kinetic, and vaccination does not prevent C3H mortality (152).

Immune mediated contact hypersensitivity reactions vary with the genetic background of the mouse. H2^k mice failed to respond to the dicyclohexylcarbodiimide (DCC) stimulus while both H2^b and H2^d mice developed a reaction (95). This indicated a specific unresponsiveness to DCC dependent reactions in H2^k mice, and corroborates the depressed cellular immune response seen in C3H mice following TC83 infection (157). Given the essential nature of the immune response to the development of DCC hypersensitivity, the failure of H2^k mice to respond indicates variability in the haplotype specific response to a given antigen (95).

Inflammatory response cytokines are affected based on haplotype. For instance, BALB/c mice with an H2^k background (BALB/k) demonstrated lower levels of IFN- γ , IL-5 and IL-2 in the lymph node compared to wild type BALB/c mice (H2^d) in response to hapten trinitrophenyl immunization (40). However, levels of IL-3, IL-4, and TNF- α were equivalent. Interestingly, the difference in haplotype also resulted in a more robust production of antibody and higher levels of IgG2a, IgG2b, and IgG3. Indicating other causes of mortality in C3H mice in VEEV models VEEV infection resulted in equivalent antibody profiles between BALB/c and C3H mice (40; 64; 157; 63).

GAS infection of C3H (H2^k) and BALB/c (H2^d) demonstrated that C3H mice had a greater inflammatory response, but ultimately failed to control the bacterial response (55). Particularly, C3H mice had elevated levels of IFN- γ , IL-1a, IFN- α , and nitric oxide in the spleen. Splenic cells of C3H mice were more responsive to stimulation with lymphotoxin- α and produced more IFN- γ , but lipopolysaccharide stimulation resulted in equivalent levels of IFN- γ production between strains. The host response to GAS in C3H indicated a genetic predisposition to produce elevated levels of inflammatory mediators.

Thus, antigen specificity determines the range of responsiveness in different haplotypes (55; 56).

In summary, C3H mice differ in key immune compartments from BL6 or BALB/c. Immune response variability is pathogen specific, and both B- and T- cellular immunity as well as cytokine production may be impacted. Thus, comparison of TC83-susceptible C3H mice to resistant BL6 could enhance understanding of immune mechanisms key in resolution of infection.

CNS ENTRY

The balance of host and viral characteristics determines outcome to infection, and minor changes in either drastically impact disease pathogenesis. However, without entry to the CNS, neurovirulence would not occur. Neuroinvasion results as viral replication begins in secondary target organs after initial replication and development of viremia (58).

However, high level viremia may not always correlate with neuropathogenesis. For instance, both virulent and attenuated strains of VEEV reach equivalent maximum concentration levels in target organs, display similar onset of neuroinvasion, and replicate growth rates despite differences in viremia in hamsters (10; 44). In addition, immunocompromised nude mice develop similar viral loads in the brain and serum compared to normal mice, but die more rapidly following infection with virulent VEEV (109).

In vivo VEEV studies support a model where virus enters the brain via infection of the olfactory epithelium regardless of route of infection (35; 157; 147; 146). Passive axonal transport may also permit entry to the brain, but infection of dental structures did not contribute to neuroinvasion (157). Thus, infection of the olfactory epithelium leads to initial neuroinvasion.

Other studies clarified mechanism of viral dissemination in the brain. Infection with VEE viral replicon particles (VRP) permitted exploration of the early mechanisms of neuroinvasion. VRP are unable to replicate beyond the first infected cell (147; 146). VRP infections demonstrated that blood brain barrier (BBB) alterations played a critical role in neurovirulence. These pathogenic BBB changes resulted from induction of the host immune response. Direct i.c. infection of VRP resulted in VEE-like encephalitis in mice and was associated with a robust, rapid immune response that compromised BBB integrity (147). Initial replication of i.c. administered VRP induced the opening of the BBB allowing a second peripheral dose of VRP to enter the brain (147; 146). When the initial opening of the BBB was inhibited by administration of MMP-9 inhibitor GM6001 (Ilomostat), a delay resulted in neuroinvasion and pathogenesis (146). Another study utilized the toxin tunicamycin to damage the ultrastructure of the BBB prior to VEEV infection. Despite the tunicamycin induced BBB damage, entry to the CNS still occurred via the olfactory system, but higher viral loads in the brain resulted in tunicamycin treated mice compared to untreated controls. Viral entry and brain viral load were similar between virulent and attenuated strains of VEEV following- tunicamycin treatment. (158).

The host inflammatory response damage to the vascular integrity of BBB enabled further entry of the virus to the compromised CNS (147; 146). The multifocal nature of the infection in the brain by five or six days post-infection indicated damage to the BBB and the free crossing of viral particles across the typically sealed barrier (186; 76; 34; 171; 144). Damage to the vascular integrity of the BBB as a result of inflammation has additional support from a range of studies examining viral entry to the CNS (37; 115; 172). Thus, CNS entry through the olfactory pathways initiated viral replication in the brain, induced a pro-inflammatory host response, damaged the BBB, and allowed for a

secondary wave of virus to enter the brain from the periphery. Work in experimental models can be extrapolated to reflect human infections, but the ability, and means, the virus utilizes to cross the BBB and enter the CNS in humans remains uncertain.

In contrast to a pathogenic effect, some components of the host response delay neuroinvasion. This is highlighted in genetically deficient mice where neuroinvasion occurs more rapidly, pathogenesis is more severe, and higher levels of mortality or earlier onset of death occurs. For instance, complement component 3 (C3) deficient mice developed more severe disease with more rapid neuroinvasion following peripheral inoculation with an attenuated VEEV mutant than control mice. Direct inoculation of the brain resulted in similar disease development indicating C3 components role in immunoprotection was in the periphery. The authors postulated that complement dependent mechanisms supported peripheral viral clearance and delayed neuroinvasion (22). However, a direct effect of C3 on the BBB was not addressed. Regardless of location or mode of action, the host response is a significant component of neuroinvasion.

Thus, initial infection of the olfactory epithelium leads to infection of the CNS; a robust proinflammatory host-response induces alterations in the BBB enhancing permeability; and a secondary influx of virus to the brain occurs. Other immune components delay viral entry to the CNS and mitigate pathogenesis, but more research is essential to understanding the specific pathogenic and protective mechanisms of action the immune system utilizes in preventing neuroinvasion.

IMMUNE RESPONSE

Viral replication at the site of inoculation, level of viremia, and subsequent spread to secondary sites are controlled by viral clearance following initiation of the host response. Given the close relation and ability of the innate immune response to modulate the later adaptive immune response needed to effectively clear virus, an early, robust,

properly directed innate immune response is essential. In the biphasic model of alphavirus infection as the primary phase of viral replication is initiated, the host begins responding to the pathogenic changes at the site of inoculation by inducing robust production of cytokines, particularly interferon (IFN), an anti-viral cytokine (58). Cytokine production also results in recruitment of other early immune effectors, such as natural killer cells (NK), capable of generating positive feedback. These factors produce an early anti-

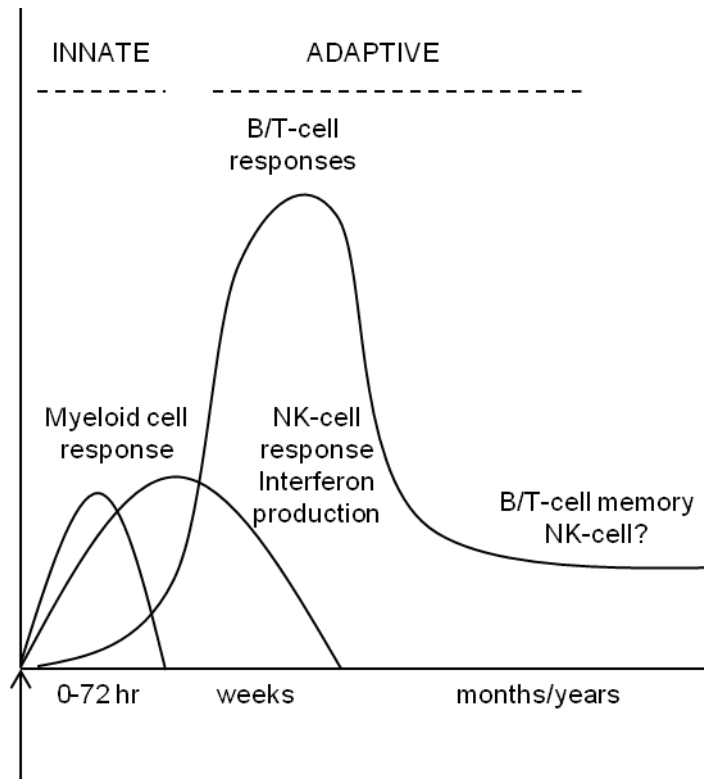


Figure 4:: Schematic diagram of the immune response to viral infection. The innate response is characterized by myeloid cell production of cytokines concurrent with dendritic cell migration and presentation of antigen in the lymph node. The NK-cell and interferon response are initiated early in infection, but wane as the adaptive immune response develops though some evidence exists for a NK-cell memory function. Adapted from: (58; 161)

viral environment in the host. However, the concurrent infection of immune cells serves to propagate the virus. Infiltration of antigen presenting cells to the nearest lymph node introducing antigen to naïve B and T-cells in the lymph nodes initiates the adaptive immune response. The adaptive immune response produces antigen-specific T and B cells. B-cells produce pathogen specific antibody. T-cells provide support to B-cell

populations and may have direct and indirect antiviral effect. Given the primary tropism of the encephalitic alphaviruses for dendritic cells, alterations in antigen presentation and subsequent modification of an efficient adaptive immune response may occur given the natural tropism of the alphavirus for immune cell populations; however, little work has been done to determine the effect of such tropism in these infections. These early responses are also required to limit peripheral replication, viremia, and spread to secondary sites of infection prior to the development of an effective adaptive immune response.

The importance of the host immune response is best illustrated by the effect of infection in its absence. Immunocompetent mice infected with VEEV developed a typical biphasic illness with an early lymphoid phase characterized by ruffling of fur and progression to hunching and later fatal CNS phase characterized by progression from ataxia to severe paralysis. In the lymphoid phase, peripheral serum viremia and replication in organs is resolved concurrent with production of IgM at 3 dpi as well as with rapid, robust production of type I IFN by 18-24 h post-infection. IgM production steadily increased till time of death; Type I IFN production began to wane after one dpi. However, mice still developed fulminant encephalitis and mean time to death was 7.8 days (34).

In contrast, severely immunocompromised SCID mice fail to develop early signs of disease and symptoms develop at 6-7 days post-infection marked by aggression and agitation with death occurring at 8-9 days post-infection. Mice fail to develop hallmark hind-limb paralysis, become less responsive and ataxic of the neurological disease in the immunocompromised host. Organ tropism differed in these mice with viral replication at or near peak titer appearing in peripheral organs until death of the animal. Unsurprisingly, patterns of antibody and type I IFN production differ from those of the

immunocompetent host. SCID mice display no neutralizing antibody production and lower levels of IFN that rise slowly and were below the limit of detection by two dpi. However, time of death is delayed in SCID mice with an average survival time of 8.9 days (34). Pathologies in the brain present as severe spongiform encephalopathy different from that of the immune competent hosts fulminate encephalitis indicative of a significant immunologic component to CNS pathology. Thus, the establishment of a functional host response in the periphery requires a competent immune system, but is unable to prevent death.

Longer time to death in SCID mice indicates a component of pathology to the immune response that may be necessary to host preservation; the protective/pathogenic dichotomy of the host response is found in a variety of disease etiologies. The changes in peripheral cellular tropism occur more rapidly than can be explained by the adaptive response. Failure to establish an anti-viral state in SCID mice likely involves the innate nonspecific response to viral pathogens, particularly the suppressed type I IFN in SCID mice (34).

Despite the importance of the earliest immune responses in preventing disease and modulating the later adaptive response, little is known regarding the specific innate mechanisms of host defense apart from an anti-viral role for type I IFN. Unfortunately, little is known about the specific mechanisms of host defense apart from an early, anti-viral role for type I IFN and a correlation of neutralizing antibody production with peripheral viral clearance. Given the importance of early intervention, a better understanding of the mechanisms of host defense during the earliest phases is crucial. In particular the role for the potent, innate immune effector natural killer cell populations has not been explored. This gap in the knowledge translates to less effective treatment of disease.

INNATE IMMUNE RESPONSE

The earliest response to infection, the innate immune response, begins at the initial site of viral replication. This phase represents a generalized response to infection and is not antigen-specific. Cytokine and chemokine secretion is initiated, and these factors recruit initial immune effector cell populations to the site of infection. These include macrophages and neutrophils. In addition, natural killer cell activation and recruitment occurs. In the microenvironment of the CNS, the strong, pro-inflammatory response that characterizes initial seeding and viral replication can cause significant damage. In addition, the innate immune response molds the later antigen-specific adaptive immune response. Thus, the innate response initially controls infection, attempts to mitigate further pathogenesis, and initiates the adaptive immune response, but may cause damage to the host (57).

Type I Interferon

Despite the importance of this initial phase of infection, little is known about the earliest protective mechanisms modulating alphavirus infection. However, all three encephalitic alphaviruses are highly susceptible to the effects of type I IFN (IFN- α and IFN- β) and, as such, resistance to type I IFN signaling and production associates with increased neurovirulence (7; 86; 80; 88; 1). Type I IFN includes IFN- α and IFN- β . Type II interferon includes IFN- γ . Most cytokines have pleiotropic roles. In other CNS disorders of non-viral etiology, type I IFN mitigates neuropathology through multiple mechanisms, but other such modes of action in the CNS have not been explored in alphaviral infections. The effects of Type I IFN depend on both the viral genome and the host response that varies with age, species, and route of inoculation.

Viral genome and type I interferon

Closely related virulent and avirulent alphaviruses demonstrate differences in ability to induce and respond to type I IFN (1, 2, 6, 8, 178). Attenuated EEEV, VEEV and WEEV strains are sensitive to type I IFN (8; 176; 6; 2). For instance, mouse attenuated EEEV strains and virulent EEEV strains differ in ability to induce IFN- α/β in lymphoid tissue with more virulent strains inducing higher levels of type I IFN. The more virulent strain caused greater disease in IFN $\alpha\beta$ deficient mice as well (1). Alterations in the type I IFN response partially explains the range of disease seen between viral strains.

Evasion and interference with the type I IFN response correlates with virulence. Interference with host gene transcription enables more virulent viruses to evade the anti-viral type I IFN response. Conversely, viral attenuation associates with an inability to regulate host gene transcription. Comparison of IFN-sensitive, avirulent strains and IFN-resistant virulent strains led to comprehensive knowledge of the genes responsible for controlling IFN resistances. For instance, priming neurons with type I IFN demonstrates VEEV's resistance to an established antiviral state. VEEV replicates and produces infectious progeny in primed cells while type I IFN priming suppresses SINV replication. VEEV partially blockaded phosphorylation of STAT1 and STAT2, type I IFN signaling pathway molecules, inhibiting type I IFN signaling. Expression of non-structural proteins mediated this effect. However, structural protein expression also inhibits interferon sensitive genes (ISG) at the post-transcriptional level (182). Thus, through viral inhibition of ISG, STAT1 and STAT2, VEEV inhibits type I IFN action and enhances viral replication (182).

Both viral structural and non-structural genes are important in virulence (58; 1; 2). NsP2, capsid, and the E2 glycoprotein are implicated in changes in virulence and

alterations in type I IFN response. EEEV and VEEV interfered with cellular transcription needed to generate type I IFN response and induced subsequent cytopathic effects in infected cells. The ability to interfere with cellular transcription is controlled by a N-terminal 35 amino acid long peptide fragment of the capsid protein composed of two domains. One domain balanced the presence of protein in the cytoplasm and nucleus and the downstream peptide may contain nuclear localization signals. These domains determined the intracellular distribution of the capsid and were essential for protein function in the inhibition of transcription and blocking type I IFN.

Capsid alterations that down regulate cellular antiviral mechanisms lead to pathogenesis. For instance, the N-terminal fragment of the VEEV capsid was replaced with the capsid of Old World alphavirus, SINV. This reduced cytopathic effects and attenuated infection *in vivo* without affecting viral replication (51). The pathogenic effect of the capsid protein appeared to work via inhibition of multiple receptor-mediated nuclear import pathways leading to downregulation of the cellular antiviral machinery. Substitution with the capsid protein of SINV had no effect on nuclear import (9). For WEEV, the recombination events leading to the formation of WEEV from SINV and EEV-like ancestors allowed WEEV to acquire capsid protein function. WEEV could then effectively evade the anti-viral effects of type I IFN. Thus, the acquisition the ability to inhibit cellular transcription and evade type I IFN led to the emergence of WEEV as a pathogenic virus (61; 52). Like New World alphaviruses, the Old World alphaviruses, SINV and SFV are both able to interfere with cellular transcription. However, different virus-specific proteins are utilized to cause this effect. For the Old World alphaviruses transcriptional shutoff depends on nsP2 (51; 52). Thus, capsid mediated inhibition of cellular transcription increases virulence of the virus.

Attenuation of TC83 resulted from mutations encoded in the 5' non-coding region and the E2 envelope glycoprotein. Studies showed E2-120 appeared to be the major structural determinant of attenuation, but genetic markers composed of genome nucleotide position 3 in the 5' non-coding region were also significant to the attenuated phenotype (97). The biological effect of the attenuating mutation in the 5' untranslated region during murine infection was traced to increased sensitivity to type I IFN (176).

Disease presentation, incidence, and epidemiology relate to the ability of viral strains to evade type I IFN. For instance, epidemiological differences in North and South American (NA, SA) isolates of EEE result from increased type I IFN sensitivity in SA isolates. Comparison of replication of NA and SA strains in Vero cells pre-treated with human IFN $\alpha\beta$ or IFN γ showed a more suppressive effect on the less virulent SA strains. However, no differences in induction of IFN *in vivo* were observed (3). Initially, epizootic potential of several VEEV strains were attributed to type I IFN resistance (80; 155). However, type I IFN levels correlated with viral load in organs of mice with both epizootic and enzootic strains (6). Host compensatory mechanisms may explain the similarity in type I IFN levels between strains. Thus, type I IFN may not be a reliable marker of epizootic or virulence potential *in vivo*.

Cellular tropism

Evasion of innate antiviral mechanisms is integral to viral survival in the host. Specific viral tropism can aid in evasion of the innate immune response. For example, altered cellular tropism may impact the level of peripheral replication, viremia and subsequent neuroinvasion and virulence. Viral tropism for the cells of the periphery varies between the three encephalitic alphaviruses. For instance, both EEE and VEE viruses cause severe morbidity and mortality in equines and humans. VEEV infected primarily DCs and macrophages of the lymphoid tissues, while EEEV replicated poorly

in lymphoid tissues and preferentially infects muscle (49). Both viruses replicate efficiently in mesenchymal cell lineages. The tropism of EEEV for non-lymphoid tissues helps the virus evade the innate immune anti-viral response *in vivo*. EEEV antagonism of type I IFN induction was shown to be cell dependent, and lower serum type I IFN levels occurred in EEEV infected mice compared to VEEV. This likely reflects the inability of EEEV to infect cells of the myeloid lineages, and contributes to differences in disease etiology (24, 49). It may also explain the higher mortality rates observed for the EEEV in human populations (49).

Altered tropism for the cells of the CNS (neurons, oligodendria, microglia, and astrocytes) does not appear to account for the changes in neurovirulence between closely related strains as both virulent and avirulent strains are capable of productive infection of neurons. However, the efficiency of replication in neurons differs dramatically with no correlation to replication in the cells of the periphery. Apoptotic cell death may be important in neuronal injury indicative of activation of cell death pathways, and VEEV is directly cytopathic to the cells of the CNS in the absence of an immune response (75; 34). Some evidence indicates maturation state of the glial and neuronal cell populations in the brain plays a role in ability to resist infection (176; 29). The susceptibility of cells in the immature CNS may explain susceptibility in pediatric patients. WEEV is more cytopathic in immature human neuronal cells than mature cells. Additionally, mature neuronal cells are more sensitive to innate immune anti-viral effectors and respond to lower concentrations of type I IFN (176; 29)

Host response and type I interferon

All three of the encephalitic alphaviruses are highly susceptible to the effects of type I IFN, and have developed effective evasion tactics to avoid the anti-viral effect. In fact, in the absence of type I IFN receptors, even attenuated virus can cause complete

mortality (142). However, prophylactic and early therapeutic treatment with type I IFN or type I IFN inducing compounds provides protection. This indicates the importance of early induction of an immune environment conducive to host protection.

Beginning with the discovery that EEEV replication was suppressed in the presence of type I IFN, Wagner et al. showed peak viral production and high levels of cytopathogenicity in chick embryos and L-cells correlated with high-level production of IFN (136, 137). In contrast, *in vivo* serum levels of type I IFN are low in EEEV infected mice compared to those of VEEV infected mice. EEEV antagonism of type I IFN induction is cell dependent, and the lower serum type I IFN levels likely reflect the inability of EEEV to infect cells of the myeloid lineages (24).

Administration of a toll-like receptor 3 (TLR 3) agonist, poly-IC, raises the serum type I IFN prior to infection. Using poly-IC, Aguilar et al. demonstrated a dose-dependent IFN-mediated protection of mice to EEE infection (3). Similar results are seen for WEEV infections. Complete survival of the hamsters results following pre-treatment with either a consensus type IFN- α or TLR3 agonist, Ampligen®. The anti-viral effect of type I IFN levels was reflected in decreased clinical symptoms and weight loss associated with a significantly lower viral load in the brain at four dpi (71). Complete survival and depression of clinical symptoms is also associated with transiently expressed, artificially high levels of IFN- α in mouse models of WEEV infection. Therapeutic treatment up to seven days prior to infection provides complete protection. Early prophylactic elevation of IFN- α at 6 hours post-infection results in increased survival rates, but fails to provide complete protection (145, 146). VEEV disease pathogenesis is similar following early induction of type I IFN. Artificial induction of signaling through administration of a TLR3 agonist or prophylactic administration of PEGylated IFN- α resulted in delayed time to death and increased survival in mouse models (72).

While the early elevation of type I IFN demonstrates some prophylactic effects in decreasing time to death or disease symptoms, in the case of intranasal or aerosol exposure, the rapid entry of the virus to the CNS may limit or alter the effectiveness of early innate immune mechanisms. The substantial difference in effectiveness of prophylactic or therapeutic elevation of type I IFN indicates the importance of rapidly modulating the immune response to create a distinct anti-viral environment. The CNS of immunologically normal mice is still invaded in the presence of very high circulating levels of type I IFN indicating that the cells that comprise the CNS may be less sensitive to the presence of type I IFN or have slower kinetics for the establishment of an effective anti-viral state (33).

In addition to acting as an antiviral, type I IFN modulates the adaptive immune response, activates NK-cells, and suppresses production of pro-inflammatory cytokines. However, these other modes of action have not been explored in alphavirus models. Early elevation of type I IFN in TC83 infected mice results in significant depression of pro-inflammatory cytokines that may contribute to pathogenesis. Due to its greater stability most studies utilize modified forms of IFN- α . To the author's knowledge no studies examining the effects of IFN- β have been performed to date. Interestingly, IFN- β treatment of multiple sclerosis, a CNS disorder, helps control the disease in some patients and indicates mechanisms other than the anti-viral effect of type I IFN may be important in control of CNS damage (43, 107). Thus, effects of type I IFN apart from an anti-viral role need to be explored for the encephalitic alphaviruses.

Natural killer cells

Natural killer cells (NK) are lymphocytes that act in an antigen-non specific manner to induce cell death. Additionally, NK cells can produce cytokines that act locally at the site of infection and modulate the later adaptive immune response.

NK-cells induce cell death through release of cytotoxic granules such as granzyme b or through induction of cell-death pathways. Cytokine receptor expression is integral to NK-cell activation and proliferation. NK-cells express receptors for IL-2, 15, 21, 18 and type I IFN. These cytokines act in activation, proliferation, and survival of NK-cell populations. Production of these cytokines primarily comes from DC.

Upon activation, NK-cells can induce lysis of cells expressing the appropriate combination of activating and inhibitory receptors. NK-cell activation requires the correct signals from the target cell. For instance, MHC-I expression inhibits NK-cell activation even in the presence of activating ligands. This prevents indiscriminate NK-cell mediated killing of self. In contrast, when MHC-I is downregulated following infection or transformation of the cell, the cell can be killed by NK-cell mediated mechanisms. NK-cells mediate cell death through antibody dependent cell cytotoxicity as well. Cross linking of Fc receptors on NK-cells to antibody expressed on infected cells results in cell death. Thus, though NK-cells do not recognize specific antigen, the immune system controls NK-cell killing.

In addition, NK-cells secrete cytokines that act directly at the site of infection and modulate the adaptive immune response. IFN- γ and TNF are produced by NK-cells and act in positive feedback cycle to activate DC populations. NK-produced IFN- γ and IL-10 also act to indirectly regulate macrophage, microglia and T-cell populations. NK-cells also act as a bridge to the adaptive immune response and can influence activation, phenotype, and expansion of B and T cell populations. While no specific role for NK cells has been demonstrated for VEEV encephalitis, an experimental model of the related Old World alphavirus, Semliki Forest, demonstrated that NK-cells are pathogenic in the brain (5). The mechanism of action was attributed to NK-cell mediated lysis. Key differences in the host response have been demonstrated between Old and New World

alphaviruses, and Old World alphaviruses may not accurately represent the naturally encephalitic and more neuroinvasive New World strains (34; 101; 99; 100; 51; 52; 9; 182).

Additionally, NK-cells have a role in non-viral etiologies of CNS disease. In models of cerebral malaria, adoptive transfer of NK-cells into NK-cell depleted mice results in a pathogenic phenotype while mice that do not receive NK cells demonstrate less severe disease (61). Models of multiple sclerosis, an autoimmune disorder of the CNS, display the opposite effect. In this model, NK-cells suppress autoimmune CD4⁺ T-cells in the brain and significant decrease in CNS damage is observed (140). Interestingly, NK-cell mediated protection is mediated by IFN- β in this model. Thus, links between IFN- β , NK-cells, CNS disorders, and alphaviral disease indicate NK-cell populations may be important in neuropathogenesis of alphaviruses, but a protective role is also possible. Further research is needed to clarify the role of NK-cells in alphaviral infection.

Given the non-specific nature of NK-cell mediated killing, control mechanisms are essential in preventing death of normal, self components. MHC-1 expression acts in an inhibitory capacity on NK-cells and expression is downregulated on transformed or infected cells permitting NK-cell lysis (93). In mice, MHC-1 specific receptors are lectin-like dimers of the Ly49 family. CD94/NKG2A interactions with MHC-1 are essential to this function. CD16, NKp46, DNAM1 and NKG2D all represent activating NK-cell receptors.

MHC expression is integral to control of NK-cell populations. The MHC region genes are named H2 and are grouped based on structure and function into I, II, III subsets. MHC-I primarily present peptides generated from intracellular antigens. H2 regions K and D in mice represent classical MHC-Ia. MHC-Ia presents antigen to

cytotoxic T-lymphocytes (CTL) and are highly polymorphic with wide tissue expression. However, expression of MHC Ia is limited in the CNS particularly on neuronal cell populations. In contrast, the non-classical MHC Ib genes have limited tissue expression and few polymorphisms. The mouse has more than 30 major histocompatibility complex (MHC) class Ib genes, most of which exist in the H2 region of chromosome 17 in distinct gene clusters. Specific MHC-Ib genes have a more specialized function than is typically found for MHC-Ia, and roles for such genes have been specifically demonstrated in the CNS (129).

A number of unique roles have been identified for several of these non-classical MHC1 genes in both immune and non immune systems. The limited expression of classical MHC-1a genes in the brain makes the unique tissue specific expression of MHC1b genes of particular importance in the CNS. Some MHC-Ib genes are uniquely expressed in the brain where they are hypothesized to control cytotoxic killing by lymphocytes (129). Thus, the known functions of the MHC-Ib genes are directly or indirectly related to NK cell functioning and control. For instance, peptide presentation by H2-T23 (Qa1) molecule may work to regulate CD8 regulatory T-cell activity, but is known to inhibit CD4 + T cell responses through CD94/NKG2A and CD94/NKG2C receptors. H2-M3 presents bacterial peptides resulting in priming of the CD8+ T cell response, and H2-T3 (TL antigen) helps form a T memory cell response (129).

Since the H2 locus partially controls NK cell interaction, changes in haplotype could affect the functioning, activation, and phenotype of NK cells for particular murine strains. For instance, the NKC gene complex has a high degree of allelic variability and more recent evidence indicates a similar degree of polymorphism in the Ly49 locus (24; 123; 124; 140). The degree of NK-cell inhibition varies based on Ly49 allelic polymorphisms. The polymorphisms in the Ly49 family enhance the repertoire of NK

cell receptors, and NK-cells display different degrees of inhibition based on these allelic polymorphisms (123; 124). A comparison of BALB/c and BL6 mice indicated that BALB/c Ly49⁺ NKC receptor gene repertoire was minimal compared to BL6 mice. Variable expression of both NK cell receptors and corresponding MHC coincide with disease susceptibility (140). Thus, not only are gene differences in MHC I expression found between C3H and BL6 mice, but differences in NK-cell associated functions may differ substantially between inbred mouse strain (140).

The differences in phenotype of TC83-mediated disease between mouse strains may be partially mediated by alterations in control of NK-cell populations. However, the a role for NK-cells has not been explored for VEEV infection. Given the anti-viral function of NK-cells coupled with the ability to induced cell death, this is a significant gap in the knowledge of the host response to VEEV.

Type II IFN

Type II IFN (IFN- γ) has anti-viral effects in a number of disease models, but its role in alphavirus encephalitis is less well understood than that of type I IFN. IFN- γ is produced by CD4⁺ T-cells and NK-cells. While a role for IFN- γ in adaptive immunity against alphaviruses is supported in the literature, the role of IFN- γ during the acute response is not known. However, animal models of infection have provided some insight into the role of IFN- γ in protection. Vaccinated mice with a deficiency in the IFN- γ receptor are only partially protected from VEEV infection indicating that type II IFN signaling may partially prevent development of encephalitis. However, unlike type I IFN signaling, type II IFN signaling is not absolutely required for effective protection (133). IFN- γ signaling does not control EEEV infection and IFN- γ receptor deficient mice demonstrate equivalent levels of viremia and mortality rates similar to wild-type mice (1). Thus, the IFN- γ response is less significant than IFN- β or IFN- α in mediating

resolution of infection. However, differences between primary infection, pre-existing immunity, and viral strain may contribute to the relative importance of IFN- γ in these different infection models.

ADAPTIVE IMMUNE RESPONSE

For the encephalitic alphaviruses, the adaptive immune response is characterized by the production of neutralizing antibody and generation of antigen specific T-cells. The adaptive immune phase typically coincides with resolution of infection and viral clearance. The following sections will detail key components of the adaptive immune response related to this project.

Lymphocyte control of infection is common in multiple viral models. Lymphocytes include T-cell, B-cell and NK-cell populations. NK-cells have been previously discussed. B-cells and T-cells represent the branches of antigen specific adaptive immunity. B-cells act in production of antibody. Antibody is an important component of protection following vaccination and acts in peripheral clearance of virus. However, the function of neutralizing antibody once neuroinvasion and viral replication in the CNS begins is less well understood.

The primary population of T-cells expresses an $\alpha\beta$ T-cell receptor. $\alpha\beta$ T-cells can be further subdivided into CD4⁺ and CD8⁺ T-cells. CD4⁺ T-cells act directly on infected cells through specific receptor-ligand interactions, indirectly through cytokine secretion or by helping B-cells. The CD4⁺ T-cell response divides into T-helper cell 1 (Th1) and T-helper cell 2 (Th2). A Th1 response is characterized by CD4⁺ T-cells secreting IFN- γ and IL-2. A Th1 response enhances the CTL response. This response is thought to mediate protection in VEEV encephalitis. In contrast, a Th2 response is associated with IL-4 production and acts in activating B-cells. This response is also immunosuppressive with robust production of inhibitory IL-10 as well as production of

IL-5, IL-6 and IL-13. CD8⁺ T-cells are cytotoxic T-lymphocytes (CTL) and induce antigen-specific cell death. In addition, CD8⁺ T-cells secrete a unique subset of cytokines that can indirectly affect the cellular response.

B-cells

Among the factors in the cell-mediated immune response that are likely/known to be responsible for resolving infection, the role of B-cells and antibody production is well-defined. Antigen specific B-cells' robust antibody production reduces peripheral replication and removes virus from the blood stream. Thus, an efficient peripheral antibody response is integral to preventing or limiting neuroinvasion from the earliest phase.

Neutralizing antibody production is a common endpoint for alphavirus vaccine studies. High levels of neutralizing antibody correlate with vaccine-mediated protection in experimental models, livestock vaccination, and accidental laboratory exposures to VEEV. In the absence of pre-existing immunity, the development of antibody is associated with viral clearance, termination of disease, and survival (77; 25). Neutralizing antibody from naturally acquired infections is long-lasting and thought to be protective in the event of re-exposure.

However, the time lag between peripheral infection and antigen-specific antibody production may permit spread and replication to secondary sites of infection, and additional cell-mediated mechanisms may be required to mediate clearance once virus reaches the secondary sites (58). Therapeutic treatment with human monoclonal antibody against E2 prevents disease, but does not prevent neuroinvasion following aerosol exposure to VEEV in mice (72; 71). In those studies, viral replication was controlled in the periphery, but not the brain. Local production of antibody in the CNS or nasal mucosa may prevent disease development following neuroinvasion, but remains to

be explored further. Peripheral produced or administered antibody action following neuroinvasion is discussed in further detail below in conjunction with CD4⁺ T-cell help.

T-cells

Once the virus enters the CNS the utility of peripherally produced antibody is uncertain, and T-cells, particularly CD4⁺ T-cells, are integral in clearance of CNS infection.

The T helper cell response was originally defined loosely *in vitro* by measuring T-cell proliferation to TC83-primed splenocytes. T-cells were derived from TC83-vaccinated C3H mice. The predominant T-cell phenotype was identified as IL-2 secreting Thy-1⁺, LYT-1⁺, LYT2⁻, and L3T4⁺ (122). This indicated a Th1 bias to the VEEV T-cell response, but early techniques of T-cell isolation resulted in mixed cell populations.

Initial studies examining the role of T-cells in the host response applied anti-thymocyte serum (ATS) in mice. This increased mean time to death by 2 days, delayed neurological signs, and increased splenic B-cells compared to controls. However, the mouse strain was TLR-4 deficient (C3H/HeJ), so results are inconclusive (179). Depletion of T-cells in wild-type CD-1 mice led to SCID-like disease development. T-cell depletion did not affect clearance of virus from the serum or production of IgM (34). This indicates the role of antibody in resolution of peripheral infection. Reconstitution of SCID mice with normal splenocytes or T-cells replicates wild-type encephalopathy and T-cells represented the majority of brain infiltrates. (34). These studies indicated a potentially pathogenic role for T-cells, and supported separation of antibody function in peripheral and brain pathologies.

However, subsequent studies indicate that CD4⁺ T-cells act in neuroprotection. Vaccinated α/β T-cell receptor knock-out mice (TCR KO) deficient in both CD4⁺ and CD8⁺ T-cells develop lethal VEEV following s.c. infection with virulent VEEV.

Vaccinated wild-type mice are completely protected. Reconstitution with CD4⁺ or CD3⁺ T-cells from vaccinated wild-type donors resulted in recovery in TCR KO mice. CD8⁺ T-cells failed to provide protection. Interactions of CD40, a receptor expressed on CD4⁺ T-cells, with CD40 ligand, expressed primarily on activating antigen presenting cells, are essential to CD4⁺ T-cell activation. CD3⁺ T-cells from CD40 deficient mice were unable to prevent encephalitis. In the context of pre-existing immunity, these studies indicate an integral role for CD4⁺ T-cells in preventing lethal encephalitis (133; 184).

TCR KO mice have impaired antibody production in the absence of a CD4⁺ T-cell help for B-cells. However, transfer of mouse hyperimmune ascitic fluids (HIAF) had no protective effect in these mice, indicating that a CD4⁺ T-helper cell function may not be the primary role of these cells (184). Thus, peripheral administration of antibody does not impact the course of VEEV encephalitis. In mice with non-functional B-cells (μ MT^{-/-}), CD4⁺ IFN- γ secreting cells reduced viral load in the brain following acute encephalitis, but, in the absence of antibody, virus persisted following survival (21). Depletion of CD4⁺ or CD3⁺ T-cells leads to earlier onset of disease and higher viral titer in the brain in μ MT^{-/-} mice. Additionally, CD4⁺ T-cells were more effective INF- γ producers than CD8⁺ T-cells in *ex vivo* assays. However, T-cell dependent B-cell activation and local production of antibody in the microenvironment of the brain may be of great functional importance. Regardless, CD4⁺ T-cells, by direct or indirect means, aid in: (1) survival and viral clearance in a model of pre-existing immunity with virulent VEEV; and (2) viral clearance and milder disease following primary infection with attenuated virus.

Though both CD4⁺ and CD8⁺ T-cells infiltrate the brain, CD8⁺ T-cells are not thought to be important in resolution of brain infection. One study demonstrated a lack of secondary cytotoxic T-lymphocyte activity in mice vaccinated i.p., s.c., i.d. with TC83

in vitro. This could not be explained by haplotype of mouse as six separate haplotypes responded in a like manner (85). In uMT KO mice, CD8⁺ depletion results in less symptomatic disease than mice depleted of CD4⁺ T-cells indicating the greater importance of CD4⁺ T-cells. However, the precise role of CD8⁺ memory T-cells and cytotoxic T-lymphocytes remains unknown.

VEEV is a highly lymphotropic virus, and disease presentation in infected mice has been compared to that of X-irradiated mice where lymphogenesis is ablated. Infection and death of lymphocytes associated with VEEV infection undoubtedly plays a part in disease phenotype and spread of virus. The ability to replicate in lymphocytes may enhance VEEV virulence. In comparison to EEEV and WEEV, TC83 replicated to higher titers in human peripheral blood leukocytes (112). Treatment of murine splenocytes with both B and T cell mitogens increases susceptibility to VEE infection and indicates the activation state of lymphocytes may be critical to lymphoid pathogenesis of VEEV. By “hijacking” the immune system, VEEV is able to replicate and spread more efficiently. This may have as yet unexplored effects on the immune response of the host.

The absence of an effective lymphocyte response leads to deregulation of the immune system. In particular, deficiencies in the CD4⁺ T-cell compartment are pathogenic and effect both antibody production and the CD8⁺ T-cell response. In addition, CD4⁺ T-cell cytokine secretion and direct interactions with infected cells may impact the course of viral infection.

Conclusions

The innate and adaptive arms of the host immune response are both key in generating protective immunity and preventing disease from VEEV. However, little is known about the specific innate immune response to the New World encephalitic

alphaviruses apart from a role for type I IFN in an antiviral capacity. Given the pleotropic effects of this cytokine, additional mechanisms of action are worth exploring. Natural killer cells are important in a number of viral infections and can have both pathogenic and protective roles in CNS disorders of varying etiologies. However, they have not been examined to date for the encephalitic alphaviruses. The early, innate response helps shape the later adaptive response phenotype. For alphaviral encephalitis, this is primarily characterized by a Th1 response and viral clearance and resolution of infection is associated with production of neutralizing antibody.

Chapter 3: Study Purpose and Design

A variety of experimental approaches to vaccine and prophylactic or therapeutic drug development have been utilized with varying degrees of success. However, little is known about the host response to alphavirus infection, particularly the very early immune response. As such, advancement of effective drug and vaccine platforms is hampered. The rapid and almost universal death of the host animal in experimental mouse models of virulent VEEV infection has deterred analysis of the correlates of protective immunity. Combined with the high level of biosafety required to handle wild-type viruses and the select agent status of the pathogen in the U.S., understanding of the host response to infection has been delayed. New research regarding the mechanisms of immunoprotection and pathogenesis in the CNS is crucial for the effective, timely development of both preventative and therapeutic measures.

STUDY PURPOSE

These studies will help define the protective and pathogenic host mechanisms utilized by the host that ultimately resolve infection or result in lethality. In turn, such knowledge can be utilized to enhance existing or novel drug and vaccine development platforms. These studies will seek to further develop a utilitarian experimental model to assess the host response to VEEV encephalitis through use of the attenuated vaccine strain of VEEV, TC83. This eliminates the restrictions placed by select agent status and permits work under BSL2 conditions. These studies will lead to a better understanding of the host response while providing a model system for the study of host pathogenesis. The evaluation of the vaccine strain is of additional interest given its use in formulation of an IND vaccine that for use in at-risk military and laboratory personnel. The specific

immune correlates resulting in lethality vs. survival following viral invasion of the host brain remain largely unknown.

Using intranasal infection with TC83, the live-attenuated, human vaccine strain of VEEV, we established an approach to compare lethal vs. non lethal brain infection. This would allow us to define the protective and pathogenic host immune response: (1) Lethal infection in C3H/HeN (C3H) mice (2) Non-lethal, acute infection with clearance of the virus in C57BL/6 (BL6) mice. The two strains display similar viral kinetics with each developing a high level viral load in the brain indicating the host response, not viral replication, is a significant contributor to outcome (Table 4). Signs of inflammation in the brain and serum neutralizing antibody levels were also similar.

Table 4: Response of C3H and BL6 mouse strains following intranasal TC83 infection.

Mouse Strain	Percent Survival	Acute disease symptoms	Viral Titer in brain (pfu/g)	Chronic virus
C3H/HeN	10%	20-30% weight loss, scruffy coat, hunched, ataxia, inactive	10^7 - 10^8	No
Wild-type C57BL/6	100%	10-15% weight loss	10^6 - 10^7	No

Profiling the host response across BL6 and C3H mice using genomics and multiplex cytokine array identified potential predictors of the disease outcome: natural killer (NK) cells and T-cells.

Determining the specific role of these immune players in viral encephalitis will be accomplished utilizing these three models of infection:

1. C3H/HeN mice will be evaluated concerning the role of natural killer cells in invasion of the CNS utilizing anti-NK-cell antibody mediated loss of function and

- gain of function through adoptive transfer of NK-cells as determined by log rank test to evaluate mortality.
2. A survival model of C3H generated by depletion of NK-cells will be evaluated to determine key factors correlated with survival using viral load, histopathology, and multiplex cytokine array.
 3. Wild type C57BL/6 mice and immunodeficient TCR KO and IL-12p40 KO mice will be evaluated to investigate T-cell activation in the brain using viral load, histopathology, and multiplex cytokine array.

HYPOTHESIS

Given the age related susceptibility to the encephalitic alphaviruses combined with the wide range of disease following infection, a comprehensive understanding of the immune response is essential to proper care, treatment and disease prevention in individuals. Thus, *we hypothesize that NK-cells contribute to susceptibility to viral encephalitis in C3H mice. In contrast, resistance in BL6 mice is mediated by T-cell activation.* The host immune response will be measured by significant differences in cytokine and antibody production. Pathogenesis of the virus will be measured by histopathological and viral load changes. Changes in the host response and pathogenesis correlated to survival and lethality will indicate the significance of T-cell and NK-cell compartments in modulating an immunoprotective or pathogenic response. Furthermore, the alterations in cytokine production or antibody levels that can correlate with survival or lethality will provide a useful measure of status of infection and may provide a unique immune signature for identification of disease in early acute infection. This will aid in identifying mechanisms of immunoprotection or pathogenesis to enhance therapeutic and vaccine development efforts.

The long term goal of this proposal is to identify immune effectors capable of influencing a neuroprotective immune response to CNS-invading viruses. The objective is to identify specific molecular and cellular markers correlating with outcome of viral CNS infection. The proposed project will study the effects of “loss and gain of function” in NK cell and T-cell compartments on the host response.

Chapter 4: Methods

ANIMAL USE:

C57BL/6, IL-12p40 KO, and TCR KO mice were purchased from Jackson Laboratories (Bar Harbor, Maine) (Table 5). C3H/HeNCrl mice were purchased from Charles River Laboratories (Charles River Strain Code 025, Wilmington, MA). All studies with VEEV strain TC83 were carried out in ABSL-2 and were approved by the Institutional Animal Care and Use Committee at the University of Texas Medical Branch.

Table 5: Description of genetically modified strains utilized in studies.

Species	Catalog	Description
C57BL/6	B6 (#000664)	Parental strain (wild type)
$\alpha\beta$ TCR KO	B6.129P2Tcrb ^{tm1Mom} /J (#002118)	Disruption of TCR β
p40 KO	B6.129S1- <i>Il12b</i> ^{tm1Jm} /J(#002693)	Disruption of p40

All studies with VEEV strain ZPC738 were carried under ABSL3 conditions. Mice were observed daily for signs of illness and weight and temperature was observed throughout the studies. Bio Medic Data Systems (BDMS) transponder model DAS-700s were utilized to track individual mice and record temperatures.

Statistical analysis:

Minimum numbers of mice needed were determined using power analysis in GraphPad® StatMate (San Diego, CA). Statistical analysis and comparison of survival for all groups over the study period was performed using log rank test at a significant level of $\alpha < 0.05$ in GraphPad® Prism (San Diego, CA).

Rationale

Previous research has utilized a variety of inbred and outbred mouse strains to model VEEV encephalitis. Both inbred and outbred strains of mice are uniformly susceptible to infection with virulent strains of VEEV by numerous routes. Inbred strains utilized include: C3H/HeN (C3H), C57BL/6 (BL6), and BALB/c. Outbred Bagg Albino Swiss mice and ICR mice have also been utilized (107; 157; 85; 89). Hamsters have also been postulated as a potential model for VEE as they are highly susceptible to infection (78). However, the lack of reagents for hamster models combined with the low number of genetically modified hamsters made such a model impractical for our uses. Inbred strains of mice provide more utility to research genetically modified strains for pathogenesis and host response studies are easily obtained. Thus, the use of inbred mouse models fit with the goals of the proposed research and had historical use in the Paessler laboratory.

While mouse strains are uniformly susceptible to virulent strains of VEEV, susceptibility to the attenuated, vaccine strain TC83 is highly variable. Intranasal infection of TC83 causes lethal VEEV-like encephalitis in C3H, but not BL6 or BALB/c. This model was proposed as an effective, easily utilized model for the evaluation of anti-virals (89). As such, it fit the model of infection in which we can use a non select agent in the BSL2.

In order to better understand the host response, we compared the response of these lethally infected mice to another inbred strain, BL6 mice. Comparison of inbred strains of mice has historically yielded important information regarding the mechanisms of immune protection. For instance, the dichotomy of the T-helper cell response differentiates BALB/c and BL/6 mice in a number of infectious disease models (70; 135; 169; 66). Thus, knowledge of differential immune response in lethal and non-lethal

infection can yield important results regarding the mechanisms of protection or pathogenesis.

VIRUS

At day 0, mice were challenged intranasally (i.n.) with $1 \times 10^{7-8}$ plaque forming units of VEEV (TC83) per animal in 40 μ l of PBS administering approximately 20 μ l per nare. Challenge with VEEV (ZPC738) was with 4×10^5 pfu in 40 μ l total volume, delivering approximately 20 μ l to each nare intranasally on Day 0. Back titration on Vero cell monolayers was utilized to confirm dosage.

Rationale

Dosage of virus was selected based on published literature. The dose selected was necessary to induce lethal encephalitis in 10% or more of C3H/HeN mice.

Intranasal route of inoculation was also chosen based on published literature as other routes do not cause high rates of mortality in C3H/HeN mice (87; 89). Additionally, since our interest was in TC83-encephalitis, i.n. infection provided a rapid means of inducing the response in the microenvironment of the brain. Furthermore, for biodefense purposes, aerosolized virus would be the likely method of release, and provided further rationale for use of this model and the i.n route of infection. Thus, due to the high mortality resulting of i.n infection with $1 \times 10^{7-8}$ pfu in C3H mice, the primary aim of studying infection of the brain, and the utility as biodefense model, we selected these parameters.

VIRAL REPLICATION IN THE TISSUES

Organ preparation

Portions of peripheral organs (lungs, liver, and spleen) and brain were collected at preselected time points post-challenge, or at time of termination, or at termination of

study. Each brain was sagittally sectioned and half-hemisphere was used to calculate viral load. Prior to homogenization, organs were weighed for later calculation of viral load/gram. Organs were then homogenized in MEM containing 10% FBS.

Plaque Assay

Viral replication in the brains and peripheral organs was assessed by plaque assay. Vero cell monolayers were seeded 48 hours prior to inoculation. On the day of inoculation, aliquots of sample were serially diluted and inoculated in duplicate onto confluent cell monolayers with 0.1 mL volumes of the test materials. Assay diluent (Dublecco's minimal essential medium containing 5%, heat inactivated (HI) FBS plus 1% penicillin/streptomycin sulfate) served as the assay negative control. Following a 60 minute adsorption, an agarose overlay was added in proportion of 33% 2x Eagles minimal essential medium, 33% assay diluents, and 33% (2%) agarose. Test cultures were maintained for 72 ± 6 h at which time, overlay was removed and crystal violet was added. Plaques in all wells containing <200 plaques were enumerated. The total number of plaques per well was calculated and the virus titer expressed as plaque-forming units per milliliter (pfu/mL).

Statistical Analysis

Statistical analysis and comparison of viral replication for all groups from plaque assay over the study period was performed using student's t test at a significant level of $\alpha < 0.05$ in GraphPad® Prism (San Diego, CA).

Rationale

Plaque assay is historically the most accurate measure of viral replication for alphaviruses and allows comparison of plaque sizes to the original inoculums as a phenotypic indicator for any significant changes in the viral genome.

Peripheral infection with TC83 is transient, mild and rapidly cleared (89). Additionally, the primary focus of this proposal is CNS infection. Thus, the entire peripheral organ was not necessary for determination of viral replication in the periphery.

To utilize mice most effectively, reducing both cost and number needed, half of each brain was taken for assessment of viral replication in the brain. Due to the disseminated nature of infection, this would not impact the calculation of viral load in the brain.

HISTOPATHOLOGY

One sagittally sectioned hemisphere of the brain was preserved in 10% formalin for 48-72 h prior to transfer to 70% ethanol solution. Sections were then fixed in paraffin and sectioned. H&E staining was largely performed by the Pathology Core at UTMB. Histopathology analysis of brain sections was performed blinded to the sample identification.

Statistical Analysis

Semi-quantitative scoring of sections was performed based on scoring system determined by trained neuropathologist. Brain sections were scored 0-3 with 0 representing no inflammation or necrosis, 1- mild/minimal inflammation (few cellular infiltrates, minimal or absent meningitis and perivascular cuffing) 2-moderate inflammation (increased cellular infiltrates, meningitis present and perivascular cuffing) 3-moderate/severe inflammation (necrosis, cellular infiltrates, diffuse meningitis, perivascular cuffing).

MICROARRAY ANALYSIS

Total RNA preparation and GeneChip processing

A midline sagittal section of each brain was removed and DNase-treated total RNA was isolated using TRIZOL Reagent followed by the RNAqueous Mini and RNeasy-Free DNAase Set according to protocols adapted from the manufacturer's instructions. Total RNA was subjected to GeneChip Expression Analysis (Affymetrix, Santa Clara, CA) according to the manufacturer's instructions [Expression Analysis Technical Manual, [Section 2: Eukaryotic Sample and Array Processing](#), Alternative protocol for One-Cycle cDNA synthesis followed by synthesis of biotin-labeled cRNA with MessageAmp Premier RNA Amplification Kit (Ambion Inc, Austin, TX)] in the Molecular Genomics Core (University of Texas Medical Branch, Galveston, TX). Total fragmented cRNA was hybridized to the Affymetrix Gene Chip Mouse Genome 430A 2.0 Array using the GeneChip Hybridization Oven 640. The chips were washed and stained in a GeneChip Fluidics Station 450 and fluorescence was detected with an Affymetrix-GS3000 Gene Array scanner using the GeneChip Operating System software (GCOS1.4).

Statistical analysis

Microarray quality assessment (*affy* (53), *affyPLM* (74) and *QCReport*, *affycoretools* packages), preprocessing (*gcrma* package (180)) and differential expression analysis (*limma* package (15; 154)) were performed with Bioconductor software packages (54) in R programming environment (73).

Hierarchical clustering of differentially expressed genes was performed in the Spotfire Decision Site 9.0 for Functional Genomics (Spotfire Inc., Somerville MA) using Unweighted Pair-Group with Arithmetic Mean and Euclidian distance method (38).

Differentially expressed genes were associated with biological functions and/or diseases or with canonical pathways in Ingenuity's Knowledge Base of the Ingenuity Pathways Analysis application (Ingenuity Systems, www.ingenuity.com). Right-tailed Fisher's exact test was used to calculate a p-value determining the probability that the association between the genes in the dataset and the canonical pathway or biological function and/or disease is caused by chance.

BIOPLEX ANALYSES OF CYTOKINE AND CHEMOKINE EXPRESSION

Brain homogenate levels of 23 cytokines and chemokines (IL-1 α , IL-1 β , IL-2, IL-3, IL-4, IL-5, IL-6, IL-9, IL-10, IL-12p40, IL-12p70, IL-13, IL-17, Eotaxin, G-CSF, GM-CSF, IFN- γ , KC, MCP-1, MIP-1 α , MIP-1 β , RANTES, and TNF- α) were determined using Bio-Plex Pro Mouse Cytokine 23-plex Assay (Bio-Rad #M60-009RDPD). Samples were collected at preselected dpi and analyzed as per manufacturer's instructions. Replicates of two or three mice per group per time point were used.

Statistical analysis.

Statistical analysis and comparison of cytokines for all groups was performed using a two-tailed unpaired student's t test with 95% confidence interval in GraphPad® Prism (San Diego, CA). In the event the F test to compare variance was significantly different, student's t test was used with Welch's correction though this reduced power of the analysis.

ADDITIONAL METHODS:

Experiment specific methods are described within that chapter.

Chapter 5: A Comparative Model of Lethal and Non-Lethal TC83-Encephalitis¹

Previous *in vivo* studies demonstrated variable susceptibility of different mouse strains to TC83-induced encephalitic disease. C3H mice are highly susceptible to disease development after intranasal infection unlike inbred strains, BALB/c and C57BL/6, which become infected but do not develop encephalitic disease (64; 157; 89). *Our approach compared lethal infection of C3H mice to non-lethal infection of BL6 mice to define the basis for resistance and susceptibility to brain infection.* This model system leads to a better understanding of host protective mechanisms in encephalitis. We initially examined viral load, symptomatic disease, and inflammation in the brains of C3H and BL6 mice following intranasal infection with TC83. At six dpi, we observed a high-titer viral load, meningitis and perivascular cuffing in the brain, low-titer viral load in peripheral organs, and similar levels of neutralizing antibody. However, no significant differences were observed in comparison to resistant BL6 mice. Thus, basic virology and pathology indicated productive, robust infection of both C3H and BL6 mice. This initial characterization provided an approach to dissect the dichotomy in clinical outcome between strains, and allowed further comparison of the host response to examine factors influencing the lethal outcome in C3H mice.

To better understand underlying differences in the host response, we compared serum neutralizing antibody, gene transcript levels, and cytokine protein levels in the brain. No differences in serum neutralizing antibody levels were observed at six dpi, but differences in gene regulation and cytokine protein production were apparent between the

¹ In revision: Taylor, K., Kolkostova, O., Patterson, M., Poussard, A., Smith, J., Estes, D.M., Paessler, S.P. (2011). Natural Killer Cell Mediated Pathogenesis Determines Outcome of Central Nervous System Infection with Venezuelan Equine Encephalitis Virus. *Vaccine*.

two strains. These factors implicated natural killer cells in the infection. Thus, viral kinetic, serum neutralizing antibody and signs of inflammation are similar between mouse strains. However, differences in the host response were apparent between C3H and BL6 by microarray and multiplex cytokine array.

Based on microarray data, cytokine data and the existing literature, *we hypothesized that NK cells contributed to TC83 disease in C3H mice.* In fact, NK-cell depleted C3H mice survived following TC83 infection. Reconstitution of naïve NK-cells to NK depleted mice reverted disease phenotype to

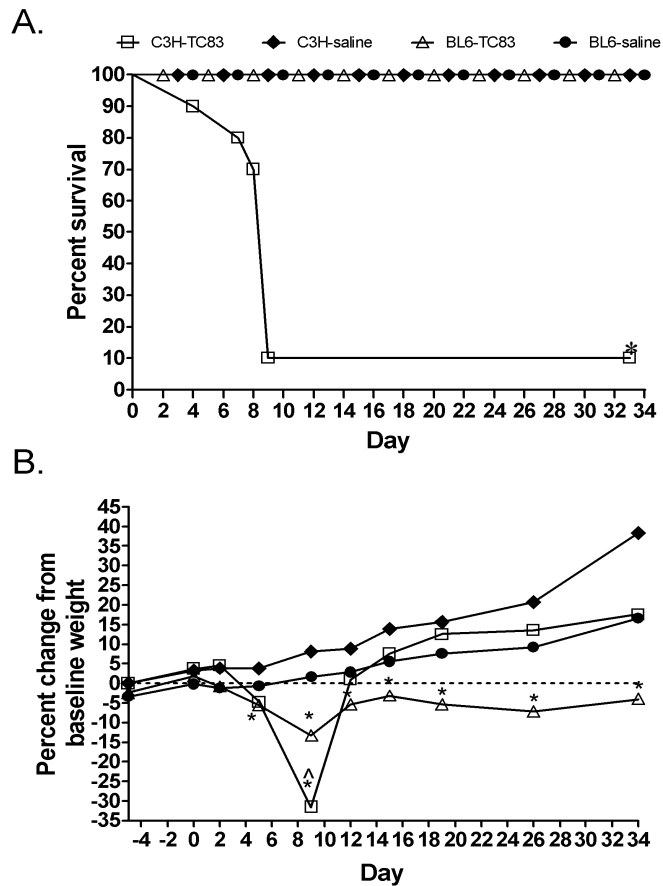


Figure 4: Pathogenesis of intranasal TC83 infection in C3H and BL6 mice. (A) Survival was significantly lower in infected C3H (n=9) mice compared to infected BL6 mice (n=3) or saline controls (n=3). (B) Infected C3H mice displayed significantly greater weight loss than infected BL6 mice or saline controls at nine dpi. BL6 mice lost significantly more weight and maintained significantly lower weights than saline controls starting at five dpi. (* denotes $p < 0.05$ compared to saline controls, ^ denotes $p < 0.05$ between infected groups).

complete lethality. This indicates an important role for this cell population in TC83 infection, and confirmed the utility of comparing lethally infected C3H mice to non-lethally infected BL6 mice.

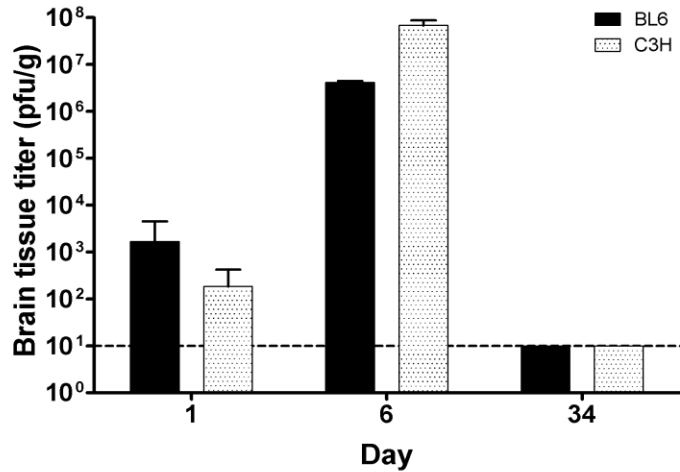


Figure 5: Similar viral kinetic in the brain between C3H and BL6 mice following intranasal TC83 infection. At one and six dpi, C3H mice and BL6 mice have no significant difference in viral load as determined by plaque assay. ($p < 0.01$). At 34 dpi, BL6 mice have no infectious virus present in the brain. The one surviving C3H animal had no virus present in the brain at 90 dpi. ($n = 3/\text{group}/\text{time point}$).

CHARACTERIZATION OF A COMPARATIVE MODEL OF LETHAL AND NON-LETHAL TC83-ENCEPHALITIS

High-levels of mortality in C3H mice, but complete survival in BL6 mice characterize intranasal TC83 infection.

C3H mice had high mortality with only 10% ($n = 1$) survival rate. Mean time to death (MTD) was 9 days. All BL6 mice and sham infected C3H and BL6 survived infection (Figure 4). Both strains of mice developed symptomatic infection characterized by rapid drop in weight compared to control, sham infected mice. C3H mice lost an average of 32.91 ± 6.11 percent of their body weight and BL6 mice lost only 13.16 ± 5.11 percent compared to baseline body weight. Between days nine and 12, BL6 mice regained an average of 5.99 ± 4.86 percent of baseline weight indicating recovery. However, BL6 mice maintained a significantly lower weight compared to sham infected BL6 controls over the study course (Figure 4). Clinical signs of disease were more severe in C3H mice and characterized by piloerection, ataxia, severe hunching, lethargy, and hypersensitivity. BL6 mice rarely

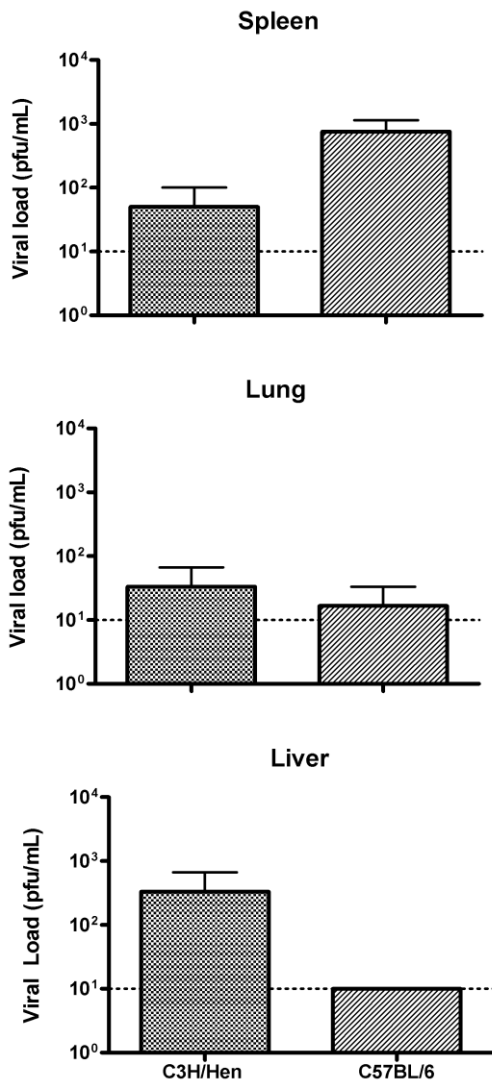


Figure 6: Infectious virus in peripheral organs of TC83 infected C3H (n=3) and BL6 mice (n=3) at six dpi determined by plaque assay. No virus was observed in any of the tested replicates at either one dpi or 34 dpi. No significant difference in viral load between for any group comparison was demonstrated ($p < 0.01$).

showed overt clinical signs of disease and only few mice exhibited hunching or piloerection (data not shown). Thus, both strains developed significant weight loss, but neurological symptoms and mortality were only recorded for C3H mice.

Both C3H and BL6 mice display high-titer viral load in the brain and low-titer viral load in peripheral organs.

Despite differences in mortality and disease severity, both strains had similar viral loads in the brain at one and six dpi indicating that level of viral replication was not a significant determinant of outcome in this model (Figure 5). At one dpi, C3H have a trend toward lower viral load in the brain compared to BL6 ($p = 0.4253$). At six dpi, C3H mice demonstrate a trend toward lower viral load in the brain compared to BL6, but this was not mathematically significant ($p = 0.0278$). Both strains developed very high levels of virus in the brain at six dpi. **Thus, six dpi marked a time of acute encephalitis with high**

titer viral load, and acted in latter studies as an ideal time to closely examine the host response. All BL6 mice and the one remaining C3H animal cleared virus to below the limit of detection by end of study (Figure 5).

Viral replication outside the CNS was not responsible for mortality either, and a similar viral kinetic between strains was observed. Viral loads in the peripheral organs

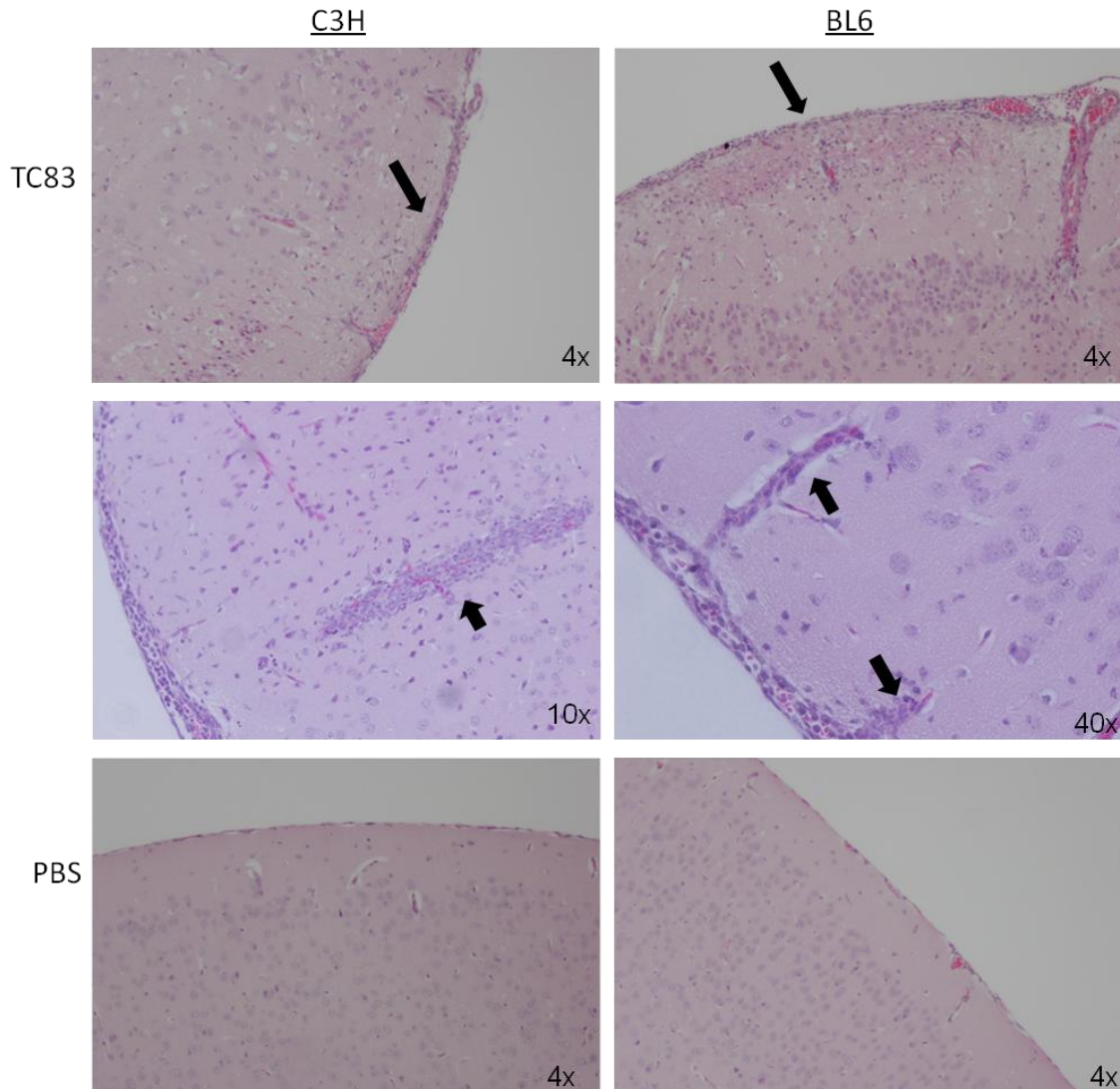


Figure 7: Meningitis and perivascular cuffing in TC83 infected C3H and BL6 mice at 6 dpi. Sham infected mice had normal brain architecture.

(liver, lung, and spleen) were present 1 and 6 dpi and ranged from below the limit of detection (10 pfu) to 10^3 pfu per gram of brain tissue. No significant difference in viral load was observed in the peripheral organs between strains. Thus, the viral kinetic appears similar in both the periphery and the brain between strains (Figure 6, Figure 5).

Similar pathology and histology scores in lethally infected C3H and resistant BL6 mice.

Histological scores of inflammation were similar between C3H and BL6. C3H mice had an overall score of 9 and BL6 had an overall score of 10.33 (**Error! Reference source not found.**). Similarities were also noted in individual regions of the brain (hippocampus, thalamus, cerebral cortex, olfactory bulb, cerebellum, striatum, and meninges between C3H and

Table 6: Histological scores of brain tissue from C3H and BL6 mice following intranasal TC83 infection at 6 dpi. Overall scores represent mean determined from means for individual brain sections.

Group	n	Hippocampus	Thalamus	Cerebral Cortex	Olfactory Bulb	Cerebellum	Striatum	Meninges	Overall Score
C3H	3	1.67±0.58	1±0	2.33±0.58	1±0	0±0	1±0	2±0	9±0
BL6	3	1.67±0.58	2±0	2.67±0.58	1±0	0.67±1.15	1±1	1.67±1.15	10.33±2.8

BL6 strains (**Error! Reference source not found.**). Both strains exhibited similar histological signs of encephalitis by H&E staining of brain tissue sections. Meningitis, and perivascular and vascular cuffing were disseminated through the brains of both strains at six dpi (Figure 7). Mononuclear cellular infiltrates were also apparent at this time point.

CHARACTERIZATION OF LETHAL AND NON-LETHAL HOST RESPONSE TO TC83-ENCEPHALITIS.

Our initial approach characterized a model of lethal vs. non-lethal encephalitis. Subsequently, we examined the host response between C3H and BL6 mice for differences in the brain in neutralizing antibody production, gene transcripts, and cytokine protein levels. No differences in neutralizing antibody were observed between mouse strains. However, gene transcript profiles and cytokine protein profiles indicated a role for natural killer cells and T-cells in TC83 infection.

High-level production of neutralizing antibody at 6 dpi characterizes TC83 infected BL6 and C3H mice.

At six dpi, antibody responses were similar between infected strains with both developing equivalent levels of neutralizing antibody at six dpi. By 12 dpi, all tested BL6 serum (9/9) displayed high titer neutralizing antibody (640-2560). The remaining C3H animal (1/1) had equivalent level of neutralizing antibody (1280) by PRNT indicating productive infection had been established despite survival of the animal.

Table 7: Serum neutralizing antibody response between C3H and BL6 mice at six dpi.

Sample	PRNT ₅₀		*Geometric mean titer
	Day six post-infection		
Sample	No. positive/total tested (% positive)	Titer range	
C3H-TC83	3/3 (100%)	20-160	320
BL6-TC83	2/2 (100%)	640-1280	960
C3H-PBS	0/2 (0%)	<20	1
BL6-PBS	0/2 (0%)	<20	1

*Geometric mean titers are reported as the reciprocal of the serum dilution corresponding to an endpoint of 50% plaque reduction. For PRNT values below the limit of detection (<20), an arbitrary value of 1 was used for calculation.

Transcriptome analysis identified immune and inflammatory genes in lethal and non-lethal host responses

Microarray analysis aided in determining specific immune compartments effecting pathogenesis and outcome following brain infection. BL6 mice were used as a control representing a non-lethal infection with complete viral clearance.

Initially, we examined C3H and BL6 mice to identify genes or functional gene groups in the brain marking lethal C3H and non lethal BL6 infections by comparison to saline controls. We then compared gene groups important in TC83 infection between infected C3H and infected BL6. Subsequently, we identified multiple genes involved in NK cell control, activation, and retention in the brains of infected mice. Interestingly, key genes that function in inhibition of NK cell action were down regulated 2-fold or greater in C3H mice compared to BL6.

To gain insight into the host response to TC83 infection, we first compared the transcriptional profiles of sham-infected C3H and BL6 mice to TC83-infected C3H and BL6 mice respectively at the peak of acute disease. This was defined as six dpi; a time associated with uniform high viral load in the brain and significant clinical symptoms.

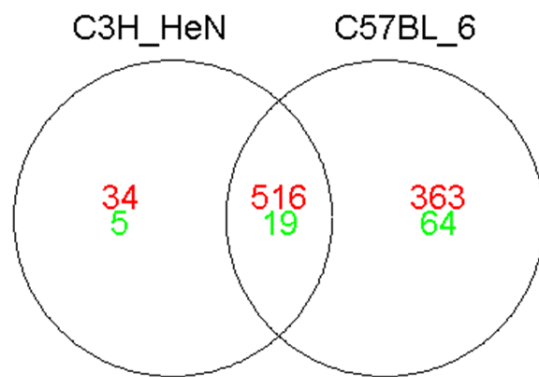


Figure 8: Comparison of genes with 2-fold or more differential expression between TC83 infected C3H and BL6 mice and saline controls. Numbers in green represent 2-fold or greater decrease in expression compared to saline. Numbers in red represent 2-fold or greater increase. C3H and BL6 shared expression of 516 up-regulated and 19 down regulated genes. C3H expressed 34 up-regulated and 5 down-regulated genes not expressed by BL6. BL6 mice uniquely expressed 363 up-regulated and 64 down-regulated genes.

Transcripts with low probability values adjusted for multiple testing ($p < 0.0001$) and \log_2 (fold change) > 1 were qualified as differentially expressed.

At six dpi, C3H displayed 2-fold or more differential expression of 574 genes. Infected mice had 24 genes more than 2-fold down-regulated and 550 transcripts more than 2 fold up-regulated in brain homogenates of TC83-infected compared to sham-infected C3H mice. In contrast, BL6 mice had 83 genes more than 2-fold down-regulated and 879 transcripts that were more than 2 fold up-regulated in brain homogenates of TC83-infected compared to sham-infected BL6 mice. Thus, based on purely number of genes differentially regulated two-fold or more, BL6 mice displayed a more robust response to TC83-infection than lethally infected C3H.

C3H and BL6 mice shared differential expression of 516 genes (Figure 8). Of the genes down regulated two-fold or greater, 64 genes in BL6 mice and 5 genes in C3H mice were uniquely differentially expressed. Of the more than 2-fold up-regulated genes, C3H mice had 34 and BL6 had 363 unique transcripts (Figure 8). Thus, BL6 mice generated a greater response to infection in the brain overall compared to C3H mice

Functional analysis was performed on differentially expressed genes through association with specific biological functions and disease. Differentially expressed genes in the brain homogenates of infected mice compared to sham infected mice included several overlapping categories related to immune and inflammatory function (antigen presentation, cell and humoral immunity, and inflammatory response) (Figure 8, Figure 9). A number of these genes in immune and inflammatory functional categories also overlapped with canonical pathways associated with cell death.

Greater than 54% (309/572) differentially expressed genes were involved in both functional categories, namely immune functioning and cell death. Unsurprisingly, other immune response transcripts across both strains were largely involved in recognition of

viral pathogens and interferon signaling, typical for alphavirus infections. However, multiple genes involved in signal transduction between natural killer cells and antigen presenting cells were also involved (*CCL13*, *CCL2*, *CCL4*, *CCL5*, *CCL7*, *CCR1*, *CCR2*, *CCR5*, *CD14*, *CD274*, *CD40*, *CD44*, *CD47*, *CD52*, *CD72*, *CD74*, *CD86*, *COL4A1*, *COL4A1*, *CSF2RB*, *CXCL10*, *CXCL12*, *CXCL9*, *FCER1G*, *FCGR1A*, *FCGR3A*, *FGL2*, *GZMB*, *H2-Id*, *H2-Q5*, *H2-T10/H2-T22*, *HBEGF*, *HCK*, *HLA-B*, *HLA-C*, *HLA-DQA1*, *HLA-DQA1*, *HLA-G*, *IFNG*, *IGFBP7*, *IL13RA1*, *IL15*, *IL15RA*, *IL1RN*, *IL1RN*, *IL2RG*, *IL2RG*, *IL6*, *IL6R*, *IL7R*, *IL7R*, *KLRC1*, *KLRD1*, *KLRK1*, *LYN*, *TLR3*, *TNFSF10*, *TYROBP*) (Figure 10). Thus, C3H and BL6 strains displayed similar functional profiles, but differential expression key individual genes within these categories.

The genes in these categories that were differentially or uniquely expressed between C3H and BL6 mice would have a significant impact on the NK cell compartment. NK-cell related genes across these functional categories were loosely

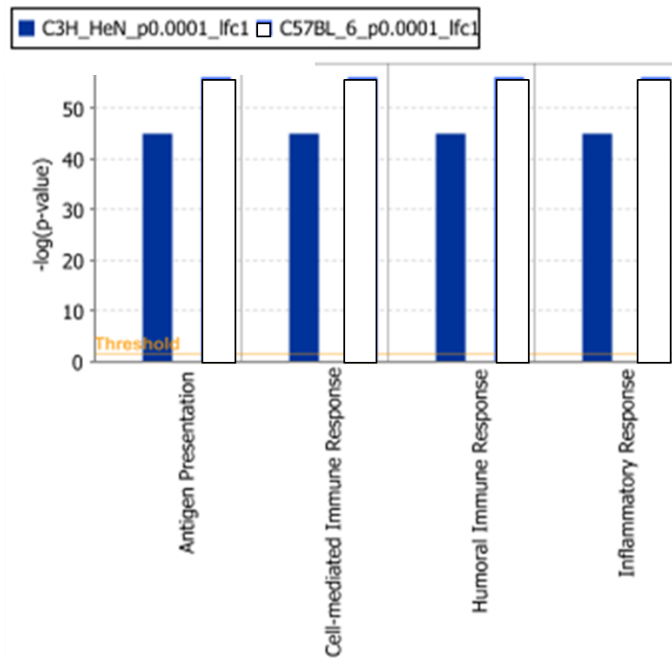
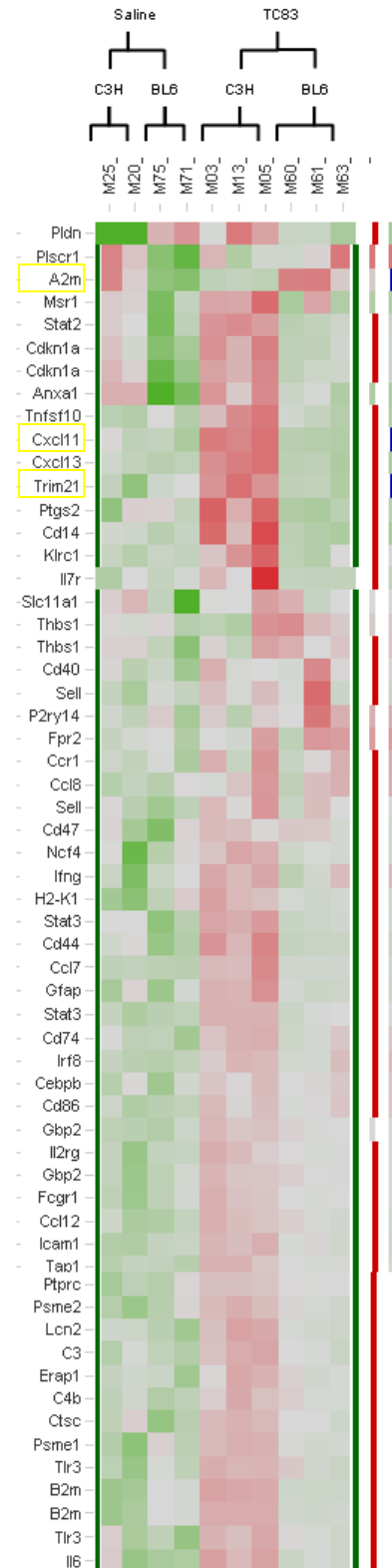
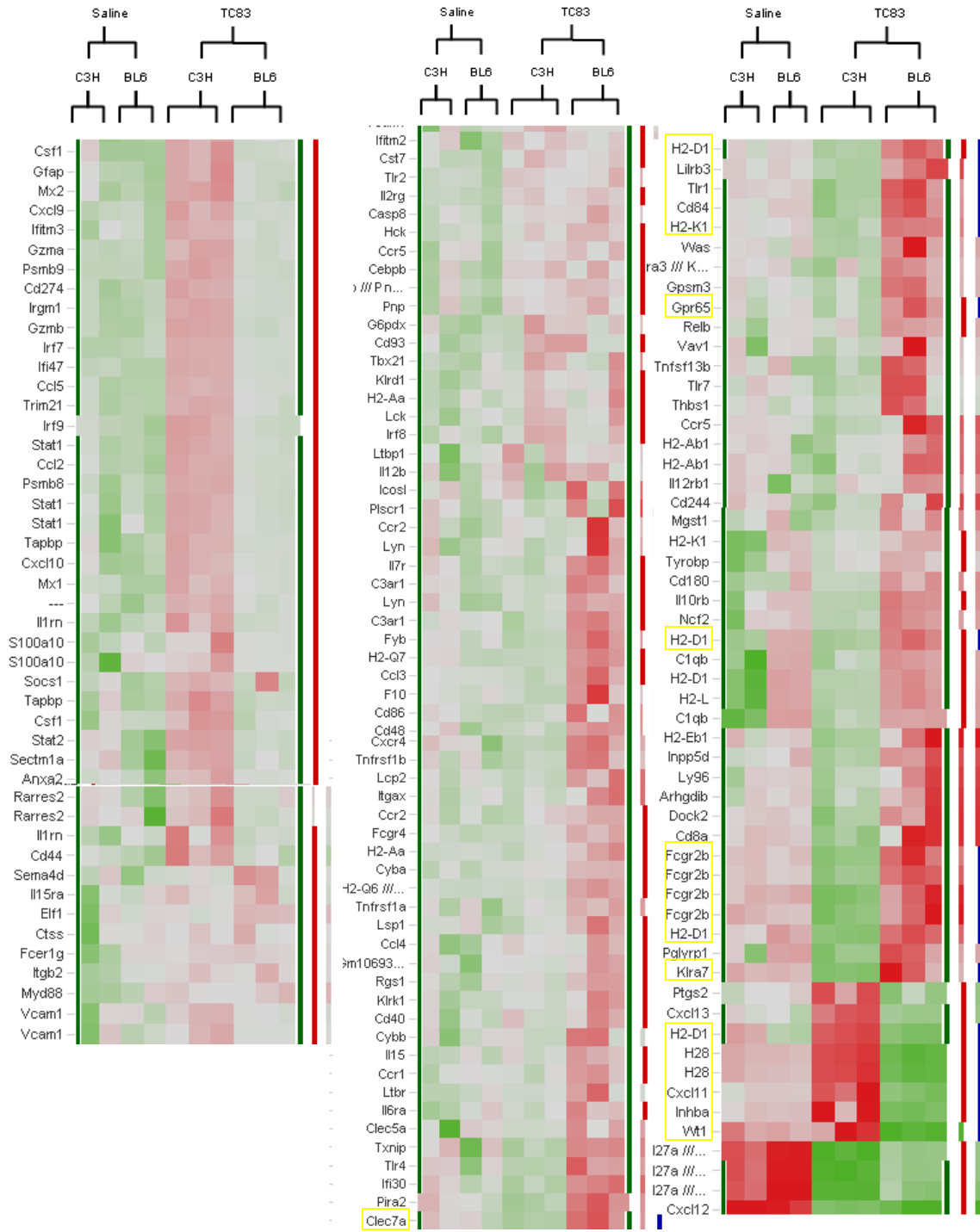


Figure 9: Analysis of top functional categories. Differentially expressed genes involved several overlapping categories related to immune and inflammatory function (antigen presentation, cell and humoral immunity, and inflammatory response) in the brain homogenates of infected mice compared to sham infected mice.

Figure 10: Alterations in immune/inflammatory functional response following TC83 infection of C3H and BL6 mice. Heat map plot of differentially expressed immune/inflammatory transcripts (from functional categories representing antigen presentation, cell-mediated immune response, humoral immune response, and inflammatory response) for C3H and BL6 infected mice. The green bar on the right indicates genes differentially expressed between BL6 and saline control. The red bar represents genes differentially expressed between C3H and saline control. The blue bar represents genes differentially expressed in interaction analysis of C3H and BL6 infected mice. Genes differentially expressed between C3H infected mice and BL6 infected mice are highlighted in yellow. Rows are arranged by hierarchical clustering following Z-score transformation of the normalized data. Columns represent mock-infected and TC83-infected animals at six dpi.. Columns represent mock-infected C3H (M25 and M20), BL6 (M1, M5) TC83-infected C3H (M3, M13, and M5), BL6 (M60, M61, M63) transcripts from brain homogenates at 6 days post challenge.





categorized by typical expression in terms of NK-cell interactions: expressed by NK-cells, expressed by NK-cell targets or indirectly related cytokines and signaling molecules.

NK-cell targets are able to prevent NK-cell mediated cytolysis via expression of inhibitory molecules. Typically, this involves self antigen presentation by classical MHC I molecules that express peptides derived from intracellular antigens. However, the unique microenvironment of the CNS has tissue specific low levels of classical MHC-I, and non-classical MHC-I expression plays an essential role in cellular control in the CNS (129; 142). Natural killer cells are capable of inducing antigen-non-specific cell death and, in the microenvironment of the brain, with tissue specific low levels of inhibitory MHC-I, can have highly pathogenic effects. The more than two-fold differential expression of non-classical MHC class I genes (*H2-LD*, *H2-Q5*, *H2-T10*, *HLA-B*, *HLA-C*, *HLA-DQA1*, *HLA-E*, *HLA-G*) between C3H and sham-infected C3H mice indicates NK-cells could play a pathogenic role in TC83 infection. Interestingly, expression of the non-classical HLA-B genes is more than two-fold lower in C3H mice compared to BL6 indicating a potential deficit in immune control in the brains of these lethally infected mice.

Unique up-regulated expression of other H2 genes, *H2-Q5* and *H2-T24*, was found in TC83-infected C3H mice. The tissue restriction of MHC-Ib molecules is particularly notable in the brain where a higher expression of H2-Q5 is found compared to other tissues in C3H mice (143). A homolog exists in BL6 mice, but has not been characterized and may explain the deficit found in BL6 mice in this experiment. Additionally, C3H mice display a two-fold or greater decrease in *thr1* compared to BL6 mice. Thus, while microarray data indicated a role for NK cells, the protective or pathogenic capacity of this cell population was uncertain.

Literature also reflects a role for H2-Q5 in control of NK-cell populations. Q5k isoforms serve an immune-protective role by donation of their Qdm leader peptide to Qa-1, the molecule capable of inhibiting CD94/NKG2A positive cytotoxic cells, such as NK-cells (143). Q5k isoforms likely play tissue specific roles in regulating immune surveillance, particularly in the CNS where their expression is high. In fact inverse distribution patterns are observed between H2-Q5 and classical H2-K/D in C3H mice. In the brain class 1a transcripts are very rare and H2-Q5 was most abundant. In contrast H2-T23 (Qa1) transcripts were ubiquitously found suggesting the peptides of H2-Q5 play a unique role in the brain. For instance, the presence of functional Qdm in the Q5 leader sequence and subsequent association with Qa1 may predispose binding to CD94/NKG2A receptors thereby inhibiting cytotoxic cells that breach the BBB (143).

Additional genes expressed by NK cells that would generate an inhibitory or activating signal were also differentially expressed. Genes encoding LAIR1, CD16a, and CD32 were more than 2 fold down regulated in C3H mice compared to BL6 mice. LAIR1 is an inhibitory receptor expressed by NK-cells while CD16/CD32 mutations have been linked to susceptibility to viral infection. These factors indicate that control of NK-cells in C3H mice differed significantly from that of non-lethally infected BL6 mice.

The contrast in more robust inflammatory response in BL6 mice and the functional significance of uniquely and differentially expressed genes between infected BL6 and C3H mice indicated alterations in the cellular immune response. Taken together, these data indicated that alterations of the immune response in C3H mice led to lethal outcome, possible related to specific cellular activation or inhibition in the brain. To continue to quantify differences in the host response between lethal and non-lethal infection, we utilized multiplex cytokine arrays to evaluate the differential production of cytokines in the brain.

Cytokine levels indicate T-cell and NK cell involvement in TC83 infection.

Levels of IL-2, an important factor in NK-cell development and maintenance, were lower than control mice at one dpi but significantly higher at six dpi (Figure 11). Resistant BL6 mice only had significantly higher levels at one dpi, but no difference at 6 dpi. The inverse relationship over time in IL-2 levels in the brain could indicate significant differences in maintenance and activation of NK-cell populations between BL6 and C3H mice (Figure 11). BL6 mice also displayed a trend toward a more robust pro-inflammatory cytokine response at one dpi with trends toward elevated levels of MCP-1, KC, IFN- γ , MIP1 α , MIP1 β , IL-1 α , IL-1 β , IL-6, IL-12p40, and RANTES compared to infected C3H mice and sham controls (data not shown).

At six dpi, both KC levels and MCP-1 levels in the brains of C3H mice were significantly higher than in resistant BL6 mice (Figure 12). MCP-1 is an important factor

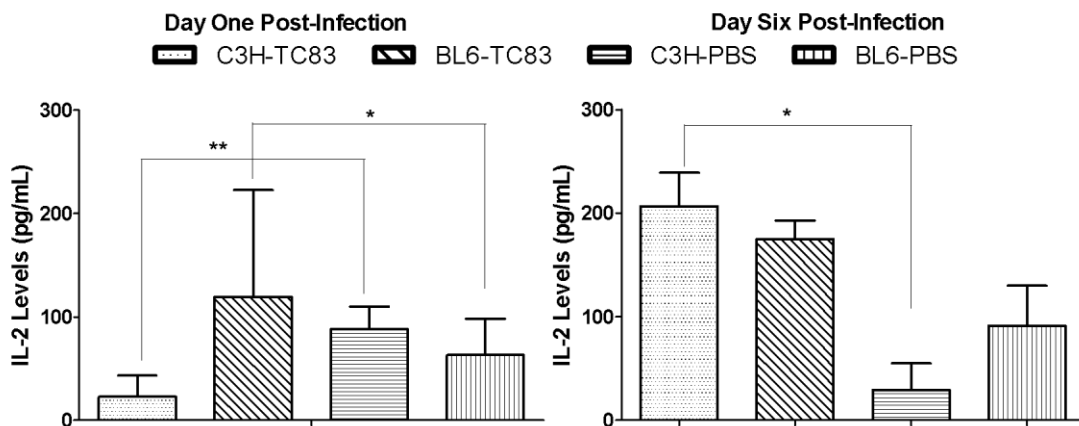


Figure 11: Inverse patterns of IL-2 expression over time in the brain in non-lethal and lethal infections. Lethally infected C3H mice (n=3) demonstrate significantly lower levels of IL-2 at one dpi, but at six dpi have significantly higher levels of IL-2 compared to saline treated C3H mice (n=2). Non-lethal infection of BL6 mice (n=3) results in early, significant increase of IL-2 at one day post-infection compared to saline treated BL6 mice (n=2), but by six dpi is not significantly different from control BL6 mice (*, p<0.05; **, p<0.005 compared to sham-infected controls) (n=3/group).

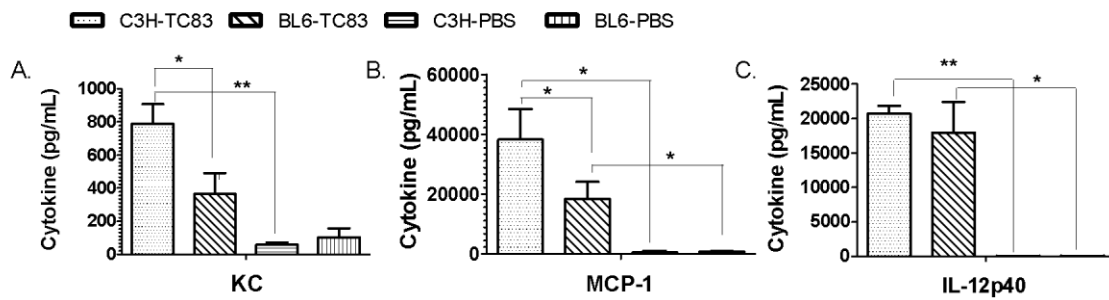


Figure 12: Significant differences in production of KC, MCP-1 and IL-12p40 at six dpi in the brain between lethal and non-lethal infections. (A) KC levels are significantly higher in lethally infected C3H mice compared to non-lethally infected BL6 mice. KC levels in C3H infected mice are significantly higher compared control C3H mice, but not in infected BL6 mice compared to control BL6 mice. (B) MCP-1 levels in infected mice are significantly elevated above control BL6 and C3H mice respectively. MCP-1 levels are significantly higher in lethally infected C3H mice compared to non-lethally infected BL6 mice. (C) IL-12p40 levels are significantly elevated in infected mice, C3H and BL6, compared to C3H and BL6 saline controls respectively (* $p < 0.05$; **, $p \leq 0.005$) (n=3/TC83 group, n=2/saline group).

enhancing NK cells and other monocytic infiltration to the CNS (36). IL-12p40 levels are also significantly elevated in both BL6 and C3H mice compared to sham-infected controls at 6 dpi (Figure 11). The balance between IL-12p40 and other inflammatory cytokines or chemokines, particularly MCP-1, has been shown in other models to be related to outcome to infection (114; 45). Thus, while active monocytic recruitment and activation occurs in both strains, the phenotypic differences in cytokine expression indicate differential activation and recruitment of specific cell populations.

Both strains displayed significant differences in IL-1 β , IL-5, MIP1 β , and RANTES when compared to sham controls (Figure 12, data not shown). In addition, C3H mice display significant differences in IL-1 α , IL-3, IL-6, IL-10, IL-12p70, IL-17, eotaxin, and G-CSF compared to sham control mice at six dpi. No significant differences in IFN- γ expression were observed between groups. However, infected C3H and BL6 mice showed a trend to increased IFN- γ expression (Figure 13).

MCP-1 levels at six dpi were corroborated by microarray assay where levels of *ccl3* and *ccl13* were more than 2-fold increased in infected C3H mice compared to sham controls. Further, MIP1 β , IL-6, and RANTES (*ccl3*, *IL-6*, *ccl5*) transcripts were more than two-fold up regulated in C3H and BL6 mice compared to controls. Additionally, the receptor transcripts for IL-2, IL-6, IL-3, IL-10, IL-17 (*IL-2RG*, *IL-6R*, *CSF2RB*, *IL-10RB*, *IL17RA*) were all 2-fold greater than sham controls.

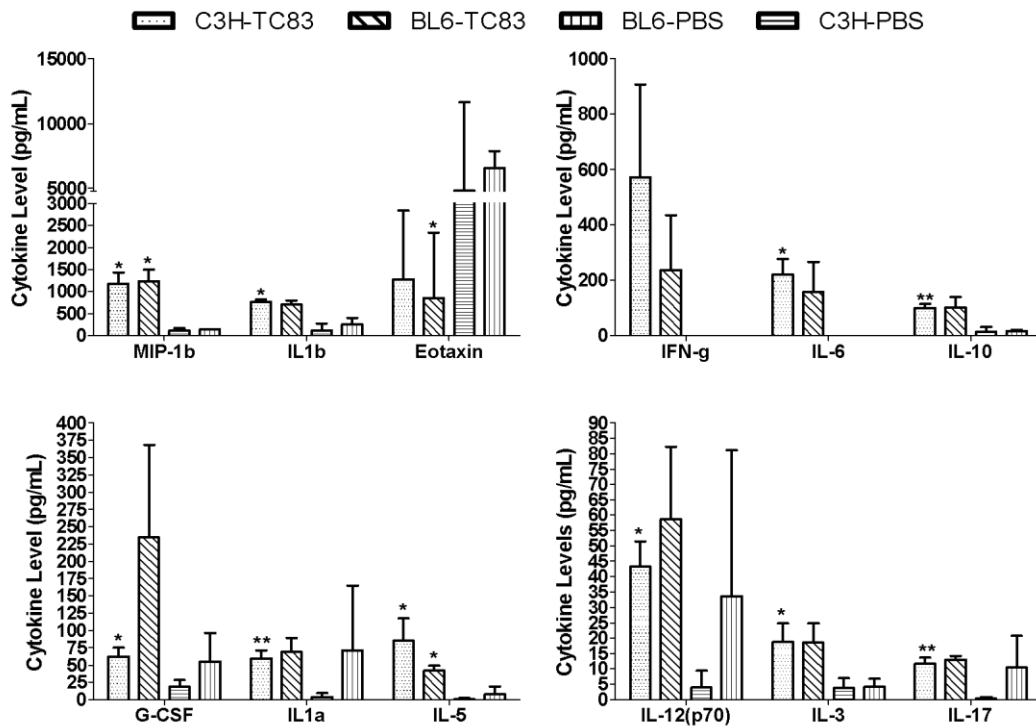


Figure 13: Unique cytokines expression profiles in the brains of C3H and BL6. All comparisons represent infected mice compared to sham control mice. C3H mice display significantly higher levels of MIP-1 β , IL-1 β , IL-1 α , IL-5, IL-10, G-CSF, IL-6, IL-12p70, IL-3, and IL-17 compared to saline treated control C3H mice. In contrast, infected BL6 mice have significant differences only in MIP1 β and IL-5 expression compared to saline treated control BL6 mice. No significant differences in IFN- γ expression were observed between groups though infected mice, C3H and BL6, show a trend to increased IFN- γ expression. Note the changing scale. (* $p < 0.05$, ** $p < 0.005$)

Thus, despite a trend toward a robust pro-inflammatory response in C3H mice, significant production differences in a subset of cytokines suggests alterations in recruitment, maintenance, and regulation of specific cell populations, particularly natural killer cells, between infected and uninfected mice.

Depletion of NK cells reverses the infection outcome in C3H mice.

In order to examine the role of NK cells in TC83-encephalitis, we utilized the common technique of anti-asialo GM1 administration to deplete NK cells from C3H mice prior to and during infection (94) .

An amelioration of disease outcome was observed following NK-cell depletion. NK cell-depleted mice had survival rates of 80-100% in repeated experiments compared to complete mortality in wild-type mice treated with a control rabbit IgG antibody. An initial pilot study demonstrated that depletion of NK cells from immunocompetent C3H/HeN mice (n=3) resulted in 100% survival compared to uniform mortality in undepleted control mice who had a mean day to death of eight days (n=5) (p=0.0082) (Figure 14). NK-cell depletion was confirmed via flow cytometry analysis of splenic lymphocytes (>90%). A repeated study to confirm findings demonstrated 80% survival in infected NK cell depleted mice (n=10) and represented a significant increase over mortality observed in NK cell competent infected mice who had a mean day to death of nine days (n=10) (p<0.0001) (Figure 14). Congruent with survival, mice depleted of NK cells lost significantly less weight than NK cell competent infected positive controls in

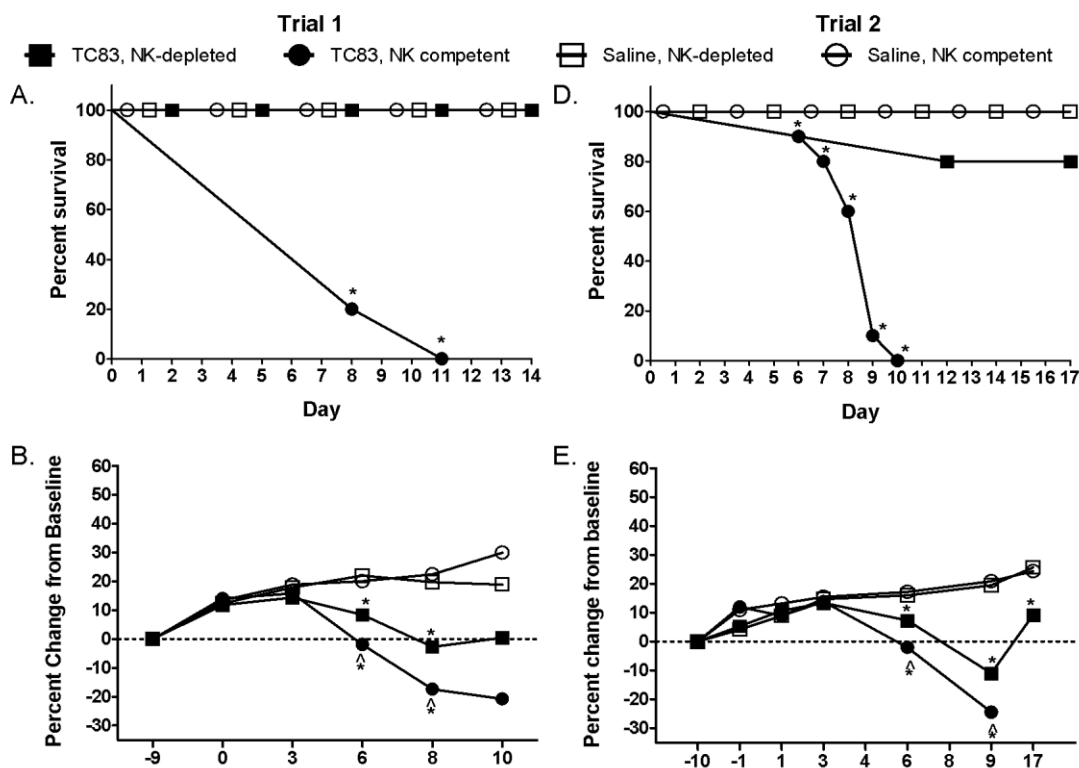


Figure 14: NK cell depletion reverses the outcome of the infection in C3H mice. (A) Depletion of NK-cells from C3H mice (n=3) resulted in 100% survival compared to 100% mortality in NK competent C3H mice who had a mean day to death of eight days (n=5) (p=0.0082). (B) Weight loss was significantly greater in infected NK competent C3H compared to NK cell depleted mice at six and eight dpi. For both infected NK-cell depleted and wt C3H weight loss was significantly greater compared to saline controls at both six and eight dpi. (C) NK-cell depleted mice had 80% survival rate, significantly higher than NK-cell competent mice. (n=10). There was no significant difference in survival between NK-cell depleted, infected mice (n=10) and saline controls (n=4). Survival in NK-cell competent infected mice (n=10) was significantly lower than saline controls (n=4). (D) Weight loss was significantly more in infected NK-cell competent C3H compared to NK-cell depleted mice at six and nine dpi. Significantly greater weight loss in NK-cell depleted mice compared to sham infected, depleted controls was maintained from six through 17 dpi. NK-cell competent C3H infected mice lost significantly more weight compared to saline controls. (*, p<0.05 compared to sham-infected control; ^ p<0.05 compared to TC83-infected group).

both trials. However, NK cell depleted mice still developed symptomatic disease losing significantly more weight than sham infected depleted mice but without developing neurological disease. Between days nine and 17 in the second trial, NK cell depleted mice regained a large percentage of body weight indicating recovery. Treatment with asialo GM-1 antibody alone did not result in clinical symptoms or weight loss compared to mice treated with control rabbit IgG (Figure 14).

Thus, NK cell depletion of C3H mice following TC83 infection results in strong protection against lethal encephalitis.

NK cells may increase viral burden in the host.

By examining viral replication, histological manifestations of encephalitis and cytokine profiles of lethally infected wild-type C3H and surviving NK cell depleted mice, we aimed to gain insight into the mechanism of NK cell action in the brain following TC83-encephalitis. While a high-titer viral load resulted in the brains of both NK cell

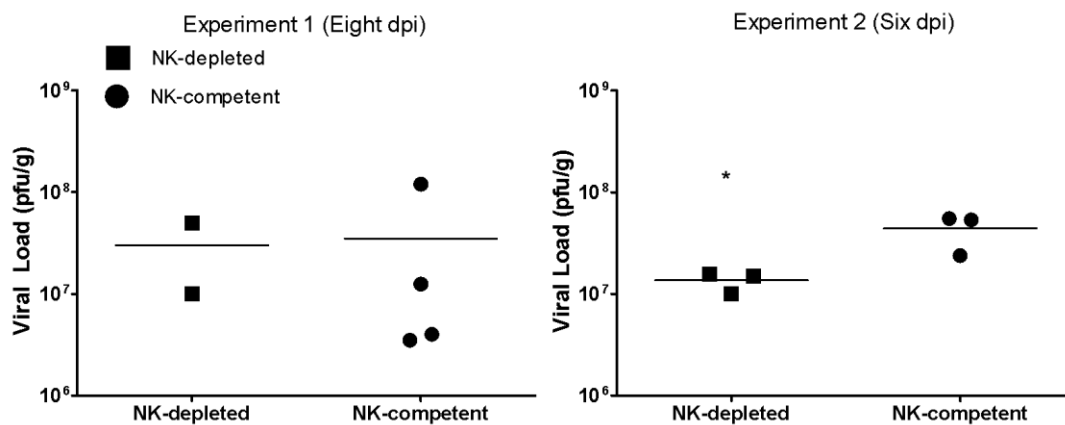


Figure 15: Viral load in the brain at eight and six dpi. (A) Viral load in the brain did not differ between NK-cell depleted and competent mice at eight dpi. Virus was not present in the brains of saline controls. (B) Viral load in the brain was significantly decreased in NK-cell depleted mice compared to NK-cell competent mice at six dpi (p=0.0422). Virus was not present in the brains of saline controls.

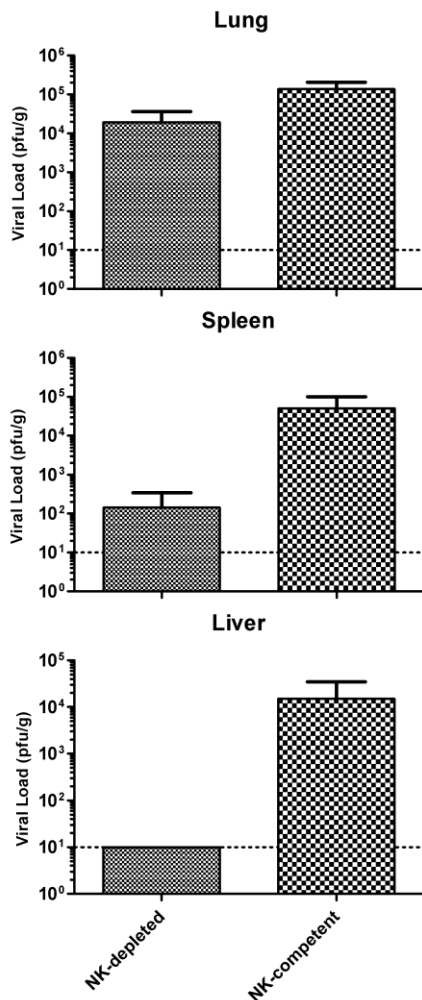


Figure 16: Viral load in liver, lung and spleen at one dpi from TC83 infected NK-cell competent (n=3) and depleted C3H mice (n=3) determined by plaque assay. No significant difference viral load was observed between any group comparison ($p < 0.05$).

depleted and wild-type mice, viral load in the brain was slightly reduced by NK cell depletion at six dpi in the second trial (Figure 15). At day eight post-infection in the first trial, no significant difference was observed (Figure 15). While no significant difference in viral load was noted in the brain at 24 h post-infection, peripheral organ viral titers (liver and spleen) demonstrated a trend toward lower viral load at this time point following NK cell depletion. By six dpi, virus was below the limit of detection and considered cleared from the periphery.

Thus, NK cell depletion appears to have a limited impact on viral load in the brain but significant one on survival.

NK cell depleted and TC83 infected mice develop lethal encephalitis following adoptive transfer of naïve NK cells.

In order to confirm the pathogenic role of NK cells, we performed a gain-of-function experiment by supplementing NK cell depleted C3H mice with naïve NK cells prior to infection.

To successfully transfer NK cells into depleted mice, treatment with anti-asialo GM1 antibody was altered from the previous trial.

Anti-asialo GM1 administration was halted 24

hours prior to infection and counteracted with mouse anti-rabbit IgG (MaR-IgG) administration. A small pilot study confirmed, that survival rates in animals depleted of NK cells in this manner remained higher than control, NK-cell competent C3H (Figure 17). Mice receiving control rabbit IgG (n=2) responded with 50% mortality. The higher mortality rate in this group is not unexpected given the low number of animals. Both mice in the anti asialo-GM1 treated group that were NK-cell depleted survived, as expected from previous experiments. Finally, when anti-asialo GM1 depletion was stopped at the time of infection, typical results occurred despite no further administration of antibody beyond day zero. Both mice in the group depleted of NK cells and receiving

mouse anti-rabbit IgG also survived indicating that altering the treatment schedule had no significant effect on outcome (Figure 17). Though mouse anti-rabbit IgG treated mice showed a trend toward greater weight loss, serum sickness was not a significant issue related to administration of anti-rabbit IgG binding to rabbit anti-asialo GM1 (data not shown).

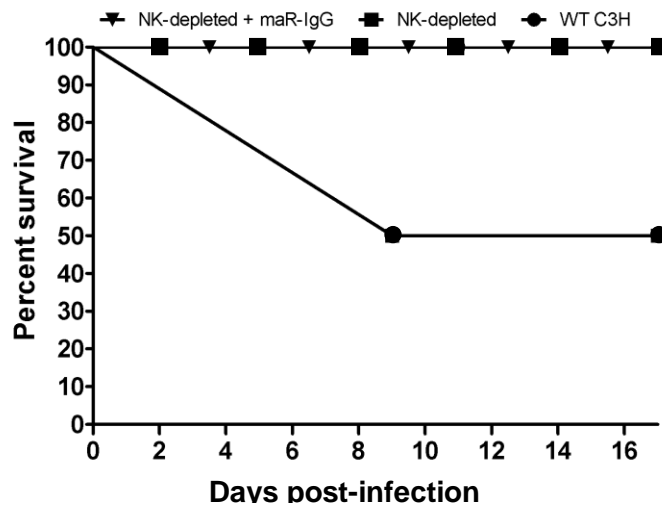


Figure 17: Survival rates are similar when anti-asialo GM1 treatment is halted at one day prior to infection and counteracted with mouse anti-rabbit polyclonal IgG (maR-IgG). C3H mice receiving polyclonal rabbit IgG had 50% mortality (n=2). Mice in the asialo-GM1 treated group that were NK-cell depleted as previously (n=2) responded with with 100% survival. Mice in the experimental group depleted of NK cells and receiving maR-IgG (n=2) responded with 100% survival.

In mice given the same treatment and 10^7 naïve NK cells, mortality increased to 100%. This was a significant difference between groups ($p=0.0495$) (Figure 18). However, upon increasing the number of mice and terminating anti-asialo GM1 treatment of mice at day zero, survival rates in NK cell depleted decreased to 40% (Figure 18). Symptomatic disease in NK-cell recipient mice resulted in weight loss equivalent to that seen in infected, wild-type mice indicating disease phenotype was restored with NK-cell transfer (Figure 18). Thus, adoptive transfer of naïve NK cells to NK cell depleted mice one day prior to infection results in reversion of disease phenotype to that seen in NK-cell competent C3H mice and complete mortality by eight dpi.

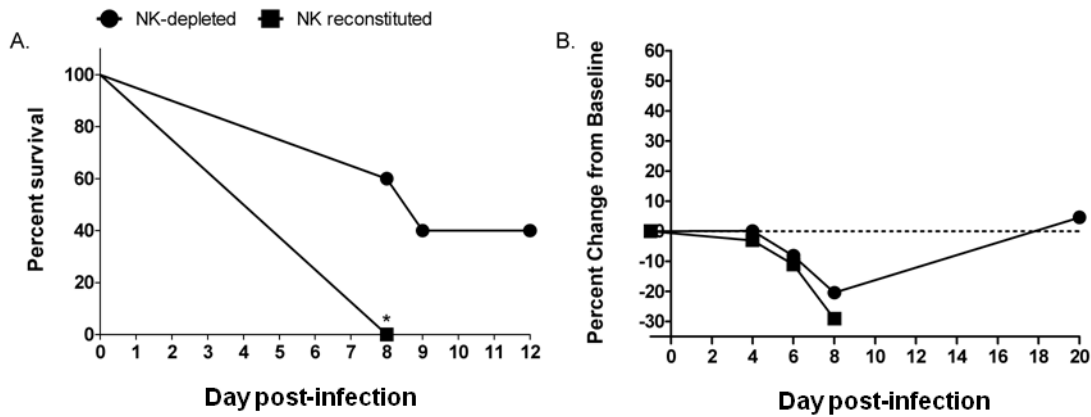


Figure 18: Pathogenesis resulting from reconstitution of naïve NK-cell cells in previously resistant NK-cell depleted C3H mice. Treatment with anti-asialo GM1 antibody was halted one day prior to infection and counteracted with treatment with mouse anti-rabbit IgG. Mice received either 10^7 naïve NK cells ($n=5$) or an equivalent amount of saline ($n=3$) i.p. 24 hours prior to infection. (A) Reconstitution of depleted mice with purified naïve NK-cells, reverted disease phenotype to uniform mortality. This was significantly different than NK-cell depleted mice that did not receive NK-cells that had a 40% survival rate ($p=0.0495$). (B) Weight loss was not significantly different between groups at any time point post infection. Surviving NK-cell depleted mice showed weight gain indicative of survival between eight and 20 dpi.

NK cells do not affect level of inflammation in the brain, but may alter phenotype of infiltrating inflammatory cells.

Histological examination of H&E stained brain tissue demonstrated similarities between infected NK cell depleted and competent mice. Both NK cell depleted and NK cell competent mice had extensive signs of inflammation throughout the brain tissue with diffuse meningitis, increased cellular infiltrates, and perivascular cuffing (Figure 19). However, despite robust pathologies in the brain, NK cell depleted mice survived infection.

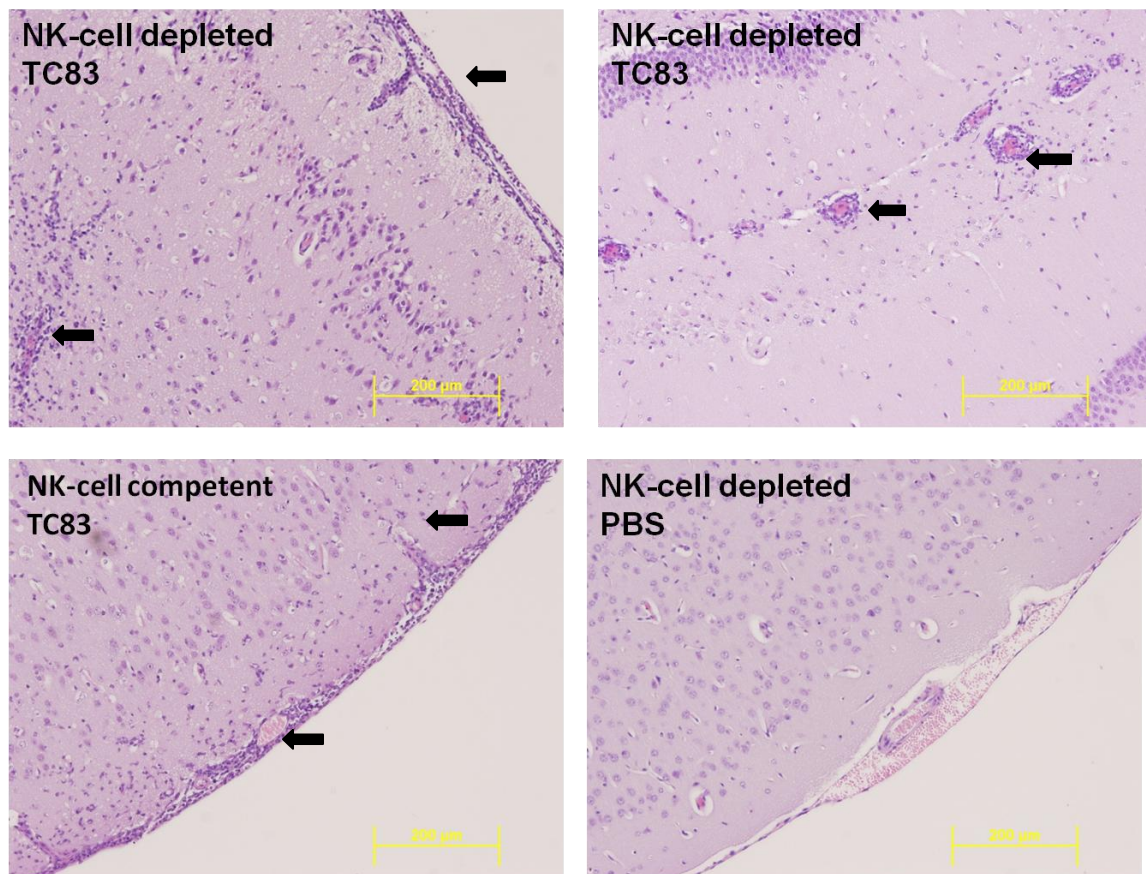


Figure 19: Meningitis and perivascular and vascular cuffing are similar between NK cell competent and NK cell depleted mice at six dpi. Sham infected controls depleted of NK cells demonstrate normal brain architecture.

Table 8: Histological scores of brain tissue from NK cell depleted and NK cell competent C3H mice following intranasal TC83 infection at 6 dpi. Overall score represents the mean of all individual brain sections.

Group	n	Hippocampus	Thalamus	Cerebral Cortex	Olfactory Bulb	Cerebellum	Striatum	Meninges	Overall Score
-NK	3	1±0	1±0	1.67±0.58	1±1.41	0±0	1.33±0.58	1.67±0.58	7±1
+NK	3	1±0	1.67±0.58	2±1	1	0±0	1.33±0.58	1.33±0.58	7.67±2.08

Preliminary flow cytometry data examining the phenotype of inflammatory cells into the brain demonstrated a trend toward increasing numbers of CD4⁺ and B220⁺ cells in the brains of NK-cell depleted infected mice indicating the cell populations may aid in generating a non-lethal infection. Neither sham-infected or NK⁺ cells are shown for the brain analysis as too few events were recorded. Spleens and brains from 3 mice/group were collected and pooled. Cells were isolated by gradient centrifugations from spleen and following collagenase digestion from the brain. Lymphocytes were then labeled with antibodies against specific cell populations (NKp46, B220, and CD4). Analysis was performed by flow cytometry. Lymphocytes isolated from brain and spleens were analyzed by flow cytometry. Splenic CD4⁺ cell populations were decreased in infected mice compared to sham depleted mice, but not sham NK-cell competent mice. Depletion in controls increased B220⁺ and CD4⁺ populations in the spleen (Figure 20). Given the lymphotropic nature of VEEV, the decreased lymphocyte cell counts are not unexpected. In sham infected mice the increased number of the cells may be a compensation mechanism for the missing NK-cell compartment. Note the ablation of NK-cells in the spleens of TC83 and sham infected NK-cell depleted mice.

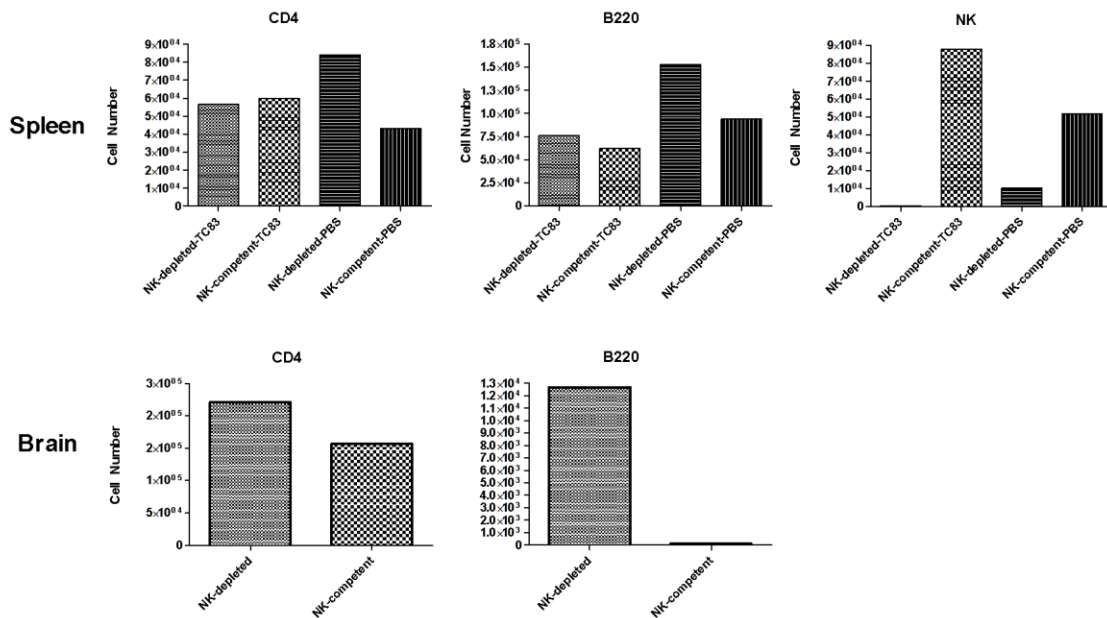


Figure 20: Alterations in the cellular immune response in the brain and spleen following NK-cell depletion and TC83 infection at six dpi. Analysis was performed by flow cytometry and represents cells pooled from 3 mice/group. Splenic B220+ cell populations were decreased in infected mice compared to saline controls, but depletion in saline controls increased these populations compared to saline competent controls. CD4+ cells were increased in infected mice compared to saline, NK-competent controls, but not saline NK-depleted controls. NK-cells are ablated in the spleens of TC83 and sham infected NK-cell depleted mice. In the brain, a trend toward increased infiltration of CD4+ and B220+ cells was observed. NK-cell populations and sham infected controls are not shown in the brain as too few events were recorded for analysis.

ADDITIONAL METHODS

Adoptive transfer

NK cells were isolated from donor C3H mice on day of adoptive transfer. Briefly, 20 donor spleens were removed and single cells suspensions generated by mechanical disruption. Splenocytes were fractionated over Lympholyte-M according to the manufacturer's protocol (Accurate Chemicals, Westbury, NY). The cells were washed

twice in MACS buffer (phosphate buffered sham, pH 7.4 supplemented with 0.5% bovine serum albumin (BSA), 2 mM EDTA) and NK cells were separated by magnetic sorting-based negative selection according to the manufacturer's instructions (AutoMacs, Miltenyi Biotec; Auburn, CA).

Five NK cell depleted mice were injected 24h prior to infection via intraperitoneal (i.p.) route with 5×10^7 NK cells obtained from naïve C3H donor mice and cells were suspended in 100 μ l of sterile phosphate-buffered sham (PBS). At time of transfer, 30 μ L of mouse-anti-rabbit IgG was administered to mice and treatment with anti-asialo GM1 was halted (Jackson Laboratory, Bar Harbor, Maine). As controls for reconstitution experiments, five NK cell depleted mice were inoculated i.p. with 100 μ l of PBS and 30 μ L of mouse-anti-rabbit IgG. At day 0, mice were challenged as previously described.

NK-cell depletion

30 μ l of rabbit anti-asialo GM1 antibody (Wako Chemicals) reconstituted in 1 mL of phosphate buffered saline (PBS) was administered intraperitoneally (i.p.) eight and four days prior to and on the day of infection and post-infection at days four, eight, and 12. Control mice received 30 μ l of polyclonal rabbit IgG at the same time point (Jackson Labs). Two NK cell depleted and two NK cell competent mice were sacrificed and spleens harvested at day 0 and day 6 to confirm NK cell depletion by flow cytometric analysis.

Flow cytometric analysis.

Cells (1×10^6 /tube) were incubated for 10 minutes on ice in 50 μ L blocking buffer (PBS/0.5% BSA). FITC-conjugated CD49b anti-mouse antibody (BD Pharmingen, San Jose, CA) was added (1:100) and cells incubated for 30 minutes at 4°C. Cells were washed in FACS buffer and fixed in PBS/2% formaldehyde for fluorescence-activated

cell sorting (FACS) analysis. Acquisition of data was performed on a FACScan flow cytometer (Becton Dickinson, San Jose, CA) and data analysis with CellQuest software (Becton Dickinson, San Jose, CA). NK cell populations were gated based on forward and side scatter and expression of CD49b. A minimum of 10,000 events were acquired for analysis. Depletion was confirmed at >90% (Figure 20) .

NK cell depletion alters cytokine profiles.

The host cytokine response was also significantly altered in NK cell depleted mice compared to infected wt C3H at both one and six dpi (Figure 23). At 24 hours post-infection, IL-12p40, a proinflammatory cytokine involved in multiple immune functions, was significantly elevated in infected wild-type mice that were not depleted of NK cells compared to infected depleted mice. Infected wild-type mice also had significantly elevated IL-12p40 levels when compared to sham infected wild-type controls. However, NK cell depleted mice showed no difference in IL-12p40 levels compared to sham-infected depleted controls. Thus, the pro-inflammatory response appears to be significantly modified following NK cell depletion and TC83 infection.

Furthermore at one dpi, both RANTES and G-CSF levels were unchanged in NK cell depleted mice compared to controls while NK cell competent mice have significant elevation of both these cytokines compared to sham-infected controls. Thus, early, acute elevation in G-CSF, RANTES and IL-12p40 may act as a marker for mortality in this model. IFN-gamma levels remained the same at one dpi though NK cell depleted mice showed a trend towards elevated IFN-gamma compared to competent infected or sham infected controls (Figure 21).

At six dpi, the host response remained altered. An overall robust pro-inflammatory response was evidenced in both competent and depleted mice. IL-3, IL-4, IL-5, IL-9, IL-10, IL-13, GM-CSF, and IFN- γ levels in NK cell competent animals were

significantly elevated compared to controls (Figure 21). IL-12p70, eotaxin, MIP1 α , MIP1 β , IL-1 α , RANTES were also significantly higher in NK-cell competent animal compared to controls (data not shown). IL-9, IL-10, IL-13, GM-CSF, and IFN- γ are significantly elevated in resistant NK cell depleted mice compared to sham controls (Figure 21). IL-1 α , MIP1 α , MIP1 β , and RANTES are also significantly higher in NK cell depleted mice compared to sham controls (data not shown). Interestingly, NK cell depletion induced significantly higher levels of TNF- α than were observed in sham controls; NK cell competent mice displayed no significant change in TNF- α levels compared to sham controls. NK cell depletion induced a cytokine profile with no significant differences in IL-2, IL-3, IL-4, IL-12p70, and eotaxin at day six post-infection from controls (Figure 21).

Interestingly, IFN- β levels correlated with NK-cell depletion regardless of infection status. The association of IFN- β with NK-cell depletion likely plays a role in the survival of NK-cell depleted mice. The means of IFN- β elevation is unknown, but is possibly due to host compensation for the absent NK-cell compartment. Alternatively, the anti-asialo GM1 treatment used to deplete NK-cells may affect IFN- β production. Regardless, the early elevation of IFN- β likely plays a role in the protective effect of NK-cell depletion in C3H mice (Figure 22).

These cytokines might provide a useful indicator of severe, fatal infection and opens the possibility for use of these cytokines in identification and treatment of viral encephalitis.

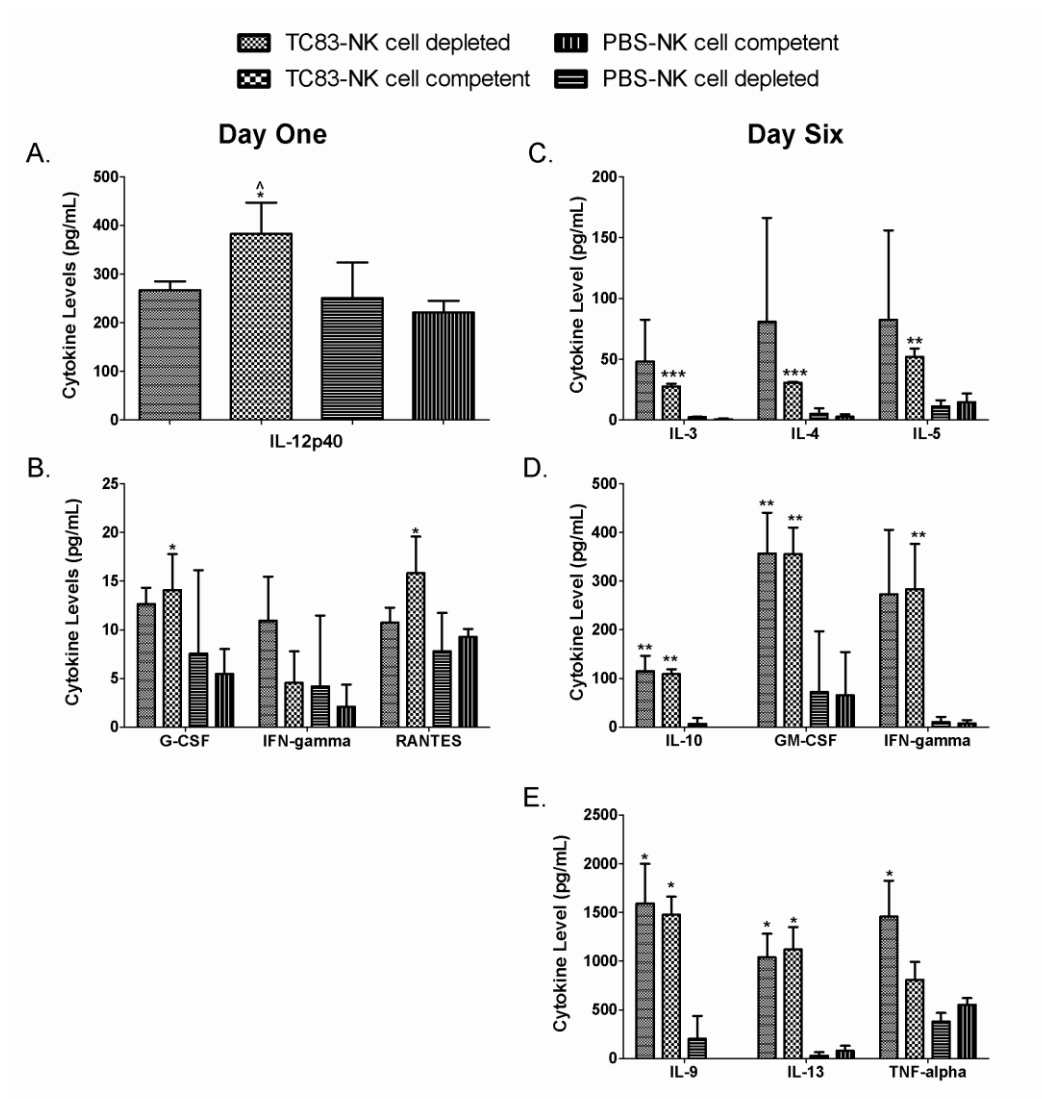


Figure 21: Alterations in cytokine profiles in the brain NK cell competent and depleted C3H at one and six dpi. (A, B) In infected NK-cell competent C3H (n=3), IL-12p40, G-CSF and RANTES levels are elevated above saline controls (n=3). (A) IL-12p40 levels are higher in infected NK-cell competent C3H than depleted mice (n=3). (C) IL-3, IL-4, and IL-5 cytokines are higher in infected wt C3H, but not NK-depleted, than controls. (D) IL-10, GM-CSF, and IFN- γ levels are elevated in infected mice. (E) IL-9 and IL-13 are elevated in infected mice compared to controls. TNF-a levels are only elevated in NK-cell competent C3H. (*, $p < 0.05$, compared to saline control) (^, $p = 0.05$ compared to infected BL6).

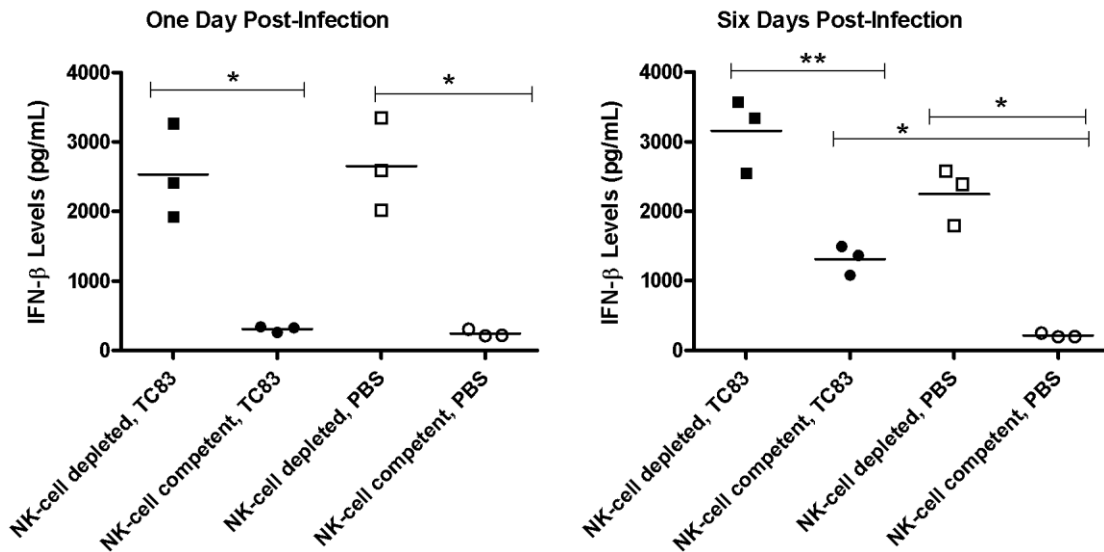


Figure 22: Significantly higher IFN- β production occurs in infected and sham NK-cell depleted mice compared to NK-competent mice at one and six dpi. (A) At one dpi, infected and sham mice depleted of NK-cells show significant elevation of IFN- β compared to infected and sham animals given a control antibody. (B) At six days post-infection, NK-competent, infected mice have significantly higher levels of IFN- β than sham controls. NK-cell depleted mice maintain significantly higher IFN- β levels compared to NK-cell competent mice (* p <0.05, ** p <0.005) (n =3/group).

DISCUSSION

The human vaccine strain of VEEV (TC83) replicates to high levels in brains of C3H and BL6 mice. Furthermore, vaccination with TC83 is associated with poor levels of seroconversion and high numbers of adverse events in humans (4).

Current literature supports lethal intranasal infection of TC83 in C3H mice as a model to evaluate antivirals against VEEV, however, no data is available that would help explain why C3H mice develop lethal disease while other strains do not (87; 89).

The results of these experiments show that qualitative differences in the host response characteristic of lethal infection identify components of the immune system

responsible for neuroprotection or pathogenesis during VEEV-like encephalitis. In our studies sham-treatment of C3H mice was associated with different transcriptome and cytokine profiles compared to lethally infected C3H mice and indicated a potential role for NK cells in pathogenesis. Previous studies of viral pathogenesis following aerosol infection with TC83 suggested that reduced cellular immune response in C3H mice might explain the decrease in rate of virus clearance compared to BALB/c mice though areas of the brain affected by viral antigen were similar (64; 157). However, no work had been performed to evaluate the specific changes in host response required for altered pathogenesis or to examine the correlates of susceptibility to TC83 challenge.

Thus, this study, through transcriptome and cytokine profiles, clearly indicated differences in the host response in the brain of infected vs. uninfected mice. Transcriptome analysis revealed fewer changes in gene expression in the robust immune pro-inflammatory response in C3H mice at the peak of acute infection compared to BL6. For the early host response capable of initial defense and later modulation of an effective adaptive response, only production of type I interferon (IFN) has a well defined role in VEEV-encephalitis (80; 176; 89; 153). Type I IFN, IFN-alpha and IFN beta, production is important early in infection as evidenced by prophylactic, but not therapeutic protection. (89). IFN also plays an important role in NK cell and adaptive immune response activation (163; 161; 162). A later adaptive immune response associated with a protective phenotype to VEEV has been primarily characterized by neutralizing antibody production and generation of IFN-gamma secreting CD4⁺ T-cells (133; 184).

The differential expression of genes involved in control of natural killer cells indicates the importance of appropriate modulation of the immune system in the response of C3H mice to TC83 infection (90). Of particular interest were the changes in non-classical MHC-1 compared to infected BL6 mice that survived infection.

Later elevation of IL-2 in lethally infected C3H mice indirectly relate to NK cell activation. Along with a later increase in IL-2 levels, KC, IL-12p40, and MCP-1 levels are elevated at the peak of acute infection in lethally infected mice indicative of robust recruitment of immune effectors. These cytokines are crucial in recruitment of monocyte cell populations, and IL-12p40 and MCP-1 act in NK-cell recruitment to the CNS. Combined with gene profiles, this evidence suggested natural killer cells as a primary early effector cell population in TC83-encephalitis (110; 20; 19).

A major finding of this study was a novel role for natural killer cells in the pathogenesis of encephalitis in C3H mice. Interestingly, depletion of this cell population resulted in a minimal but statistically significant suppression of viral replication at day six post-infection, possibly indicative of more rapid clearance as seen in BL6 mice.

The mechanism of NK cell induced pathogenesis remains to be determined. NK cells may be acting directly through cell to cell interactions and cellular cytotoxicity as demonstrated for Semliki Forest virus (5). NK cells may also indirectly affect the environment of the brain through cytokine secretion. Alternatively, the phenotype and cell-to cell interactions of NK cells may be altered by the specific strain of mouse either through changes in H2 alleles altering cytotoxicity or by generation of different phenotypes via altered cytokine secretion patterns. Interestingly, MHC-1 expression inhibits SINV replication in a haplotype and allele specific manner between H2^K (CBA) and H2^D (BALB/c) mice (Ref). Alterations in the cytotoxic T lymphocyte response were also observed. H-2^K mice were unable to inhibit SINV in comparison to H2^D. However, single gene transfection of H-2^D MHC 1 in cells expressing H-2^K resulted in resistant cell populations. This occurs at the stage of viral RNA replication and gene expression in the cells (62).

The threshold of infection determined by amplification of the virus at the initiation site of infection is determined by viral replication and the innate host response. Alterations in either result in changes in susceptibilities. However, given the similarities in viral load in survivors and lethally infected mice, this may not be the mechanism in our model. The change in susceptibility to CTL response may explain the response we see in NK-cell depleted mice especially given the similar role MHC plays in control of NK-cell mediated lysis (62). Blastocyte MHC, a MHC Ib gene, is implicated in evasion of some tumor cells from NK cell attack (164). In the context of VEEV infection of the CNS the cellular evasion induced by alterations in NK-cell responsiveness may result in survival. Murine cytomegalovirus resistance has been linked to NK-cells under control of the H-2^k in MA/my mice (181). However, allelic susceptibility conferred substantial differences in control of that virus. This was eventually linked to the MHC class I d locus prompting expansion and activation of NK cells. Thus, NK-cells, anti-viral interferon, and the H-2 locus are linked in the literature in multiple models of infection.

Cytokines indicative of type I IFN production were produced in C3H mice as well as in C3H depleted mice. Given the importance of type I IFN in both resistance to alphavirus infection as well as activation and determination of phenotype for NK cells, the pathogenesis of NK cell populations in C3H mice may be linked to type I IFN.

In summary, these studies provide a unique profile of the host response demonstrating correlates of both a protective and pathogenic host response in the CNS to viral encephalitis. Additionally, a unique role for NK cells in the pathogenesis of TC83-encephalitis was shown for the first time. Nevertheless, the precise mode of action NK cells utilize to induce pathogenesis in the brain of C3H mice remains to be determined.

Chapter 6: A model of viral persistence following acute TC83-encephalitis in mice.

Previous *in vivo* studies demonstrated variable susceptibility of different mouse strains to TC83 encephalitic disease. C3H mice are highly susceptible to disease development after intranasal infection unlike inbred strains (BALB/c and C57BL/6) (64; 157; 89), which become infected but do not develop encephalitic disease. We successfully compared lethal infection in C3H mice to non-lethal infection in BL6 mice to identify NK cells as critical in disease in C3H mice. To determine the basis for resistance in C57BL/6 (BL6) mice to TC83 lethality, we modified the host immune response in key compartments through the use of genetically deficient BL6 mice. Prior data from our laboratory demonstrated that vaccinate BL6 mice are resistant to virulent VEEV infection(134, 188). Vaccinated BL6 mice tolerated a high-level of viral load in the brain without developing encephalitic disease following s.c. infection with virulent VEEV. However, vaccinated α/β T-cell receptor deficient (TCR KO) mice, with defective CD4+ and CD8+ T-cell responses, develop fatal VEEV encephalitis. Adoptive transfer of CD4+ T-cells generated in wild-type vaccinated mice ameliorates the disease in α/β TCR KO mice and demonstrates the importance of the host response (188). Additional literature in conjunction with these studies supports a specific role for T helper type I cells (Th1), IFN- γ secreting CD4+ T cells, as the primary immunoprotective population. Additional studies reveal that neutralizing antibody may not be the primary mechanism preventing pathogenesis in the CNS.

Thus, we hypothesized T-cell activation contributed to protection in BL6 mice following TC83 infection. We utilized intranasal infection with TC83 in α/β TCR KO mice and IL-12p40 KO mice on a BL6 background to determine if these

immunocompromised mice were resistant to TC83 encephalitis. IL-12p40 KO mice have deficits in the IL-12p40 subunit, and lack the ability to generate cytokines, IL-12, IL-23, the bioactive homodimer, IL-12p80 or the agonistic IL-12p40 monomer. IL-12 is integral in the generation of effective innate immunity and acts as a key bridge to adaptive immunity. Specifically, IL-12p40 KO mice have depressed Th1-IFN- γ development (68).

Thus, IL-12 and IL-12 receptor interactions are critical to the functioning of cellular populations identified as key in TC83 encephalitis: NK cells and T-cells. Production of IL-12 is a requisite to developing cell-mediated immune responses to intracellular pathogens. Like NK-cells, IL-12 is a functional bridge between innate and adaptive immune responses, and strongly influences both NK-cell and T-cell mediated immune responses making IL-12 necessary for proper generation of an immune response to VEEV.

CHARACTERIZATION OF A COMPARATIVE MODEL OF VIRAL PERSISTENCE AND CLEARANCE FOLLOWING ACUTE TC83-ENCEPHALITIS IN MICE

TCR KO mice develop acute encephalitis followed by low level, unresolved viral infection of the brain.

In an initial pilot study, we utilized intranasal inoculation of two doses of TC83, 10^7 and 10^8 pfu/mL in TCR KO mice and compared to sham infected TCR KO or TCR KO given SIN/ZPC, a chimeric vaccine candidate with the structural proteins of VEE and the non-structural proteins of Sindbis (130; 131).

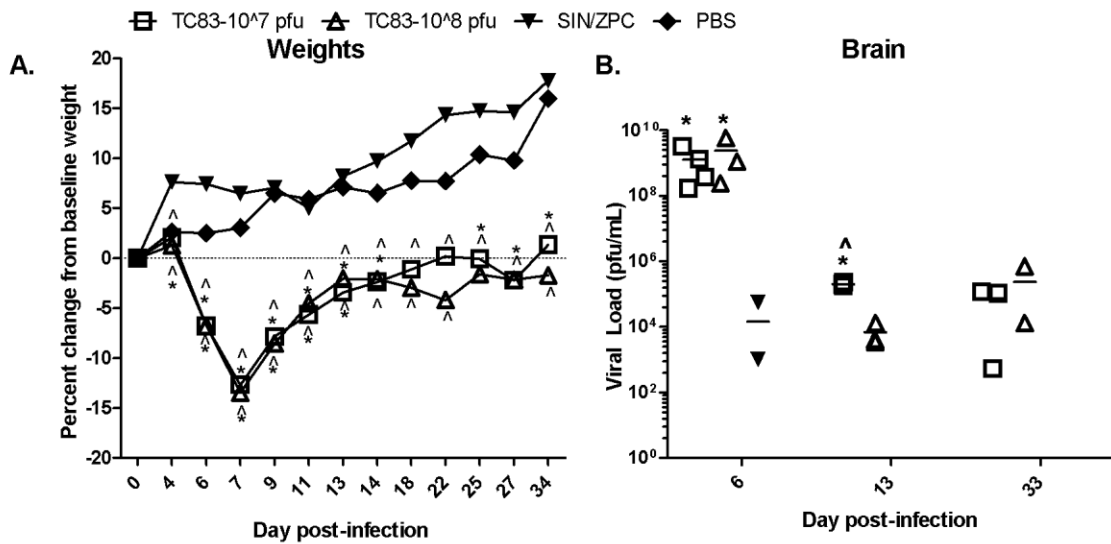


Figure 23: Weight loss and viral load in the brain of TCR KO mice intranasally infected with 10^7 or 10^8 pfu of TC83. Control mice received PBS or 10^7 pfu of SIN/ZPC (n=3/group). (A) TC83 infected TCR KO mice lost significantly more weight than SIN/ZPC or PBS controls and maintained weight loss to 34 dpi. (B) At six dpi, a significantly higher viral load is present in the brains of TC83 infected mice compared to saline controls. SIN/ZPC infected mice display low virus levels. At 13 dpi, TCR KO mice infected with 10^7 pfu TC83 had significantly higher virus levels in the brain than PBS or SIN/ZPC controls. TC83 infected TCR KO mice maintained infectious virus in the brain to 33 dpi. (* denotes group compared to saline; ^, compared to SIN/ZPC) ($p < 0.05$).

Surprisingly, given the highly immunocompromised status of the TCR KO mice, no animals in any group succumbed to infection. However, TC83 infected mice displayed symptomatic disease, TC83 infected TCR KO mice developed infrequent, mild clinical signs of illness, and lost significantly more body weight than control mice (data not shown, Figure 23). This indicated productive infection of mice.

Mice maintained weight from time of initial infection to four dpi. At six dpi, TC83 infected mice had lost significantly more weight than positive (SIN/ZPC) and PBS controls, and maintained significantly greater weight loss to 14 dpi (Figure 23). SIN/ZPC mice maintained initial weight and gained more weight than sham-infected controls

indicative of the high degree of attenuation of the virus. At 14 dpi, mice infected with 10^8 pfu of TC83 were not significantly different than PBS controls, but mice infected with 10^7 pfu were. By 18 dpi, TC83 infected mice had regained weight, but were still significantly lower than SIN/ZPC mice. TC83 infected mice lost significantly more weight than SIN/ZPC infected mice, and maintained greater weight loss until termination of the study. Interestingly, at 25 dpi, mice infected with 10^7 pfu of TC83 displayed a significant drop in weight relative to PBS controls that was maintained till study termination at 34 dpi (Figure 23). Thus, symptomatic disease could be quantified by weight loss in $\alpha\beta$ TCR KO mice though few overt clinical signs of illness were apparent (piloerection, hunching, lethargy, etc.).

When viral load in the brain was examined, TCR KO mice infected with TC83 at 10^7 and 10^8 pfu (4/4, 3/3) developed a high viral load in the brain at six dpi ranging from 10^8 - 10^{10} pfu/g. TCR KO mice maintained infectious virus in the brain at 33 dpi. SIN/ZPC appeared at a low level at 6 dpi, and not all replicates demonstrated plaque-producing virus (2/4). Viral load decreased by 13 dpi in TC83 infected groups (3/3, 3/3) and was absent in SIN/ZPC infected mice (0/2) indicating T-cell independent control mechanisms in resolution of disease. However, at 33 dpi, both groups of TC83 infected mice (3/3, 2/3) maintained a similar viral load to that seen at time of initial resolution (Figure 23). Though TCR KO mice completely survived infection, a chronic brain infection was established in the absence of $\alpha\beta$ T-cells.

TCR KO, but not BL6 or IL-12p40 KO mice develop asymptomatic, non-lethal chronic TC83 infection of the brain.

In order to confirm and better characterize the viral persistence in TCR KO mice, we repeated the study but lengthened the time to termination and included wild-type BL6 mice as controls. We also included IL-12p40 KO mice on a BL6 background to explore

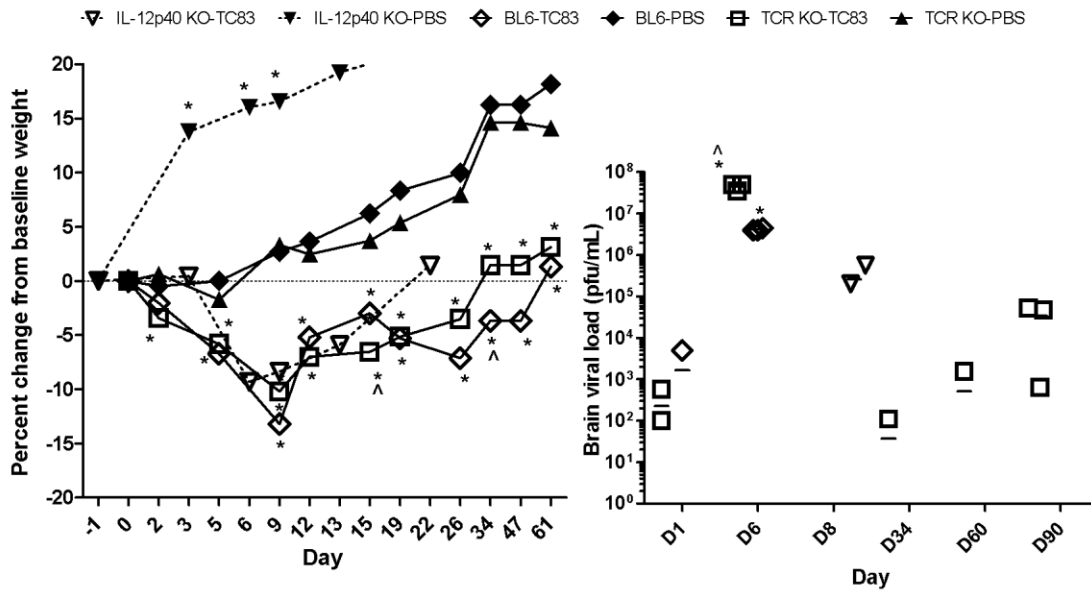


Figure 24: Weight loss and viral load in the brains of TCR KO, IL-12p40 KO, and BL6. (A) TCR KO and BL6 mice maintained significantly greater weight loss than sham controls to 61 dpi. IL-12p40 KO maintained significantly greater weight loss to 13 dpi, and no significant difference was observed by 22 dpi. Dashed line indicates separate experiment. (B) Viral load peaked at six dpi for TCR KO and BL6, but virus was maintained in the brain to 90 dpi in TCR KO mice. IL-12p40 KO mice had an expected viral load at eight dpi. Points represent individual mice (n=3/group) (p<0.05 - * denotes group compared to sham-infected; ^, compared to infected BL6).

the role of T-cell activation in development of chronic disease. In this study, we utilized a dose of 10⁷ pfu/mL of TC83 administered intranasally as few significant differences were observed at the higher dose.

Interestingly, TC83 persisted in the brains of TCR KO mice to 90 dpi, and they maintained similar levels of virus to that found at time of initial recovery. In contrast, no virus was found in the brains of BL6 or IL-12p40 KO mice past eight dpi. In TCR KO, 1:3 replicates had confirmed virus on 34 and 60 dpi, but by 90 dpi 3:3 replicates demonstrated the presence of virus in the brain (Figure 24). Viral load in the brain also

showed a trend toward increase over time in the brains of persistently infected TCR KO mice.

IL-12p40 KO mice recovered from infection more rapidly with weight gain beginning at 9 dpi. Weights were not statistically different between sham and TC83 infected IL-12p40 presented at 22 dpi. In contrast, TCR KO and BL6 mice do not begin to regain weight until 12 dpi, and maintain significantly greater weight loss till termination of the study. The more rapid recovery of IL-12p40 KO than TCR KO or BL6 mice indicated a potentially pathogenic role for IL-12p40 in disease development (Figure 24). Interestingly, significant variations in weight occurred between wild-type BL6 mice and TCR KO mice at 15 dpi and 34 dpi perhaps indicative of alterations in viral load over time in these mice or maintenance of viral load below the level of detection in BL6 mice (Figure 24). Thus, symptomatic disease, as measured by significant weight loss compared to sham controls, developed following TC-83 infection in IL-12p40 KO, TCR KO and BL6 mice, but TCR KO and BL6 mice maintained significantly greater weight loss than controls till end of study.

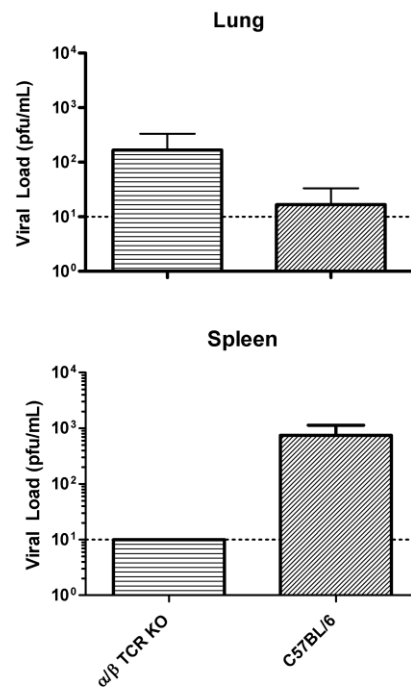


Figure 25: Viral load in the peripheral organs of BL6 (n=3) and TCR KO (n=3) mice infected intranasally with TC83 at six dpi. Virus levels were determined by plaque assay. No virus was found in the liver. No significant difference in viral load was observed in lung or spleen ($p < 0.05$).

Visceral organs, lung and spleen, had low level of infectious virus present during acute infection only at six dpi in few replicates, 1/3 and 2/3 respectively in BL6 mice. TCR KO mice developed detectable levels of virus in the lung only (1/3). Neither BL6 or TCR KO displayed infectious virus in the liver (Figure 25).

Reduction of viral infection in TCR KO mice occurred in the absence of both $\alpha\beta$ T –cells and significant levels of neutralizing antibody, indicative of compensation by other immune effectors such as NK cells (Table 9).

Table 9: Serum neutralizing antibody at 12 dpi in TC83 infected TCR KO and BL6 mice.

Sample	PRNT ₅₀		*Geometric mean titer
	Day twelve post-infection		
Sample	No. positive/total tested (% positive)	Titer range	
TCR KO-TC83	8/9 (100%)	40-160	93
BL6-TC83	9/9 (100%)	640-2560	1351
TCR KO-PBS	0/2 (0%)	<20	1
BL6-PBS	0/2 (0%)	<20	1

*Geometric mean titers are reported as the reciprocal of the serum dilution corresponding to an endpoint of 50% plaque reduction. For PRNT values below the limit of detection (<20), an arbitrary value of 1 was used for calculation.

Characterization of chronic viral isolates

Given the relatively high rate of mutation in replicating alphaviruses, we expected to find significant differences in viral isolates from chronically infected mice. However, initial plaque assay of the virus from chronically infected mice demonstrated no significant differences in plaque size from original inoculums. However, plaque morphology did vary between original inoculum and chronic isolates indicating some changes in viral populations in chronically infected mice (Figure 26).

DPI Chronic infection Original inoculum

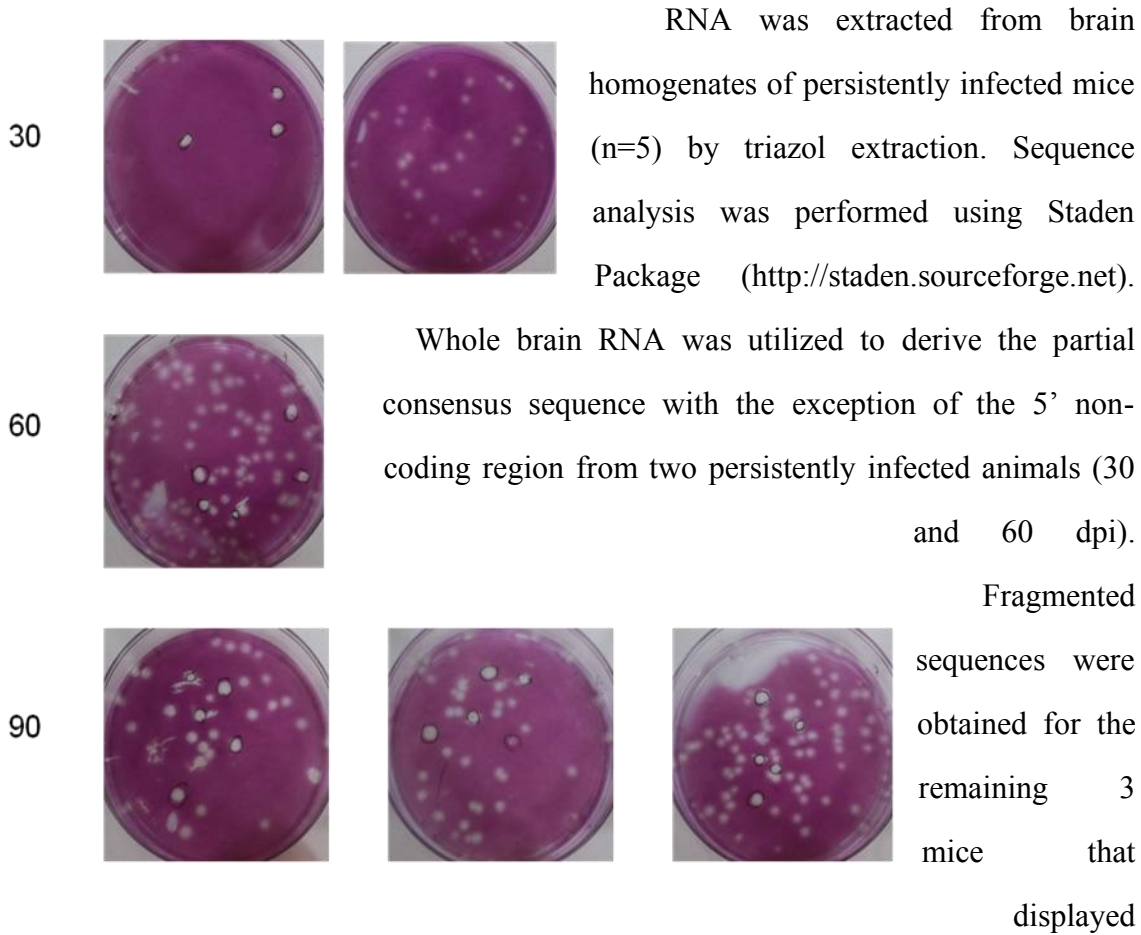


Figure 26: No significant changes in plaque size from original inoculum in chronically infected mice at 30 (n=1), 60 (n=1), and 90 (n=3) dpi. Plaque morphology does differ with some plaques displaying well defined edges and others appearing more unfocused at the periphery. However, all mutations found

in persistently infected mice were also present in the original inoculums, and did not result in any coding changes to the viral genome. Due to degradation of the sample, the 5' non-coding region and additional sequencing from the remaining three mice were not completed.

TCR KO mice display a chronic inflammatory response in the brain.

TCR KO mice display similar encephalitic histological features to BL6 mice at six dpi. However, at 30 dpi signs of inflammation are still present in the brains of TCR KO mice. Interestingly, lymphocytic cuffing of blood vessels and mononuclear cells infiltrates, are apparent in TCR KO mice at 30 dpi (Figure 27). Additionally neutrophilic infiltrates associated with neuronal necrosis are apparent in the brain tissue at this time point.

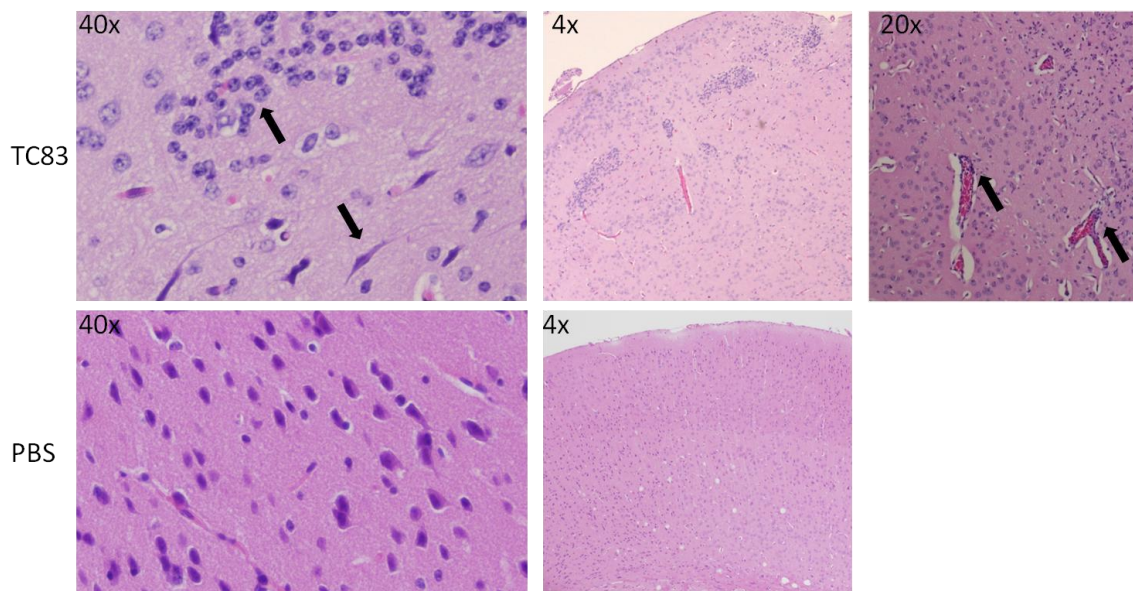


Figure 27: Neutrophil infiltrates, activated microglia, meningitis, and perivascular cuffing in the brains of TCR KO mice infected intranasally with TC83 at 30 dpi. Microglia also show signs of activation with elongated processes.

An on-going pro-inflammatory cytokine response characterizes chronically infected TCR KO mice.

Levels of IL-12p40 are similar at initial time points during acute infection between infected BL6 and TCR KO mice with both significantly elevated compared to controls at six dpi. Only TCR KO mice demonstrated a significant difference compared to controls at 34 dpi. Interestingly, a trend toward maintained of elevated IL-12p40

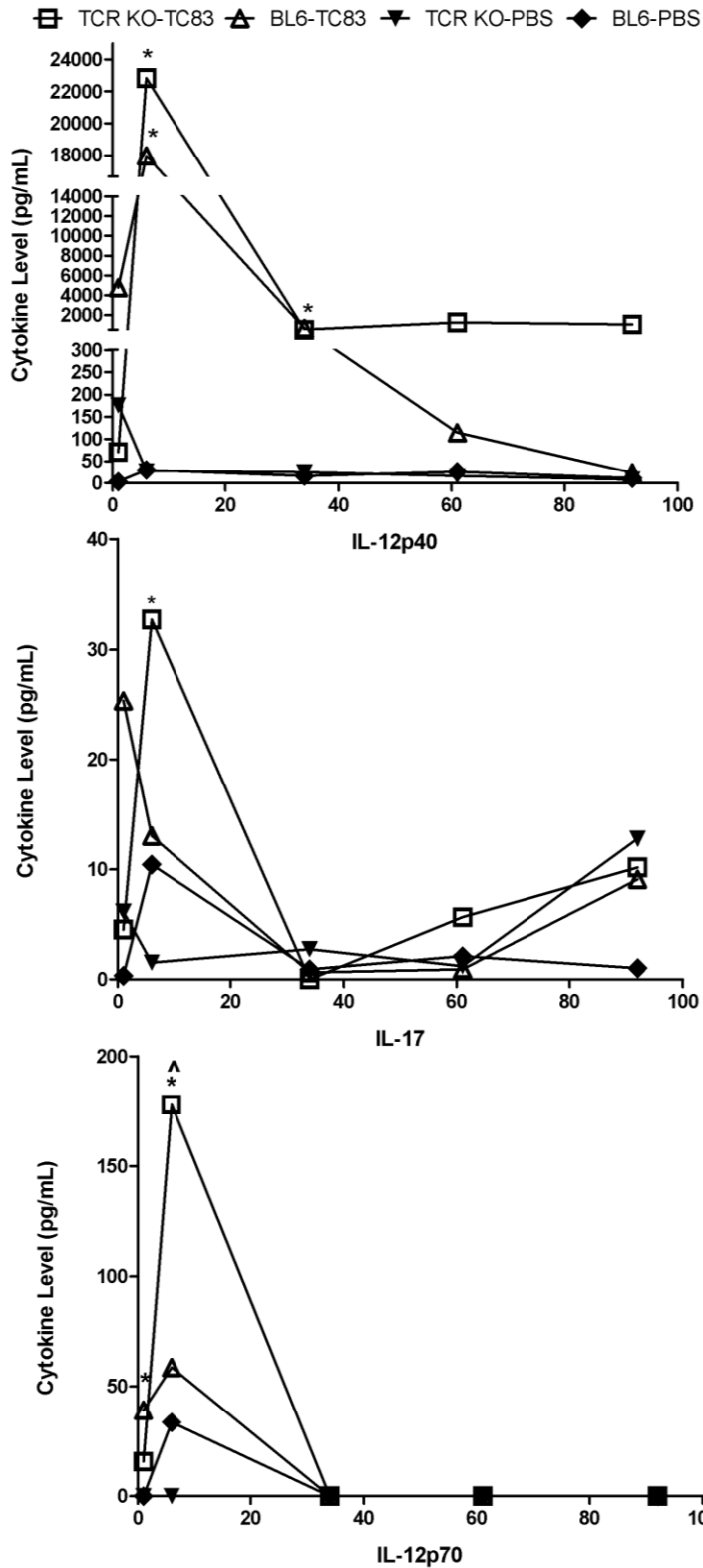
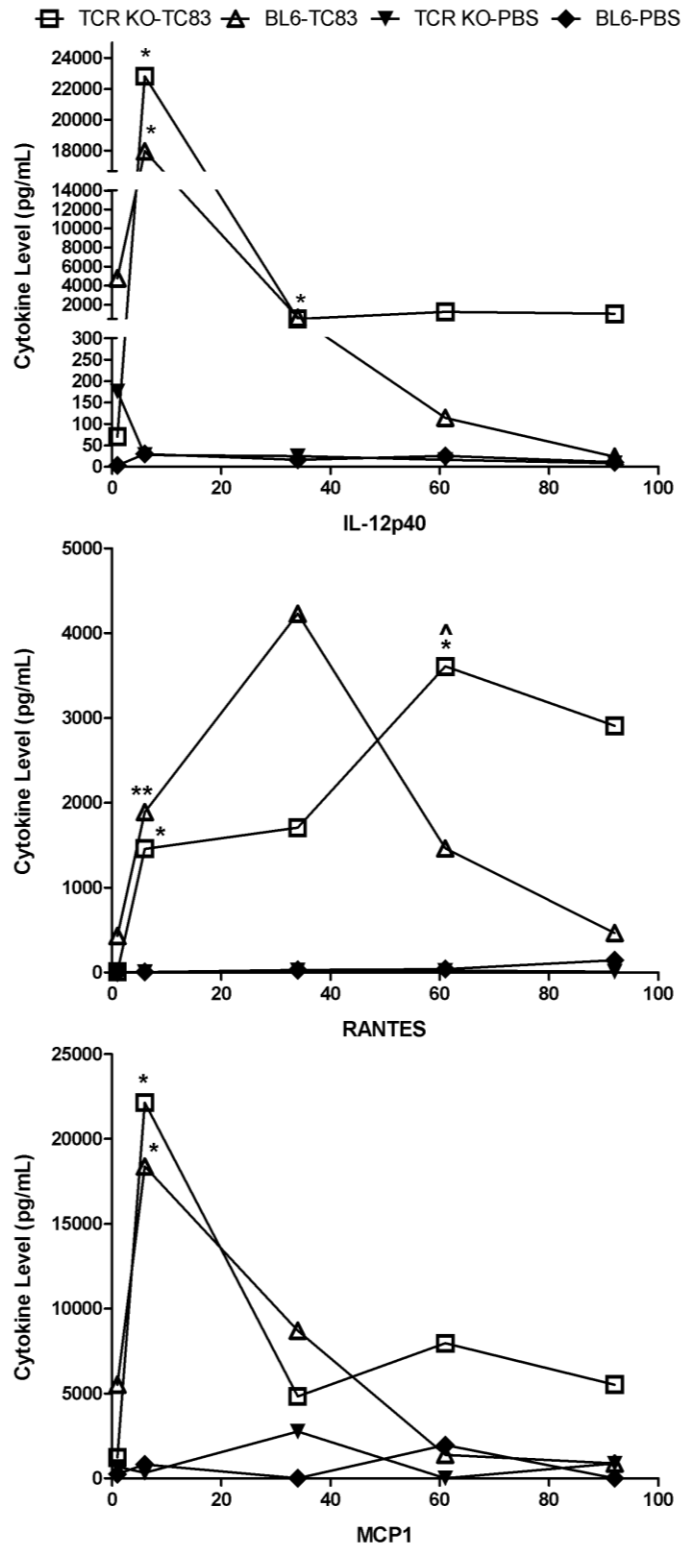


Figure 28: Expression of IL-12p40 and related cytokines over time. IL-12p40 levels are significantly higher than controls in BL6 and TCR KO mice at 6 dpi, but only in TCR KO mice at 30 dpi. IL-17 and IL-12p70 levels are significantly higher in TCR KO mice, but not BL6 at six dpi compared to controls. IL-12p70 levels are significantly higher in infected TCR KO mice compared to BL6. No differences between sham infected and TCR KO mice were observed. (* denotes $p < 0.05$ compared to sham-infected; ^, denotes $p < 0.05$ compared to infected BL6)

Figure 29: Chronic elevation of RANTES, IL-12p40, and MCP1 in the brains of infected TCR KO mice. IL-12p40 is significantly different from controls at six and 30 dpi in TCR KO mice. RANTES is significantly different at six and 60 dpi TCR KO mice compared to controls. In addition, RANTES is significantly higher compared to infected BL6 mice.



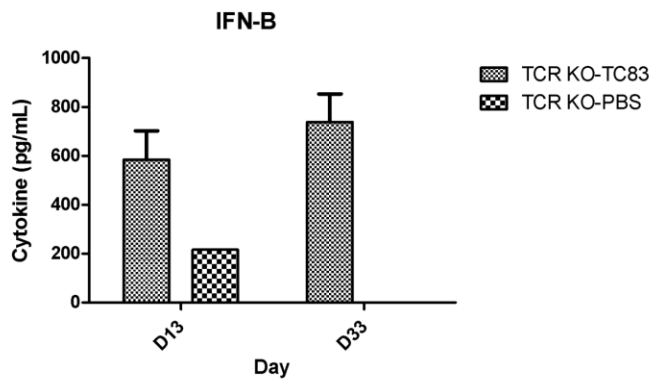


Figure 30: IFN- β levels in the brains of infected and sham infected TCR KO mice at 13 and 33 dpi (n=3/group). IFN- β levels display a trend toward elevation at 13 and 33 dpi compared to sham-infected controls. No significant difference between groups was observed. (p<0.05).

levels was demonstrated at 61 and 92 dpi while in contrast BL6 mice demonstrate a trend toward steady decline from six dpi through 92 dpi. These levels are not contributing toward IL-12p70 levels in late infection in TCR KO as these mimic BL6 and demonstrate a steady decline to baseline. Indirectly, IL-12p40 production is not attributed to IL-23 generation as IL-17 levels demonstrate the same declining

trend from 6 dpi onward (Figure 28). RANTES and MCP-1 demonstrate the same trend toward maintenance of elevated levels during chronic infection (Figure 29). IFN- β levels also remain elevated in chronically infected TCR KO mice to 33 dpi (Figure 30). In contrast, the cytokine levels in BL6 mice steadily drop from six to 60 dpi returning to baseline by 90 dpi (Figure 29). The delayed return to baseline indicates BL6 mice may maintain virus below the limit of detection by plaque assay; however, the slow decline could be attributed to regenerative process in the brain.

Cytokine profiles identify chronically infected TCR KO mice.

At one dpi, IL-10 and IL-5 were significantly higher than controls in TCR KO mice while in BL6 mice IL-10, IL-5, IL-3, IL-12p70, and GM-CSF were all significantly higher than sham controls indicating an early and more robust immune response in wild-

type mice. IL-10, IL-5, IL-3 and TNF- α levels were all significantly higher between infected TCR KO and BL6 mice (Table 10).

Table 10: Cytokine protein levels at one, six, 30, and 90 dpi that are significantly elevated ($p < 0.05$) in : (1) chronically infected TCR KO mice compared to sham (2) BL6 infected compared to sham (3) TCR KO infected animals compared to BL6 infected.

DPI	TCR KO (TC83/Saline)	BL6 (TC83/Saline)	TC83 (TCR KO/BL6)
1	IL-10 IL-5	IL-10 IL-5 IL-3 IL-12p70 GM-CSF	IL-10 IL-5 IL-3 TNF- α
6	IL-1a IL-1b IL-2 IL-3 IL-4 IL-5 IL-6 IL-10 IL-12p40 IL-12p70 IL-17 IL-13 GM-CSF MCP-1 MIP-1a MIP-1b RANTES	IL-1b IL-3 IL-5 IL-12p40 GM-CSF MCP-1 MIP-1b RANTES	IL-1a IL-1b IL-6 IL-12p70 KC
30	IL-12p40 TNF- α	IL-13	
60	RANTES		RANTES

At six dpi, TCR KO had significantly higher levels of IL-1 α , IL-1 β , IL-2, IL-3, IL-4, IL-5, IL-6, IL-10, IL-12p40, IL-12p70, IL-17, IL-13, GM-CSF, MCP-1, MIP-1 α , MIP-1 β , and RANTES. In contrast, comparison of BL6 to sham controls demonstrated

only IL-1b, IL-3, IL-5, IL-12p40, GM-CSF, MCP-1, MIP-1b, and RANTES as being significantly greater. IL-1 α , IL-1 β , IL-6, IL-12p70 and KC levels were significantly different between infected TCR KO and BL6 groups at this time point (Table 10).

By 30 dpi, the acute highly proinflammatory phase of cytokine production had decreased and only IL-12p40 and TNF- α remained significantly higher than controls for TCR KO mice. BL6 mice maintained elevated levels of IL-13 compared to controls. At 60 dpi, only RANTES remained significantly elevated from controls in TCR KO mice; this was also significantly higher than BL6 infected mice (Table 10). No significant changes were observed at 90 dpi.

Whole transcriptome analysis of the brain indicates significant alterations of the host response.

Whole transcriptome analysis of TCR KO mice compared to sham controls and BL6 mice compared to sham-infected controls at the peak of acute infection, six dpi, revealed multiple genes with greater than two fold differences. Unsurprisingly, transcripts for CD3g and CD8a were not present in the brains of TCR KO mice, but were expressed at levels two fold higher in infected BL6 mice. However, the gene encoding the IL-12 receptor β -1 that the IL-12p40 subunit uses in signaling, *IL-12RB1*, was not altered in comparison to sham controls in TCR KO mice but was more than two-fold greater than controls in wild-type BL6 (**Error! Reference source not found.**). In addition, several other genes were uniquely expressed in BL6 mice that are indirectly related to IL-12R β -1 signaling. These include: *IL-6R*, *ITGAX*, *TLR4*, and *TBX21* genes. IL-6/IL-6R interactions are related to T-cell activation and effector function, and TLR4 is directly related to production of IL-12 subunits and IL-12 related cytokines. *TBX21* encodes t-bet, a transcription regulator, that stimulates production of IL-4, IL-17a, and IFN- γ . All three cytokines are integral to

Table 11: Fold change in IL-12p40 and related cytokine gene expression in infected BL6 and TCR KO mice compared to sham controls.

Unique gene expression					
BL6/Saline			TCR KO/Saline		
Symbol	Fold Change	p-value	Symbol	Fold Change	p-value
CD3G	5.51	1.26E-05	CCR7	3.81	3.10E-05
CD8A	2.90	2.13E-05	IL1b	3.07	3.35E-06
IL12RB1	5.54	3.93E-06			
IL6R	3.26	2.50E-06			
ITGAX	5.32	3.24E-05			
TLR4	2.96	2.18E-07			
TBX21	2.52	9.22E-05			
Shared gene expression					
CCL5	339.28	2.13E-12	CCL5	318.09	2.54E-12
CD40	4.04	1.51E-07	CD40	4.56	6.36E-08
CD44	14.12	5.28E-07	CD44	8.34	3.65E-05
CD86	12.47	1.83E-07	CD86	7.64	9.51E-07
CEBPB	9.27	3.54E-07	CEBPB	6.02	4.13E-06
CSF2RB	6.79	2.09E-05	CSF2RB	4.56	2.34E-05
CXCL10	899.48	1.01E-12	CXCL10	1087.06	8.11E-13
CXCL9	205.79	3.67E-10	CXCL9	210.42	3.90E-10
FCER1G	37.09	3.39E-08	FCER1G	27.48	9.74E-08
FCGR3A	87.37	8.32E-09	FCGR3A	20.25	5.32E-07
ICAM1	29.58	4.50E-10	ICAM1	40.96	1.93E-10
IFNAR2	4.98	6.89E-07	IFNAR2	3.14	2.33E-05
IFNG	11.89	1.65E-06	IFNG	5.76	5.63E-05
IL10RA	4.98	3.11E-06	IL10RA	4.26	1.13E-05
IL12B	16.55	6.74E-05	IL12B	40.13	2.61E-05
IL15	4.88	5.69E-09	IL15	4.80	7.29E-09
IL15RA	4.11	4.49E-06	IL15RA	4.29	4.67E-06
IL2RG	68.97	1.20E-09	IL2RG	50.82	5.76E-09
IL6	18.58	3.12E-08	IL6	102.05	3.43E-10
IRGM	120.00	1.47E-11	IRGM	123.08	1.58E-11
KLRK1	6.65	7.29E-09	KLRK1	3.40	7.10E-07
STAT1	93.18	4.41E-11	STAT1	78.20	7.33E-11
STAT2	19.95	8.23E-08	STAT2	23.42	3.30E-08
STAT3	9.15	8.79E-09	STAT3	7.07	5.68E-08
TLR2	6.91	1.18E-05	TLR2	12.58	1.18E-06
TNFRSF1A	6.57	2.73E-06	TNFRSF1A	4.06	5.75E-05
TNFRSF1b	4.94	7.19E-07	TNFRSF1b	4.65	1.38E-06
VCAM1	7.92	6.37E-06	VCAM1	6.35	3.42E-05

an effective T-cell response. Expression of *ITGAX*, encoding CD11C, is also indicative of a Th1 mediated response, particularly given the ability of IFN- γ to induce CD11c expression in microglia. Interestingly, the chemokine receptor gene *CCR7* is uniquely expressed in TCR KO. However, T-cells, B cells, mature dendritic cells, and, importantly, microglia express the receptor. *CCR7* aids cells in migration of these cells to cognate ligands, CCL19 and CCL21 (**Error! Reference source not found.**).

T-cell absence mediates a chronic infection and inflammatory response of the brain.

We demonstrated long-term viral replication occurred in the brain of TC83 infected mice without causing clinical signs of encephalitis. This coincided with maintenance of inflammation in the brain and elevated levels of proinflammatory cytokines. The chronic host response identified infected mice. This established a novel model to study the impact of chronic viral infection on brain function. While IL-12p40 was not essential to survival, mice deficient in the subunit recovered more rapidly indicating a pathogenic role for IL-12p40.

A PROPOSED ROLE FOR IL-12P40 IN TC83 INFECTION OF BL6 AND C3H MICE.

IL-12p40 was implicated in the described TC83 studies through the more rapid recovery of IL-12p40 KO mice than wild-type BL6 or TCR KO following TC83 infection (Figure 24). In addition, non-lethally infected, NK-cell depleted C3H mice have lower levels of IL-12p40 than lethally infected NK-cell competent mice, and IL-12 receptor transcript levels are depressed in C3H and TCR KO mice compared to BL6 (Figure 21, Figure 10, Table 11). These factors indicated IL-12p40 might be important to disease development. Thus, *we hypothesized IL-12p40 was pathogenic in C3H and BL6 murine models.* To test our hypothesis, we used IL-12p40 KO on BL6 background that are resistant to TC83 infection (Jackson Laboratories, B6.129S1-II12btm1Jm/J) and

lethal infection of C3H mice. We supplemented mice with daily 300 ng/mouse in 200 uL PBS of IL-12p40 monomer give i.p. (Cell Sciences CN# CRI199B). Five treatment groups were used:

1. Early treatment from zero-four dpi, infected with TC83
2. Late treatment from three to eight dpi, infected with TC83
3. Untreated, infected with TC83
4. Early treatment from zero-four dpi, infected with PBS
5. Untreated, infected with PBS

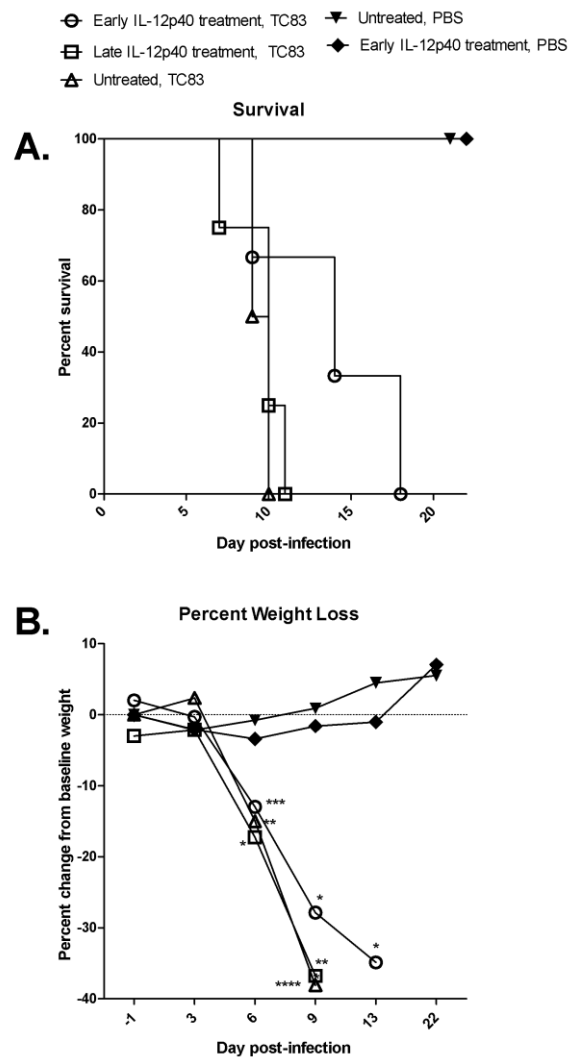
Dividing early and late treatment allowed exploration of innate vs. adaptive role for IL-12p40. Mice were infected intranasally with TC83 as previously described and survival, disease development, and viral load in the brain evaluated.

IL-12p40 treatment of C3H mice extends mean time to death, lessens disease, and reduces viral load in the brain.

IL-12p40 treatment of C3H mice had no significant effect on survival curves, and all TC83 infected groups were similar. A significant increase in survival was observed between sham infected controls and TC83 infected groups ($p < 0.05$) (Figure 31). However, early IL-12p40 treatment extended time to death in C3H mice (MTD=14) compared to untreated mice or mice receiving later IL-12p40 treatment (MTD=9, MTD=10). A decrease in symptomatic disease correlated with the longer survival time in mice treated early in infection. Symptomatic disease in mice treated early in infection slowed weight loss, and animals showed a trend toward less weight loss than either untreated mice or mice in the late treatment group. The extended time to death and decrease in symptomatic disease indicated IL-12p40 might play an early, protective role in infection.

Interestingly at eight dpi, viral loads in the brain showed a trend toward decrease in the IL-12p40 treated groups compared to untreated mice or mice in the late treatment group (Figure 32). There was no significant difference in viral load for any group comparison ($p < 0.05$). Thus, IL-12p40 may help in generating an anti-viral state in the brain.

Figure 31: IL-12p40 treatment of C3H mice delays time to death and reduces symptomatic disease following intranasal TC83 infection. Two treatments were given to TC83 infected mice; the early treatment group received 300 ng of IL-12p40 daily from zero to four dpi and the late treatment group from five to eight dpi. (A) TC83 infected C3H mice treated early (n=3) had a MTD of 14 dpi. The late treatment (n=4) and untreated (n=2) infected mice had MTD of 10 and 9 dpi respectively. Untreated (n=3) and treated (n=2) sham infected mice survived completely. There was no significant difference in survival curves in TC83 infected mice ($p < 0.05$). (B) Infected mice treated early lost less weight than untreated or late treatment groups. (* represents comparison to PBS control, * $p < 0.05$, ** $p < 0.005$, *** $p < 0.001$, **** $p < 0.0001$)



IL-12p40 treatment of IL-12p40 KO mice reduces symptomatic disease and viral load in the brain.

Like TCR KO and BL6, IL-12p40 KO mice completely survived lethal brain infection. However, symptomatic disease as measured by weight loss varied by treatment group. IL-12p40 KO mice receiving early treatment with IL-12p40 monomer recovered more rapidly from infection than mice receiving a later dosage regime or untreated mice. Mice treated early did display symptomatic disease dropping significantly more weight than treated, sham infected controls. However, weight was only significantly lower than control at 6 dpi, and no significant difference was observed in weight at nine to 22 dpi. In contrast, mice in the later treatment group maintained significantly greater weight loss than treated controls from six through 12 dpi. Untreated, infected mice maintained significantly more weight loss than sham, untreated controls beginning at three dpi and lasting through 12 dpi. IL-12p40 monomer treatment did demonstrate trend toward toxic effect on treated sham controls as these mice maintained significantly lower weight than sham, untreated counterparts till 22 dpi. Thus, early protection may be partially mediate through IL-12p40 dependent mechanisms (Figure 33).

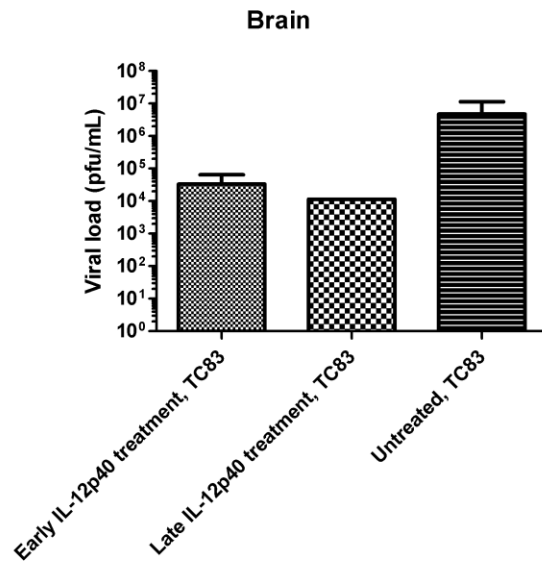


Figure 32: IL-12p40 treatment of C3H mice reduces viral load in the brain following TC83 infection at eight dpi. Both early (n=3) and late (n=1) treatment groups displayed a trend toward lower viral load in the brain at 8 dpi compared to untreated, infected mice (n=2). No significant differences were observed for any group comparison ($p < 0.05$).

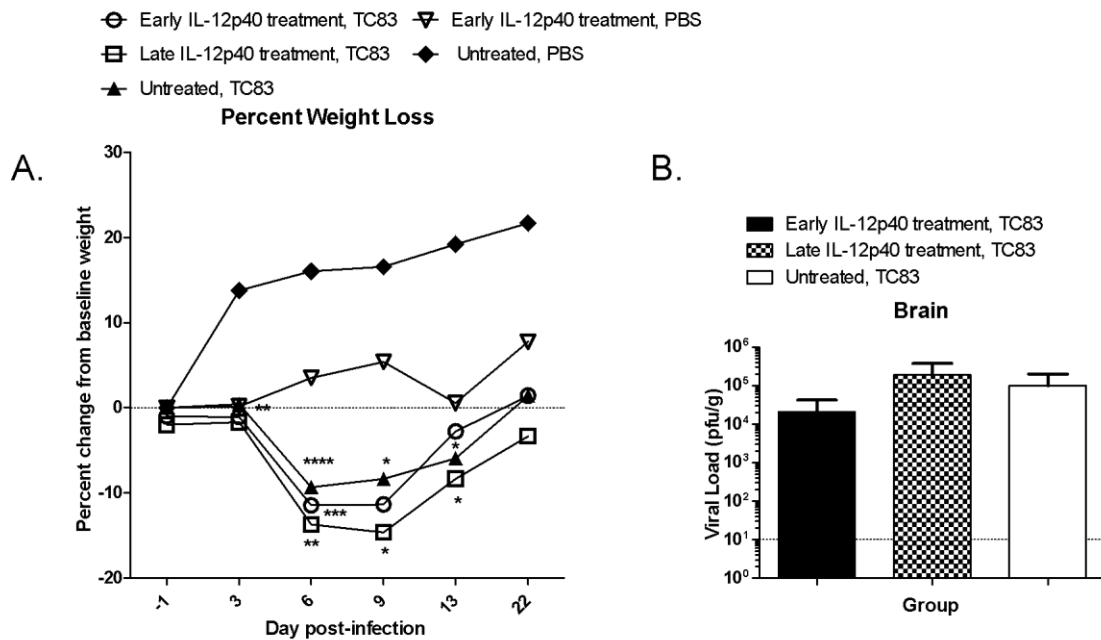


Figure 33: IL-12p40 KO mice treated early with IL-12p40 monomer display less symptomatic disease and lower viral load in the brain. Early treatment (n=3) results in more rapid recovery as measured by weight loss, but later treatment (n=3) has no effect on recovery of weight compared to untreated, infected mice (n=2). Sham infected mice treated early (n=2) maintain lower weights than untreated, sham infected mice (n=2). Viral load in the brain is reduced in mice treated early with IL-12p40 compared to mice receiving treatment later or untreated mice. This difference was not significant. (p<0.05) (* represents comparison to PBS control, * p<0.05, **p<0.005, *** p<0.001, ****p<0.0001)

Viral load in the brain reflected disease pathogenesis. Mice treated early displayed a trend toward lower viral load in the brain at 8 dpi than infected, untreated mice or the mice treated later in infection (Figure 33).

Clinical hematology and biochemistry parameters vary little between infection in early IL-12p40 treated mice, untreated mice, and uninfected, untreated mice at eight dpi.

Peripheral parameters of infection as measured by clinical hematology and biochemistry levels varied little regardless of status of the animal. Values were measured

from blood serum drawn at eight dpi. Mean corpuscular volume values were significantly higher for the early treatment group (n=3) compared to uninfected mice (n=2) in the clinical biochemistry panel ($p < 0.05$). No other group comparisons or values were significantly changed ($p < 0.05$). Values for clinical biochemistry were calculated as the mean of two separate runs.

With the exception of significantly lower serum albumin, phosphorus and calcium levels in the early treatment group (n=3) compared to uninfected controls (n=2), no other parameters were significantly altered in the hematology panel ($p < 0.05$). No comparisons could be made to untreated, infected mice as numbers were too low (n=1). The similarity between groups indicates control of the host response in BL6 mice influencing a positive outcome to infection in the periphery.

The effect of IL-12p40 on TC83 infection of C3H and BL6 mice.

In C3H mice, IL-12p40 treatment extended time to death and lowered viral load in the brain. In IL-12p40 KO mice on a BL6 background IL-12p40 treatment resulted in a more rapid recovery and lower viral load in the brain. These studies indicated a trend in the importance of IL-12p40 in generating an early antiviral state in TC83 infection, but the mechanism of IL-12p40 action is unknown.

A POTENTIAL ROLE FOR IL-12P40 IN WILD-TYPE VEEV INFECTION.

To further explore the role of IL-12p40 in viral encephalitis, we reverted to a model utilizing the more virulent strain of VEEV (ZPC738). *We hypothesized that VEEV infection would be lethal in vaccinated mice lacking IL-12p40 and this effect would be dependent on the absence of IL-12p40 primed T-cells.* IL-12p40 KO and TCR KO mice on a BL6 background were used for this experiment. Mice were vaccinated three times at two week intervals with the previously described vaccine candidate SIN/ZPC.

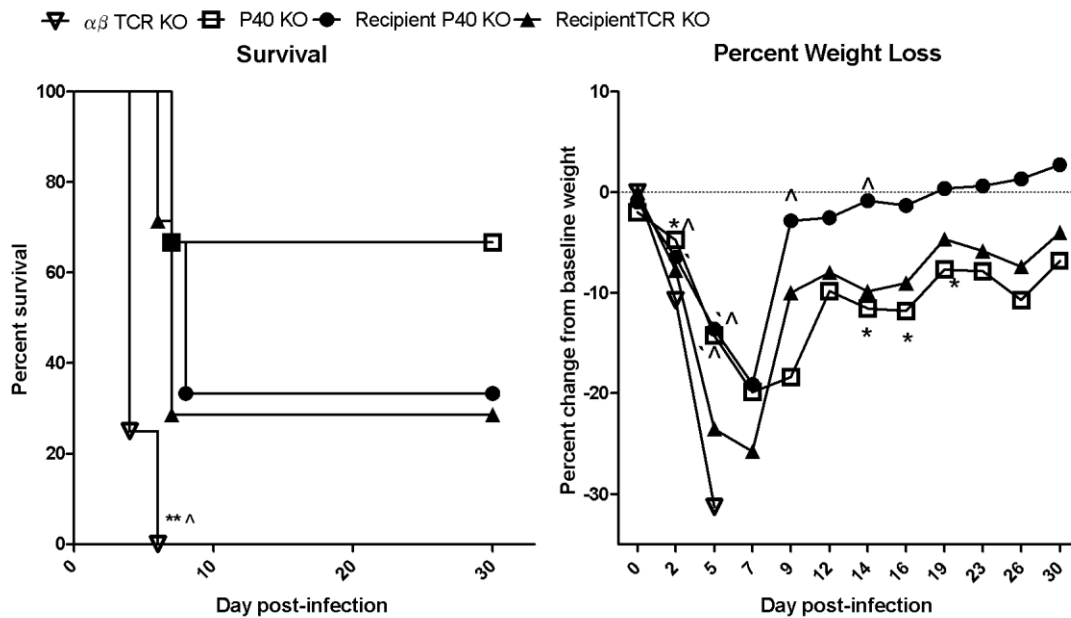


Figure 34: T-cell mediated recovery in TCR KO and IL-12p40 KO mice. IL-12p40 KO mice (n=5) had a 67% survival rate following VEEV challenge. IL-12p40 KO receiving T-cells (n=10) had a 33% survival rate, but this was not significantly different. TCR KO mice had 0% survival in the absence of T-cells (n=5), but in recipient groups had a 29% survival rate, a significant difference (n=10). IL-12p40 KO mice receiving T-cells weighed more than recipient TCR KO mice and IL-12p40 KO mice that did not receive T-cells between nine and 18 dpi. (*denotes $p < 0.05$ in comparison the recipient of the same strain; ^denotes $p < 0.05$ to recipient of the different strain; `denotes $p < 0.05$ compared to the control and recipient of the different strain)

Vaccination is protective in wild-type BL6 mice. A separate group of wild-type BL6 mice were vaccinated on the same schedule. We tested the ability of IL-12p40 KO mice to resist lethal challenge following adoptive transfer of CD3⁺ T-cells generated via vaccination in wild-type controls. Mice were challenged with wild-type VEEV. TCR KO mice that received T-cells had significantly greater survival rates than control TCR KO mice (Figure 34). IL-12p40 KO mice that received T-cells had similar survival rates to controls. However, vaccinated IL-12p40 KO controls had significantly greater survival than TCR KO controls, indicating that IL-12p40 is not absolutely required for survival.

However, differences in weight loss indicated that antigen primed T-cells mitigated symptomatic disease in IL-12p40 KO mice. IL-12p40 KO mice lost significantly more weight than IL-12p40 KO mice receiving T-cells at 14, 19, and 23 dpi indicating that antigen-specific T-cells primed in the presence of IL-12p40 mitigate symptomatic disease. Both groups of IL-12p40 KO mice maintained more weight than TCR KO mice with recipient and control TCR KO mice weighing significantly less than IL-12p40 groups at 5 dpi than IL-12-p40 groups.

Thus, IL-12p40 is not an absolute requirement for vaccine-induced protection against wild-type VEEV. Additionally, CD3⁺ T-cells developed in vaccinated IL-12p40 competent mice increase the rate of recovery in vaccinated IL-12p40 KO mice. This data indicates a role for IL-12p40 in the activation and development of protective T-cell populations.

DISCUSSION

Chronic infection following alphaviral encephalitis has been reported in the literature in different models. In a model of pre-existing immunity, $\delta\gamma$ TCR KO mice developed chronic viral infection with VEEV (ZPC) (133). These T-cells are thought to bridge innate and adaptive immune responses in a tissue specific manner. Attenuated strains of VEEV also induce chronic infection in μ MT KO mice that lack functional B-cell responses (21). Chronic inflammation was observed in the brains of some aerosol TC83 vaccinated BALB/c mice after challenge, but this was interpreted as residual inflammation due to the vaccine virus (157; 63). In combination with our model of chronic infection in $\alpha\beta$ TCR KO mice where a vaccine strain of virus TC83 administered intranasally resulted in long-term viral persistence, data indicates that T-cells are crucial to complete viral clearance and resolution of infection.

While brain viral load was maintained at levels similar to those seen a time of initial recovery in the pilot study at 12 dpi, TCR KO mice displayed a trend toward increased viral load over time. Perhaps significant variations in viral load occur over time with virus maintained at levels below the detection of the immune system until replication initiates a response resulting in subsequent reduction. This hypothesis would explain both the variable weight loss differences in BL6 and TCR KO at 15 and 34 dpi, and the increasing nature of both viral load and number of viral replicates seen at 91 dpi. Whether additional flux in viral load occurred between 34, 61, and 94 dpi is uncertain and requires additional study. However, this was beyond the scope of these experiments.

Pro-inflammatory cytokines in BL6 mice did not return to baseline till 60-90 dpi. This could be explained by either (1) regenerative process in the brain after TC83-encephalitis, or (2) continuous presence of virus below the limit of detection. Both are distinct possibilities and further testing is necessary to differentiate the precise cause for the very slow decline in these cytokine levels.

Given the importance of IL-12 in generating an effective T-cell response, we examined the effect on TC83 encephalitis. Survival was similar to wild type with TC83 and IL-12 was not absolutely required in a vaccine model of VEEV (ZPC) infection. However, weight loss indicated disease development. Subsequent gain of function experiments indicated that early administration of IL-12 and more rapid generation of a host response had a moderately attenuating effect on disease phenotype. However, this was not true of later administration that resulted in more symptomatic disease.

Interestingly trends toward lower viral load in treated mice and few alterations in clinical biochemical and hematology parameters leads to the question of a potential anti-viral effect for IL-12p40. Given the negative regulation between anti-viral type I IFN this would be a novel finding. Unlike TCR KO mice IL-12p40 mice did not develop a

chronic viral infection of the brain and, similar to wild-type BL6, cleared virus completely from the brain. This indicates that IL-12p40 is not essential for the generation of T-effector cell populations needed to clear virus from the brain. However, this may be attributed to compensatory, overlapping immune mechanisms as has been demonstrated previously in the literature (119; 120; 68).

In a vaccination model followed by VEEV (ZPC) infection, adoptive transfer of T-cells into IL12p40 KO mice had a significant attenuating affect on disease development and recovery though no differences in survival compared to controls were noted.

In conclusion, IL-12 shows promise early in infection in generating a robust protective T-cell response and mitigating symptomatic disease. However, the novel finding of viral persistence in the brains of TCR KO mice combined with indicators of persistence below the limit of detection in BL6 mice requires further study. The unique novel expression of key cytokines in TCR KO mice indicates that chronically infected individuals may be identified in the absence of isolation of virus.

Chapter 7: Conclusions

By using a comparative model of lethal and non-lethal TC83 infection, we identified key immune compartments that determined the course of infection. In summary, TC83 susceptible C3H mice survived infection in the absence of functional NK cells. This indicated the importance of this cell population in TC83 infection, and was a novel finding for VEE infections. TC83 resistant BL6 mice did not require T-cells for survival, but, in the absence of T-cells developed a chronic brain infection. Chronic brain infection coincided with development of a chronic inflammatory response in the brain. This provides a novel model to study the role of T-cells in persistent viral infection, as well as the chronic responses to infection in the brain. The importance of IL-12p40 in TC83 and wild-type VEEV infection and activation of immunoprotective T-cells was less well defined, and we can only speculate that IL-12p40 acted early in the development of protective T-cell populations.

Neuroinvasive viruses are not always neurovirulent. TCR KO, IL-12p40 KO and wild-type BL6 tolerated a high-level viral load in the brain following TC83 infection. In addition, chronically infected TCR KO mice had viral loads equivalent to lethally infected C3H mice at the peak of acute disease indicating that factors apart from viral load impact the course of disease following infection. TCR KO mice were asymptomatic. Likewise, NK-cell depleted C3H mice that survive infection developed a similar viral load in the brain compared to NK-cell competent mice that die. While this was mathematically significant in 1:2 experiments, the biological significance is uncertain. Previous studies demonstrated vaccinated mice tolerate a very high titer viral load in the brain, but survive infection with wild-type VEEV. Thus, neuroinvasion and level of viral replication in the brain does not determine outcome.

Given the asymptomatic nature of TC83 brain infection in TCR KO, BL6, and IL-12p40 KO, in human infections, we speculate alphaviruses can, and do, invade the CNS. The question of why some individuals develop significant neurological manifestations and others remain asymptomatic remains. While an age-related susceptibility occurs for alphavirus infections, the reasons for greater mortality, sequelae, and disease severity in pediatric populations are not defined for viral encephalitis. These questions are ubiquitous for viral encephalitis of many etiologies, and a better understanding of the factors influencing the host response to neuroinvasion are critical in influencing effective treatment and prevention strategies. Apart from experimental models, these questions are difficult, if not impossible, to test. Based on data generated mouse models, we conjecture that CNS susceptibility and disease occur partially independently of neuroinvasion and viral replication.

However, neuroinvasion and viral replication in the CNS undoubtedly modify the homeostasis of this delicate microenvironment and the role of the CNS in behavioral and cognitive functioning make any changes to the CNS of significant concern. Behavioral changes have been noted in pediatric cases, and indicate the variability of outcome following neuroinvasion. Behavioral changes marked by increased aggression have also been noted in murine models of TC83 vaccination. Thus, while disease may be asymptomatic or mild, the nature of the CNS means minute disruptions can have a significant impact on function. While mice may appear asymptomatic, their basic needs are met, and higher level cognitive process has not been evaluated in experimental models. The neuroinvasive nature of a live, attenuated vaccine strain TC83 calls into question the true safety of such a vaccine strategy. To truly understand the impact of neuroinvasion and viral replication in the CNS, behavioral and cognitive function in experimental models should be explored experimentally.

Studying the functional changes in experimental models is also important in models of chronic disease. The asymptomatic, chronic viral persistence in TCR KO mice indicates that virus can persist long-term in the absence of clinical symptoms. The translation of this research to humans indicates that virus can be maintained in the brain. The implications for infected individuals are unclear, but post-infectious neurological manifestations may occur as indicated by behavioral changes and neurological sequelae following acute disease. The slow resolution of neurological sequelae in reported cases of viral encephalitis may be indicative of delayed viral clearance. However, regenerative processes in the brain following rapid viral clearance could result in the same phenotype. In flavivirus infection, chronic symptoms may result from persistent renal infection indicating the ability of these viruses to persist in human systems. The unique nature of the CNS makes studying chronic infection difficult. However, persistent infection of humans is a possibility, and further exploration in experimental models may yield useful data regarding the role of persistent virus following alphavirus infection.

Based on our experimental mouse model, the host response and genetic variability influence outcome to infection. C3H mice died following TC83 infection. In contrast, all mice on a BL6 background survived infection. Even immunocompromised TCR KO and ILp40 KO mice survived. However, $\alpha\beta$ T-cell deficient mice develop a chronic brain infection. Comparison of the host response in these two inbred strains indicated NK-cells in infection, and C3H mice depleted of NK-cells survived TC83 infection. The high degree of allelic variability in receptors governing the NK-cell response may provide clues regarding the susceptibility of individuals to infection. Thus, genetic differences in inbred strains translated to differences in host response to virus. The comparison of the host response between mouse strains validated the importance of NK cells in VEEV-

caused encephalitis. We speculate that similar genetic and host response alterations in humans translate to susceptibility to viral encephalitis.

The discovery of the importance of NK-cells in TC83 disease in C3H mice identified novel innate immune effectors for VEEV infection. Since early intervention is crucial in alphavirus infections, this may provide a novel strategy for modulation of the earliest immune responses. However, NK-cells serve a number of functions including secretion of cytokines and induction of cell death. NK-cells are also lymphocytes and as such susceptible to infection with VEE viruses. Whether NK-cells provide a means for viral spread following infection, and if NK-cells are susceptible to TC83 infection are questions that should be addressed. Thus, to provide a usable intervention point, the precise mechanism of NK-cell mediated pathogenesis should be explored.

The absence of T-cells resulted in chronic infection of TCR KO mice following TC83 infection. Differences in viral populations over time may explain the chronic nature of infection, though preliminary data indicated this was not the case. Further examination of viral subpopulations is crucial in understanding the nature of chronic viral infection. These mice also had low levels of neutralizing antibody due to the lack of T-cell help for B-cells. The role of T-cells in mediating viral clearance is uncertain, and adoptive transfer studies looking at T-cell mediated clearance following establishment of a chronic viral state should be pursued. This might also clarify the role of endogenously and exogenously produced antibody in clearance of virus from neurons. Thus, a more specific mechanism for $\alpha\beta$ T-cells in resolution of chronic infection remains to be determined.

In C3H mice, IL-12p40 treatment extended time to death and lowered viral load in the brain. In IL-12p40 KO mice on a BL6 background, IL-12p40 treatment resulted in a more rapid recovery and lower viral load in the brain. These studies indicated a trend in

the importance of IL-12p40 in generating an early antiviral state in TC83 infection, but the mechanism of IL-12p40 action is unknown. In wild-type VEEV infection, IL-12p40 was not an absolute requirement for vaccine-induced protection. Additionally, CD3+ T-cells developed in vaccinated IL-12p40 competent mice increase the rate of recovery in vaccinated IL-12p40 KO mice. IL-12 induces IFN- γ production from NK and T cells, enhances the CTL activity of NK cells, and favors the generation of CD8 T-cells. IL-12 acts in three stages: (1) In early infection IL-12 induces IFN-gamma from NK and T cells resulting in cellular activation and inflammation; (2) IL-12 dependent IFN-gamma production and IL-12 itself acts to prime T-cells toward Th1 differentiation; and (3) finally, IL-12 continues to contribute to IFN-gamma production and aids in proliferation of now differentiated Th1 cells in response to APC (119; 68). Experimental data indicated a role for IL-12p40 in the activation and development of protective T-cell populations early in infection. However, the functional significance of IL-12p40 is uncertain.

Finally, by modifying specific immune compartments in both C3H and BL6 mice, changes to the phenotype of cellular infiltrates likely occur. In addition, these modifications may change neuronal and microglial cell populations. The influence of specific immune effectors recruited to the CNS and activation or phenotype of resident CNS cells can strongly influence an anti-viral state in the brain. To fully understand the neuroprotective and neuropathogenic mechanisms in the CNS, the global effects of immunomodulation of the host response should be explored.

In conclusion, we demonstrate a comparative murine model of lethal and non lethal viral encephalitis identified immune compartments crucial viral encephalitis. Using this system, we identified T-cells and NK-cells. Subsequently, we showed that the systemic depletion of NK cells enables C3H mice to tolerate the brain infection without

dying. A role for NK-cells had not previously been explored for VEEV. Absence of T-cells in BL6 mice resulted in a chronic viral infection, but not lethality. Chronic brain infection resulted in a chronic inflammatory response. This provides a novel model to study the effect of long-term viral replication in the brain.

Bibliography

1. Aguilar, P. V., A. P. Adams, et al. (2008). "Structural and nonstructural protein genome regions of eastern equine encephalitis virus are determinants of interferon sensitivity and murine virulence." J Virol **82**(10): 4920-4930.
2. Aguilar, P. V., L. W. Leung, et al. (2008). "A five-amino-acid deletion of the eastern equine encephalitis virus capsid protein attenuates replication in mammalian systems but not in mosquito cells." J Virol **82**(14): 6972-6983.
3. Aguilar, P. V., S. Paessler, et al. (2005). "Variation in interferon sensitivity and induction among strains of eastern equine encephalitis virus." J Virol **79**(17): 11300-11310.
4. Alevizatos, A. C., R. W. McKinney, et al. (1967). "Live, attenuated Venezuelan equine encephalomyelitis virus vaccine. I. Clinical effects in man." Am J Trop Med Hyg **16**(6): 762-768.
5. Alsharifi, M., M. Lobigs, et al. (2006). "NK cell-mediated immunopathology during an acute viral infection of the CNS." Eur J Immunol **36**(4): 887-896.
6. Anishchenko, M., S. Paessler, et al. (2004). "Generation and characterization of closely related epizootic and enzootic infectious cDNA clones for studying interferon sensitivity and emergence mechanisms of Venezuelan equine encephalitis virus." J Virol **78**(1): 1-8.
7. Armstrong, J. A., L. C. Freeburg, et al. (1971). "Effect of interferon on synthesis of Eastern equine encephalitis virus RNA." Proc Soc Exp Biol Med **137**(1): 13-18.
8. Aronson, J. F., F. B. Grieder, et al. (2000). "A single-site mutant and revertants arising in vivo define early steps in the pathogenesis of Venezuelan equine encephalitis virus." Virology **270**(1): 111-123.
9. Atasheva, S., N. Garmashova, et al. (2008). "Venezuelan equine encephalitis virus capsid protein inhibits nuclear import in Mammalian but not in mosquito cells." J Virol **82**(8): 4028-4041.
10. Austin, F. J. and W. F. Scherer (1971). "Studies of viral virulence. I. Growth and histopathology of virulent and attenuated strains of Venezuelan encephalitis virus in hamsters." Am J Pathol **62**(2): 195-210.
11. Bale, J. F., Jr. (1999). Viral Infections of the Nervous System. Pediatric Neurology: Principles and Practice. K. F. Swaiman, Ashwal, S. St. Louis, MO, Mosby, Inc. **2**: 1001-1024.
12. Barrera, R., C. Ferro, et al. (2002). "Contrasting sylvatic foci of Venezuelan equine encephalitis virus in northern South America." Am J Trop Med Hyg **67**(3): 324-334.

13. Barrera, R., N. Torres, et al. (2001). "Characterization of enzootic foci of Venezuelan equine encephalitis virus in western Venezuela." Vector Borne Zoonotic Dis **1**(3): 219-230.
14. Beck, C. E. and R. W. Wyckoff (1938). "Venezuelan Equine Encephalomyelitis." Science **88**(2292): 530.
15. Benjamini, Y. and Y. Hochberg (1995). "Controlling the False Discovery Rate - a Practical and Powerful Approach to Multiple Testing." Journal of the Royal Statistical Society Series B-Methodological **57**(1): 289-300.
16. Berge, T. O., I. S. Banks, et al. (1961). "Attenuation of Venezuelan equine encephalomyelitis virus by in vitro cultivation in guinea pig heart cells." Am. J. Hyg. **73**: 209.
17. Bernard, K. A., W. B. Klimstra, et al. (2000). "Mutations in the E2 glycoprotein of Venezuelan equine encephalitis virus confer heparan sulfate interaction, low morbidity, and rapid clearance from blood of mice." Virology **276**(1): 93-103.
18. Bianchi, T. I., G. Aviles, et al. (1993). "Western equine encephalomyelitis: virulence markers and their epidemiologic significance." Am J Trop Med Hyg **49**(3): 322-328.
19. Biron, C. A. (2010). "Expansion, maintenance, and memory in NK and T cells during viral infections: responding to pressures for defense and regulation." PLoS Pathog **6**(3): e1000816.
20. Biron, C. A. (2010). "More things in heaven and earth: defining innate and adaptive immunity." Nat Immunol **11**(12): 1080-1082.
21. Brooke, C. B., D. J. Deming, et al. (2010). "T cells facilitate recovery from Venezuelan equine encephalitis virus-induced encephalomyelitis in the absence of antibody." J Virol **84**(9): 4556-4568.
22. Brooke, C. B., A. Schafer, et al. (2012). "Early activation of the host complement system is required to restrict central nervous system invasion and limit neuropathology during Venezuelan equine encephalitis virus infection." J Gen Virol **93**(Pt 4): 797-806.
23. Brown, F. (1993). "Review of accidents caused by incomplete inactivation of viruses." Dev Biol Stand **81**: 103-107.
24. Brown, M. G., A. A. Scalzo, et al. (2001). "Natural killer gene complex (Nkc) allelic variability in inbred mice: evidence for Nkc haplotypes." Immunogenetics **53**(7): 584-591.
25. Calisher, C. H. (1994). "Medically important arboviruses of the United States and Canada." Clin Microbiol Rev **7**(1): 89-116.
26. Calisher, C. H., F. A. Murphy, et al. (1980). "Everglades virus infection in man, 1975." South Med J **73**(11): 1548.

27. Casals, J., E. C. Curnen, et al. (1943). "Venezuelan Equine Encephalomyelitis in Man." J Exp Med **77**(6): 521-530.
28. Casamassima, A. C., L. W. Hess, et al. (1987). "TC-83 Venezuelan equine encephalitis vaccine exposure during pregnancy." Teratology **36**(3): 287-289.
29. Castorena, K. M., D. C. Peltier, et al. (2008). "Maturation-dependent responses of human neuronal cells to western equine encephalitis virus infection and type I interferons." Virology **372**(1): 208-220.
30. CDC (2009). Confirmed and Probable Eastern Equine Encephalitis Cases, Human, United States, 1964-2009, Centers for Disease Control.
31. CDC (2009). Confirmed and Probable Western Equine Encephalitis Cases, Human, United States, 1964-2009,. W. D. 07202010.
32. CDC. (2009). "Fact Sheet: Arboviral Encephalitis." Retrieved November 11, 2011, 2011.
33. CFSPH (2008). Eastern Equine Encephalomyelitis, Western Equine Encephalomyelitis and Venezuelan Equine Encephalomyelitis. Iowa City, Iowa, The Center for Food Security and Public Health and the Institute for International Cooperation in Animal Biologics.
34. Charles, P. C., J. Trgovcich, et al. (2001). "Immunopathogenesis and immune modulation of Venezuelan equine encephalitis virus-induced disease in the mouse." Virology **284**(2): 190-202.
35. Charles, P. C., E. Walters, et al. (1995). "Mechanism of neuroinvasion of Venezuelan equine encephalitis virus in the mouse." Virology **208**(2): 662-671.
36. Chen, Y., J. M. Hallenbeck, et al. (2003). "Overexpression of monocyte chemoattractant protein 1 in the brain exacerbates ischemic brain injury and is associated with recruitment of inflammatory cells." J Cereb Blood Flow Metab **23**(6): 748-755.
37. Cook, S. H. and D. E. Griffin (2003). "Luciferase imaging of a neurotropic viral infection in intact animals." J Virol **77**(9): 5333-5338.
38. Datta, S. and S. Datta (2006). "Evaluation of clustering algorithms for gene expression data." BMC Bioinformatics **7 Suppl 4**(Suppl 4): S17.
39. de la Monte, S., F. Castro, et al. (1985). "The systemic pathology of Venezuelan equine encephalitis virus infection in humans." Am J Trop Med Hyg **34**(1): 194-202.
40. Dieli, F., G. L. Asherson, et al. (1995). "Major histocompatibility complex control of the class of the immune response to the hapten trinitrophenyl." Immunology **84**(3): 355-359.
41. Eddy, G. A., D. H. Martin, et al. (1972). "Field studies of an attenuated Venezuelan equine encephalomyelitis vaccine (strain TC-83)." Infect Immun **5**(2): 160-163.

42. Edelman, R., M. S. Ascher, et al. (1979). "Evaluation in humans of a new, inactivated vaccine for Venezuelan equine encephalitis virus (C-84)." J Infect Dis **140**(5): 708-715.
43. Ehrenguber, M. U., M. Renggli, et al. (2003). "Semliki Forest virus A7(74) transduces hippocampal neurons and glial cells in a temperature-dependent dual manner." J Neurovirol **9**(1): 16-28.
44. Ehrenkranz, N. J. and A. K. Ventura (1974). "Venezuelan equine encephalitis virus infection in man." Annu Rev Med **25**: 9-14.
45. Elhofy, A., J. Wang, et al. (2005). "Transgenic expression of CCL2 in the central nervous system prevents experimental autoimmune encephalomyelitis." J Leukoc Biol **77**(2): 229-237.
46. Feemster, R. F. (1938). "Outbreak of Encephalitis in Man Due to the Eastern Virus of Equine Encephalomyelitis." Am J Public Health Nations Health **28**(12): 1403-1410.
47. Ferro, C., J. Boshell, et al. (2003). "Natural enzootic vectors of Venezuelan equine encephalitis virus, Magdalena Valley, Colombia." Emerg Infect Dis **9**(1): 49-54.
48. Frolov, I. (2004). "Persistent infection and suppression of host response by alphaviruses." Arch Virol Suppl(18): 139-147.
49. Gardner, C. L., C. W. Burke, et al. (2008). "Eastern and Venezuelan equine encephalitis viruses differ in their ability to infect dendritic cells and macrophages: impact of altered cell tropism on pathogenesis." J Virol **82**(21): 10634-10646.
50. Gardner, C. L., J. Yin, et al. (2009). "Type I interferon induction is correlated with attenuation of a South American eastern equine encephalitis virus strain in mice." Virology **390**(2): 338-347.
51. Garmashova, N., S. Atasheva, et al. (2007). "Analysis of Venezuelan equine encephalitis virus capsid protein function in the inhibition of cellular transcription." J Virol **81**(24): 13552-13565.
52. Garmashova, N., R. Gorchakov, et al. (2007). "The Old World and New World alphaviruses use different virus-specific proteins for induction of transcriptional shutoff." J Virol **81**(5): 2472-2484.
53. Gautier, L., L. Cope, et al. (2004). "affy--analysis of Affymetrix GeneChip data at the probe level." Bioinformatics **20**(3): 307-315.
54. Gentleman, R. C., V. J. Carey, et al. (2004). "Bioconductor: open software development for computational biology and bioinformatics." Genome Biol **5**(10): R80.

55. Goldmann, O., G. S. Chhatwal, et al. (2003). "Immune mechanisms underlying host susceptibility to infection with group A streptococci." J Infect Dis **187**(5): 854-861.
56. Goldmann, O., A. Lengeling, et al. (2005). "The role of the MHC on resistance to group a streptococci in mice." J Immunol **175**(6): 3862-3872.
57. Griffin, D. E. (2005). "Neuronal cell death in alphavirus encephalomyelitis." Curr Top Microbiol Immunol **289**: 57-77.
58. Griffin, D. E. (2007). Alphaviruses. Fields Virology. D. M. H. Knipe, P. Philadelphia, Wolters Kluwer Health/Lippincott Williams & Wilkins. **1**: 1023-1054.
59. Grimley, P. M. and R. M. Friedman (1970). "Arboviral infection of voluntary striated muscles." J Infect Dis **122**(1): 45-52.
60. Groot, H. (1971). Venezuelan Encephalitis. Proceedings of the Workshop-Symposium on Venezuelan Encephalitis Virus, Washington, D.C., Pan American Health Organization.
61. Hahn, C. S., S. Lustig, et al. (1988). "Western equine encephalitis virus is a recombinant virus." Proc Natl Acad Sci U S A **85**(16): 5997-6001.
62. Hahn, Y. S., A. Guanzone, et al. (1999). "Class I MHC molecule-mediated inhibition of Sindbis virus replication." J Immunol **162**(1): 69-77.
63. Hart, M. K., K. Caswell-Stephan, et al. (2000). "Improved mucosal protection against Venezuelan equine encephalitis virus is induced by the molecularly defined, live-attenuated V3526 vaccine candidate." Vaccine **18**(26): 3067-3075.
64. Hart, M. K., W. Pratt, et al. (1997). "Venezuelan equine encephalitis virus vaccines induce mucosal IgA responses and protection from airborne infection in BALB/c, but not C3H/HeN mice." Vaccine **15**(4): 363-369.
65. Hawley, R. J. and E. M. Eitzen, Jr. (2001). "Biological weapons--a primer for microbiologists." Annu Rev Microbiol **55**: 235-253.
66. Hemmers, S. and K. A. Mowen (2009). "T(H)2 bias: Mina tips the balance." Nat Immunol **10**(8): 806-808.
67. Holbrook, M. R. and B. B. Gowen (2008). "Animal models of highly pathogenic RNA viral infections: encephalitis viruses." Antiviral Res **78**(1): 69-78.
68. Holscher, C. (2004). "The power of combinatorial immunology: IL-12 and IL-12-related dimeric cytokines in infectious diseases." Med Microbiol Immunol **193**(1): 1-17.
69. Howitt, B. (1938). "Recovery of the Virus of Equine Encephalomyelitis from the Brain of a Child." Science **88**(2289): 455-456.

70. Hsieh, C. S., S. E. Macatonia, et al. (1995). "T cell genetic background determines default T helper phenotype development in vitro." J Exp Med **181**(2): 713-721.
71. Hunt, A. R., R. A. Bowen, et al. (2011). "Treatment of mice with human monoclonal antibody 24h after lethal aerosol challenge with virulent Venezuelan equine encephalitis virus prevents disease but not infection." Virology **414**(2): 146-152.
72. Hunt, A. R., S. Frederickson, et al. (2006). "A humanized murine monoclonal antibody protects mice either before or after challenge with virulent Venezuelan equine encephalomyelitis virus." J Gen Virol **87**(Pt 9): 2467-2476.
73. Ihaka, R. and R. Gentleman (1996). "R: A Language for Data Analysis and Graphics." J. Comput. Graph. Stat. **5**(3): 299-314.
74. Irizarry, R. A., B. Hobbs, et al. (2003). "Exploration, normalization, and summaries of high density oligonucleotide array probe level data." Biostatistics **4**(2): 249-264.
75. Jackson, A. C. and J. P. Rossiter (1997). "Apoptotic cell death is an important cause of neuronal injury in experimental Venezuelan equine encephalitis virus infection of mice." Acta Neuropathol **93**(4): 349-353.
76. Jackson, A. C., S. K. SenGupta, et al. (1991). "Pathogenesis of Venezuelan equine encephalitis virus infection in mice and hamsters." Vet Pathol **28**(5): 410-418.
77. Jahrling, P. B. (1975). "Interference between Virulent and Vaccine Strains of Venezuelan Encephalitis-Virus in Mixed Infections of Hamsters." J Gen Virol **28**(Jul): 1-8.
78. Jahrling, P. B., E. Dendy, et al. (1974). "Correlates to increased lethality of attenuated Venezuelan encephalitis virus vaccine for immunosuppressed hamsters." Infect Immun **9**(5): 924-930.
79. Jahrling, P. B. and L. Gorelkin (1975). "Selective clearance of a benign clone of Venezuelan equine encephalitis virus from hamster plasma by hepatic reticuloendothelial cells." J Infect Dis **132**(6): 667-676.
80. Jahrling, P. B., E. Navarro, et al. (1976). "Interferon Induction and Sensitivity as Correlates to Virulence of Venezuelan Encephalitis Viruses for Hamsters." Arch Virol Suppl **51**(1-2): 23-35.
81. Jahrling, P. B. and W. F. Scherer (1973). "Homegeneity of Venezuelan encephalitis virion populations of hamster-virulent and benign strains, including the attenuated TC83 vaccine." Infect Immun **7**(6): 905-910.
82. Johnson, B. J., R. M. Kinney, et al. (1986). "Molecular determinants of alphavirus neurovirulence: nucleotide and deduced protein sequence changes during attenuation of Venezuelan equine encephalitis virus." J Gen Virol **67** (Pt 9): 1951-1960.

83. Johnson, R. T. (1996). "Acute encephalitis." Clin Infect Dis **23**(2): 219-224; quiz 225-216.
84. Johnston, L. J., G. M. Halliday, et al. (2000). "Langerhans cells migrate to local lymph nodes following cutaneous infection with an arbovirus." J Invest Dermatol **114**(3): 560-568.
85. Jones, L. D., A. M. Bennett, et al. (2003). "Cytotoxic T-cell activity is not detectable in Venezuelan equine encephalitis virus-infected mice." Virus Res **91**(2): 255-259.
86. Jordan, G. W. (1973). "Interferon sensitivity of Venezuelan equine encephalomyelitis virus." Infect Immun **7**(6): 911-917.
87. Julander, J. G., R. A. Bowen, et al. (2008). "Treatment of Venezuelan equine encephalitis virus infection with (-)-carbodine." Antiviral Res **80**(3): 309-315.
88. Julander, J. G., V. Siddharthan, et al. (2007). "Effect of exogenous interferon and an interferon inducer on western equine encephalitis virus disease in a hamster model." Virology **360**(2): 454-460.
89. Julander, J. G., R. Skirpstunas, et al. (2008). "C3H/HeN mouse model for the evaluation of antiviral agents for the treatment of Venezuelan equine encephalitis virus infection." Antiviral Res **78**(3): 230-241.
90. Kamath, A. B., J. Alt, et al. (2004). "The major histocompatibility complex haplotype affects T-cell recognition of mycobacterial antigens but not resistance to Mycobacterium tuberculosis in C3H mice." Infect Immun **72**(12): 6790-6798.
91. Kamrud, K. I., K. D. Alterson, et al. (2008). "Analysis of Venezuelan equine encephalitis replicon particles packaged in different coats." Plos One **3**(7): e2709.
92. Karabatsos, N., A. L. Lewis, et al. (1988). "Identification of Highlands J virus from a Florida horse." Am J Trop Med Hyg **39**(6): 603-606.
93. Karre, K., H. G. Ljunggren, et al. (1986). "Selective rejection of H-2-deficient lymphoma variants suggests alternative immune defence strategy." Nature **319**(6055): 675-678.
94. Kasai, M., T. Yoneda, et al. (1981). "In vivo effect of anti-asialo GM1 antibody on natural killer activity." Nature **291**(5813): 334-335.
95. Kato, H., M. Hayashi, et al. (2002). "MHC restriction in contact hypersensitivity to dicyclohexylcarbodiimide." Food Chem Toxicol **40**(11): 1713-1718.
96. Kelser, R. A. (1937). "Transmission of the Virus of Equine Encephalomyelitis by Aedes Taeniorhynchus." Science **85**(2198): 178.
97. Kinney, R. M., G. J. Chang, et al. (1993). "Attenuation of Venezuelan equine encephalitis virus strain TC-83 is encoded by the 5'-noncoding region and the E2 envelope glycoprotein." J Virol **67**(3): 1269-1277.

98. Kinney, R. M., B. J. Johnson, et al. (1989). "The full-length nucleotide sequences of the virulent Trinidad donkey strain of Venezuelan equine encephalitis virus and its attenuated vaccine derivative, strain TC-83." *Virology* **170**(1): 19-30.
99. Kolokoltsov, A. A., E. H. Fleming, et al. (2006). "Venezuelan equine encephalitis virus entry mechanism requires late endosome formation and resists cell membrane cholesterol depletion." *Virology* **347**(2): 333-342.
100. Kolokoltsov, A. A., E. Wang, et al. (2006). "Pseudotyped viruses permit rapid detection of neutralizing antibodies in human and equine serum against Venezuelan equine encephalitis virus." *Am J Trop Med Hyg* **75**(4): 702-709.
101. Kolokoltsov, A. A., S. C. Weaver, et al. (2005). "Efficient functional pseudotyping of oncoretroviral and lentiviral vectors by Venezuelan equine encephalitis virus envelope proteins." *J Virol* **79**(2): 756-763.
102. Koskiniemi, M., M. Korppi, et al. (1997). "Epidemiology of encephalitis in children. A prospective multicentre study." *Eur J Pediatr* **156**(7): 541-545.
103. Kubes, V. (1944). "Venezuelan-Type Equine Encephalomyelitis Virus in Trinidad." *Science* **99**(2559): 41-42.
104. Kubes, V. and A. Diamante (1942). "Cross-immunity Studies: Between Venezuelan Equine Encephalomyelitis Virus and Eastern, Western, and Argentine Virus." *Can J Comp Med Vet Sci* **6**(12): 357-359.
105. Kubes, V. and F. A. Rios (1939). "The Causative Agent of Infectious Equine Encephalomyelitis in Venezuela." *Science* **90**(2323): 20-21.
106. Kubes, V. and F. A. Rios (1939). "Equine Encephalomyelitis in Venezuela: Advance Data Concerning the Causative Agent." *Can J Comp Med* **3**(2): 43-44.
107. Kuehne, R. W., W. D. Sawyer, et al. (1962). "Infection with aerosolized attenuated Venezuelan equine encephalomyelitis virus." *Am J Hyg* **75**: 347-350.
108. Large, A. (1867). "Fatal epidemic among horses in America." *The Veterinarian* **67**: 655-660, 727-279.
109. LeBlanc, P. A., W. F. Scherer, et al. (1978). "Infections of congenitally athymic (nude) and normal mice with avirulent and virulent strains of Venezuelan encephalitis virus." *Infect Immun* **21**(3): 779-785.
110. Lee, S. H., T. Miyagi, et al. (2007). "Keeping NK cells in highly regulated antiviral warfare." *Trends Immunol* **28**(6): 252-259.
111. Leon, C. A. (1975). "Sequelae of Venezuelan equine encephalitis in humans: a four year follow-up." *Int J Epidemiol* **4**(2): 131-140.
112. Levitt, N. H., H. V. Miller, et al. (1979). "Interaction of alphaviruses with human peripheral leukocytes: in vitro replication of Venezuelan equine encephalomyelitis virus in monocyte cultures." *Infect Immun* **24**(3): 642-646.

113. Liu, C., D. W. Voth, et al. (1970). "A comparative study of the pathogenesis of western equine and eastern equine encephalomyelitis viral infections in mice by intracerebral and subcutaneous inoculations." J Infect Dis **122**(1): 53-63.
114. Liu, T., T. Matsuguchi, et al. (2002). "Differences in expression of toll-like receptors and their reactivities in dendritic cells in BALB/c and C57BL/6 mice." Infect Immun **70**(12): 6638-6645.
115. Lossinsky, A. S. and R. R. Shivers (2004). "Structural pathways for macromolecular and cellular transport across the blood-brain barrier during inflammatory conditions. Review." Histol Histopathol **19**(2): 535-564.
116. Lucas, R. E. and M. Qiao (1999). "A case of encephalitis in central Australia due to Ross River virus?" Aust N Z J Med **29**(2): 268-270.
117. Ludwig, G. V., M. J. Turell, et al. (2001). "Comparative neurovirulence of attenuated and non-attenuated strains of Venezuelan equine encephalitis virus in mice." Am J Trop Med Hyg **64**(1-2): 49-55.
118. Luers, A. J., S. D. Adams, et al. (2005). "A phylogenomic study of the genus Alphavirus employing whole genome comparison." Comp Funct Genomics **6**(4): 217-227.
119. Magram, J., S. E. Connaughton, et al. (1996). "IL-12-deficient mice are defective in IFN gamma production and type 1 cytokine responses." Immunity **4**(5): 471-481.
120. Magram, J., J. Sfarra, et al. (1996). "IL-12-deficient mice are defective but not devoid of type 1 cytokine responses." Ann N Y Acad Sci **795**: 60-70.
121. Marr, J. (2002). Encephalitis. Case based Pediatrics for Medical Students and Residents. L. Yamamoto, Inaba, A., Okamoto, J., Patrinos, M., Yamashiroya, V. . Honolulu, HI, Department of Pediatrics, University of Hawaii, John A. Burns School of Medicine. **VI**.
122. Mathews, J. H. and J. T. Roehrig (1989). "Specificity of the murine T helper cell immune response to various alphaviruses." J Gen Virol **70 (Pt 11)**: 2877-2886.
123. Mehta, I. K., H. R. Smith, et al. (2001). "A "chimeric" C57l-derived Ly49 inhibitory receptor resembling the Ly49D activation receptor." Cell Immunol **209**(1): 29-41.
124. Mehta, I. K., J. Wang, et al. (2001). "Ly49A allelic variation and MHC class I specificity." Immunogenetics **53**(7): 572-583.
125. Meyer, K. F., C. M. Haring, et al. (1931). "The Etiology of Epizootic Encephalomyelitis of Horses in the San Joaquin Valley, 1930." Science **74**(1913): 227-228.
126. Mims, C. A., F. A. Murphy, et al. (1973). "Pathogenesis of Ross River virus infection in mice. I. Ependymal infection, cortical thinning, and hydrocephalus." J Infect Dis **127**(2): 121-128.

127. Murphy, F. A. and S. G. Whitfield (1970). "Eastern equine encephalitis virus infection: electron microscopic studies of mouse central nervous system." Exp Mol Pathol **13**(2): 131-146.
128. Nicolosi, A., W. A. Hauser, et al. (1986). "Epidemiology of central nervous system infections in Olmsted County, Minnesota, 1950-1981." J Infect Dis **154**(3): 399-408.
129. Ohtsuka, M., H. Inoko, et al. (2008). "Major histocompatibility complex (Mhc) class Ib gene duplications, organization and expression patterns in mouse strain C57BL/6." BMC Genomics **9**: 178.
130. Paessler, S., R. Z. Fayzulin, et al. (2003). "Recombinant sindbis/Venezuelan equine encephalitis virus is highly attenuated and immunogenic." J Virol **77**(17): 9278-9286.
131. Paessler, S., H. Ni, et al. (2006). "Replication and clearance of Venezuelan equine encephalitis virus from the brains of animals vaccinated with chimeric SIN/VEE viruses." J Virol **80**(6): 2784-2796.
132. Paessler, S. and S. C. Weaver (2009). "Vaccines for Venezuelan equine encephalitis." Vaccine **27 Suppl 4**: D80-85.
133. Paessler, S., N. E. Yun, et al. (2007). "Alpha-beta T cells provide protection against lethal encephalitis in the murine model of VEEV infection." Virology **367**(2): 307-323.
134. Paredes, A., K. Alwell-Warda, et al. (2001). "Venezuelan equine encephalomyelitis virus structure and its divergence from old world alphaviruses." J Virol **75**(19): 9532-9537.
135. Pie, S., P. Matsiota-Bernard, et al. (1996). "Gamma interferon and interleukin-10 gene expression in innately susceptible and resistant mice during the early phase of Salmonella typhimurium infection." Infect Immun **64**(3): 849-854.
136. Pittman, P. R., R. S. Makuch, et al. (1996). "Long-term duration of detectable neutralizing antibodies after administration of live-attenuated VEE vaccine and following booster vaccination with inactivated VEE vaccine." Vaccine **14**(4): 337-343.
137. Porterfield, J. S. (1975). "The basis of arbovirus classification." Med Biol **53**(5): 400-405.
138. Porterfield, J. S. (1986). Comparative and historical aspects of the Togaviridae and Flaviviridae. The Togaviridae and Flaviviridae. S. S. Schlesinger, M.J. New York, Plenum Press. **1-19**.
139. Prater, M. R., R. M. Gogal, Jr., et al. (2003). "Immunotoxic effects of cis-urocanic acid exposure in C57BL/6N and C3H/HeN mice." Photochem Photobiol **77**(4): 383-389.

140. Proteau, M. F., E. Rousselle, et al. (2004). "Mapping of the BALB/c Ly49 cluster defines a minimal natural killer cell receptor gene repertoire." Genomics **84**(4): 669-677.
141. Rennels, M. B. (1984). "Arthropod-borne virus infections of the central nervous system." Neurol Clin **2**(2): 241-254.
142. Renthal, N. E., P. A. Guidry, et al. (2011). "Isoforms of the nonclassical class I MHC antigen H2-Q5 are enriched in brain and encode Qdm peptide." Immunogenetics **63**(1): 57-64.
143. Rivas, F., L. A. Diaz, et al. (1997). "Epidemic Venezuelan equine encephalitis in La Guajira, Colombia, 1995." J Infect Dis **175**(4): 828-832.
144. Roy, C. J., D. S. Reed, et al. (2009). "Pathogenesis of aerosolized Eastern Equine Encephalitis virus infection in guinea pigs." Virol J **6**: 170.
145. Ryman, K. D. and W. B. Klimstra (2008). "Host responses to alphavirus infection." Immunol Rev **225**: 27-45.
146. Schafer, A., C. B. Brooke, et al. (2011). "The role of the blood-brain barrier during Venezuelan equine encephalitis virus infection." J Virol **85**(20): 10682-10690.
147. Schafer, A., A. C. Whitmore, et al. (2009). "Replicon particles of Venezuelan equine encephalitis virus as a reductionist murine model for encephalitis." J Virol **83**(9): 4275-4286.
148. Schlesinger, S. a. S., M.J. (2001). Togaviridae: The viruses and their replication. . Fields' Virology. D. M. K. a. P. M. Howley. Philadelphia, Lippincott, Williams and Wilkins: 895-916.
149. Schoneboom, B. A., M. J. Fultz, et al. (1999). "Astrocytes as targets for Venezuelan equine encephalitis virus infection." J Neurovirol **5**(4): 342-354.
150. Scrimgeour, E. M. (1999). "Suspected Ross River virus encephalitis in Papua New Guinea." Aust N Z J Med **29**(4): 559.
151. Sidwell, R. W., L. P. Gebhardt, et al. (1967). "Epidemiological aspects of venezuelan equine encephalitis virus infections." Bacteriol Rev **31**(1): 65-81.
152. Siegert, J., I. Sastalla, et al. (2006). "Vaccination equally enables both genetically susceptible and resistant mice to control infection with group A streptococci." Microbes Infect **8**(2): 347-353.
153. Simmons, J. D., L. J. White, et al. (2009). "Venezuelan equine encephalitis virus disrupts STAT1 signaling by distinct mechanisms independent of host shutoff." J Virol **83**(20): 10571-10581.
154. Smyth, G. K. (2004). "Linear models and empirical bayes methods for assessing differential expression in microarray experiments." Stat Appl Genet Mol Biol **3**: Article3.

155. Spotts, D. R., R. M. Reich, et al. (1998). "Resistance to alpha/beta interferons correlates with the epizootic and virulence potential of Venezuelan equine encephalitis viruses and is determined by the 5' noncoding region and glycoproteins." Journal of Virology **72**(12): 10286-10291.
156. Staab, E. V., S. J. Normann, et al. (1970). "Alterations in reticuloendothelial function by infection with attenuated Venezuelan equine encephalitis (VEE) virus." J Reticuloendothel Soc **8**(4): 342-348.
157. Steele, K. E., K. J. Davis, et al. (1998). "Comparative neurovirulence and tissue tropism of wild-type and attenuated strains of Venezuelan equine encephalitis virus administered by aerosol in C3H/HeN and BALB/c mice." Vet Pathol **35**(5): 386-397.
158. Steele, K. E., P. Seth, et al. (2006). "Tunicamycin enhances neuroinvasion and encephalitis in mice infected with Venezuelan equine encephalitis virus." Vet Pathol **43**(6): 904-913.
159. Steele, K. E. and N. A. Twenhafel (2010). "Pathology of animal models of alphavirus encephalitis." Vet Pathol **47**(5): 790-805.
160. Sudia, W. D. and V. F. Newhouse (1975). "Epidemic Venezuelan equine encephalitis in North America: a summary of virus-vector-host relationships." Am J Epidemiol **101**(1): 1-13.
161. Sun, J. C., J. N. Beilke, et al. (2009). "Adaptive immune features of natural killer cells." Nature **457**(7229): 557-561.
162. Sun, J. C. and L. L. Lanier (2009). "Natural killer cells remember: an evolutionary bridge between innate and adaptive immunity?" Eur J Immunol **39**(8): 2059-2064.
163. Swann, J. B., Y. Hayakawa, et al. (2007). "Type I IFN contributes to NK cell homeostasis, activation, and antitumor function." J Immunol **178**(12): 7540-7549.
164. Tajima, A., T. Tanaka, et al. (2003). "Blastocyst MHC, a putative murine homologue of HLA-G, protects TAP-deficient tumor cells from natural killer cell-mediated rejection in vivo." J Immunol **171**(4): 1715-1721.
165. Tenbroeck, C., E. W. Hurst, et al. (1935). "Epidemiology of Equine Encephalomyelitis in the Eastern United States." J Exp Med **62**(5): 677-685.
166. Tenbroeck, C. and M. H. Merrill (1933). "A Serological Difference Between Eastern and Western Equine Encephalomyelitis Virus." Proceedings of the Society for Experimental Biology and Medicine **31**: 217-220.
167. Tigertt, W. D. and W. G. Downs (1962). "Studies on the virus of Venezuelan equine encephalomyelitis in Trinidad, W.I. I. The 1943-1944 epizootic." Am J Trop Med Hyg **11**: 822-834.
168. Turell, M. J., R. F. Tammariello, et al. (1995). "Nonvascular delivery of St. Louis encephalitis and Venezuelan equine encephalitis viruses by infected mosquitoes (Diptera: Culicidae) feeding on a vertebrate host." J Med Entomol **32**(4): 563-568.

169. Ulett, G. C., N. Ketheesan, et al. (2000). "Cytokine gene expression in innately susceptible BALB/c mice and relatively resistant C57BL/6 mice during infection with virulent *Burkholderia pseudomallei*." Infect Immun **68**(4): 2034-2042.
170. Velasquez, J. (1939). "Enfermedades de los animales transmisibles al hombre: peste loca." Salud y Sanidad **8**: 22.
171. Vogel, P., W. M. Kell, et al. (2005). "Early events in the pathogenesis of eastern equine encephalitis virus in mice." Am J Pathol **166**(1): 159-171.
172. Wang, T., T. Town, et al. (2004). "Toll-like receptor 3 mediates West Nile virus entry into the brain causing lethal encephalitis." Nat Med **10**(12): 1366-1373.
173. Weaver, S. C. (2005). "Host range, amplification and arboviral disease emergence." Arch Virol Suppl(19): 33-44.
174. Weaver, S. C. and A. D. Barrett (2004). "Transmission cycles, host range, evolution and emergence of arboviral disease." Nat Rev Microbiol **2**(10): 789-801.
175. Weaver, S. C., C. Ferro, et al. (2004). "Venezuelan equine encephalitis." Annu Rev Entomol **49**: 141-174.
176. White, L. J., J. G. Wang, et al. (2001). "Role of alpha/beta interferon in Venezuelan equine encephalitis virus pathogenesis: effect of an attenuating mutation in the 5' untranslated region." J Virol **75**(8): 3706-3718.
177. Whitley, R. J. and D. W. Kimberlin (1999). "Viral encephalitis." Pediatr Rev **20**(6): 192-198.
178. Willems, W. R., G. Kaluza, et al. (1979). "Semliki forest virus: cause of a fatal case of human encephalitis." Science **203**(4385): 1127-1129.
179. Woodman, D. R., A. T. McManus, et al. (1975). "Extension of the mean time to death of mice with a lethal infection of Venezuelan equine encephalomyelitis virus by antithymocyte serum treatment." Infect Immun **12**(5): 1006-1011.
180. Wu, Z., R. A. Irizarry, et al. (2004). A Model-Based Background Adjustment for Oligonucleotide Expression Arrays. **99**: 909-917.
181. Xie, X., M. D. Stadnisky, et al. (2009). "MHC class I Dk locus and Ly49G2+ NK cells confer H-2k resistance to murine cytomegalovirus." J Immunol **182**(11): 7163-7171.
182. Yin, J., C. L. Gardner, et al. (2009). "Similarities and differences in antagonism of neuron alpha/beta interferon responses by Venezuelan equine encephalitis and Sindbis alphaviruses." J Virol **83**(19): 10036-10047.
183. Young, N. A. and K. M. Johnson (1969). "Antigenic variants of Venezuelan equine encephalitis virus: their geographic distribution and epidemiologic significance." Am J Epidemiol **89**(3): 286-307.

184. Yun, N. E., B. H. Peng, et al. (2009). "CD4+ T cells provide protection against acute lethal encephalitis caused by Venezuelan equine encephalitis virus." Vaccine **27**(30): 4064-4073.
185. Zacks, M. A. and S. Paessler (2010). "Encephalitic alphaviruses." Vet Microbiol **140**(3-4): 281-286.
186. Zlotnik, I., S. Peacock, et al. (1972). "The pathogenesis of western equine encephalitis virus (W.E.E.) in adult hamsters with special reference to the long and short term effects on the C.N.S. of the attenuated clone 15 variant." Br J Exp Pathol **53**(1): 59-77.

Vita

Katherine Taylor was born in Amarillo, Texas on August, 7 1983 to Gregory and Cathy Taylor. She graduated from Texas A&M University on May 12th, 2006 with a B.S. in biomedical science. She worked in a plant genomics laboratory for most of her undergraduate time. After completing her teaching certification for 8th-12th grade science, she returned to Texas A&M University as a research assistant and studied identification system for fungal plant infections. In fall of 2007, she entered graduate school at the University of Texas Medical Branch. During her time at UTMB, she studied immune mechanisms of resolution of infection to multiple pathogens including Venezuelan equine encephalitis virus, Burkholderia pseudomallei, and Mycobacterium tuberculosis.

Education

B.S., May 2006, Texas A&M University, College Station, Texas

Publications

1. Judy, B.M., **Taylor, K.**, Deeraksa, A., Johnston, K., Endsley, J.J., Aronson, J.F., Estes, D.M. & Torres, A.G. (2011). Therapeutic CpG oligonucleotides dampen host inflammatory response and reduce lung injury in an acute respiratory model of Melioidosis. *Plos One*. In revision.

2. **Taylor, K.**, Kolkostova, O., Patterson, M., Poussard, A., Smith, J., Estes, D.M., Paessler, S.P. (2011). Natural Killer Cell Mediated Pathogenesis Determines Outcome of Central Nervous System Infection with Venezuelan Equine Encephalitis Virus. *Vaccine*.
 3. Whitlock, G.C., Robida, M.D., Judy, B.M., Qazi, O., Brown, K.A., Deeraksa, A., **Taylor, K.**, Massey, S., Loskutov, A., Borovkov, A.Y., Brown, K., Cano, J.A., Torres, A.G., Estes, D.M. & Sykes, K.F. (2011). Protective antigens against glanders identified by expression library immunization. *Frontiers in Science*. In revision.
 4. Patterson, M., Poussard, A., **Taylor, K.**, Seregin, A., Smith, J., Peng, B.-H., Walker, A., Linde, J., Smith, J., Salazar, M. & Paessler, S. (2011). Rapid, non-invasive imaging of alphaviral brain infection: Reducing animal numbers and morbidity to identify efficacy of potential vaccines and antivirals. *Vaccine*.
 5. Burrell AM, **Taylor KG**, Williams RJ, Cantrell RT, Menz MA, Pepper AE. (2011) A comparative genomic map for *Caulanthus amplexicaulis* and related species (Brassicaceae). *Mol Ecol* 20:784-98.
 6. Atasheva S, Wang E, Adams AP, Plante KS, Ni S, **Taylor K**, Miller ME, Frolov I, Weaver SC. (2009) Chimeric alphavirus vaccine candidates protect mice from intranasal challenge with western equine encephalitis virus. *Vaccine* 27: 4309-431.
1. Slobodan Paessler and **Katherine Taylor** (2011). Encephalitic Development in Alphaviral Infection, Non-Flavivirus Encephalitis, Sergey Tkachev (Ed.), ISBN: 978-953-307-720-8, InTech,

2. G. C. Whitlock, A. Deeraksa, O. Qazi, B. M. Judy, **K. Taylor**, K. L. Propst, A. J. Duffy, K. Johnson, G. B. Kitto, K. A. Brown, S. W. Dow, A. G. Torres and D. M. Estes. Protective response to subunit vaccination against intranasal *Burkholderia mallei* and *B. pseudomallei* challenge. 3rd Vaccine Global Congress, Singapore 2009. R. Spier. Amsterdam, Elsevier Science Bv. **2**: 73-77.

1. **Taylor K**, Borisevich V, Kolokoltsova O, Smith J, Smith J, Poussard A, Estes M, Paessler S. Identification of natural killer cells as a key determinant of survival in alphaviral encephalitis. Poster presentation at American Society of Virology Annual Meeting, July 2011.
2. **Taylor K**, Borisevich V, Kolokoltsova O, Smith J, Smith J, Poussard A, Estes M, Paessler S. A novel role for natural killer cells in VEEV pathogenesis. Oral and Poster presentation and American Association of Immunologists, San Francisco, CA, May 2011.
3. **Taylor K**, Kolokoltsova O, Borisevich V, Peng B, Smith S, Yun N, Estes M, Paessler S. Oral and poster presentation at American Association of Immunologists, Baltimore, MA, May 7-11 2010.
4. **Taylor K**, Kolokoltsova O, Borisevich V, Peng B, Smith S, Yun N, Estes M, Paessler S. A novel model to study encephalitis: Lessons learned from a non-lethal response. Poster presentation at Fourth Annual DHS University Network Summit, Washington D.C., March 8-12 2010
5. **Taylor K**, Kolokoltsova O, Borisevich V, Peng B, Smith S, Yun N, Estes M, Paessler S. Lethal vs. non-lethal viral encephalitis. Poster presentation at Keystone Symposia: Viral Immunity, Banff, Alberta, Canada March 21-27 2010.

6. Patterson M, Seregin A, **Taylor K**, Poussard A, Smith J, Smith J, Salazar M, Paessler S. In VIVO Imaging of Alphavirus Infection: Visualizing the Early CNS Infection Using Non-Invasive Technique. Poster presentation at National Student Research Forum March 2010.
7. **Taylor K**, Deerakasa A, Judy B, Estes M. B and C Class CpG Protect against Intranasal Challenge by *B. pseudomallei* in a Mouse Model. Poster presentation at Third Annual DHS University Network Summit, Washington D.C. March 17-19 2009
8. Burrell M, Cantrell R, **Taylor K**, Sedio B, Reddy U, Pepper A. Development of Molecular and Genetic Tools to Study the Evolution of Serpentine Speciation in the Streptanthoid Complex, Brassicaceae. Poster presentation at Fifth International Conference on Serpentine Ecology, Siena, Italy May 9-13, 2006.
9. Burrell M, Cantrell R, **Taylor K**, Reddy U, Pepper A. Molecular resources for population-genetic and functional ecological-genetic studies in the Streptanthoid Complex of genera (Brassicaceae). Poster presentation at Annual Conference of the Botanical Society of America, Austin, TX August 13-17 2005.

Permanent address: P.O. Box 106 Wellborn, TX 77845

This dissertation was typed by Katherine G. Taylor

